Progetto S2

Valutazione del potenziale sismogenetico e probabilità dei forti terremoti in Italia

Assessing the seismogenic potential and the probability of strong earthquakes in Italy

Scientists in charge: Dario Slejko (INOGS-Trieste) and Gianluca Valensise (INGV)

Final report of activity (1 June 2005 - 31 July 2007)

Table of contents

Generalities

Project S2 has been a large project with a multifaceted nature. Its four tasks pursued - we hope successfully – quite distinct goals that would justify independent projects. What was it then that made it worthwhile to pursue these goals together within a single, large - and admittedly quite difficult to handle - project? We believe the key word to explain why it did make sense to plan our project as we did was *challenge*.

Scientists involved in Task 1 were ready to challenge themselves and the community around them by proposing the Seismogenic Areas, an innovative concept aimed at supplying a complete geologic record of seismogenic activity, or at least at supplying a scheme whose incompleteness can be assessed and dealt with area by area.

Many scientists – unfortunately not all – in Task 2 finally developed an appreciation for the difference between a study of active faulting and a study for the identification of a seismogenic source: between mapping in great detail the complexity of surface processes on the one hand, and identifying the full set of geological occurrences associated with the activity of a large fault on the other (with lesser detail of course, but with an improved appreciation for the scale and hierarchy of the tectonic processes that actually generate damaging earthquakes).

Scientists in Task 3 were ready to start developing GPS-derived velocity and strain models at the scale of whole Italy. They were also ready to challenge themselves with the preparation of a highly computation-intensive, Finite Elements geodynamic model of peninsular Italy incorporating highly scattered data with a final detail of 10-20 km. A model that could be extensively tested against stress, focal mechanism, active faulting and GPS data that were unavailable until just a few years ago.

And finally, scientists in Task 4 were ready to incorporate detailed knowledge on active faulting and tectonic rates into their models of earthquake occurrence, which were all based on earthquake catalogues until the beginning of this decade.

To sum up, the project attempted to assess earthquake probabilities by capturing and bringing together innovative ideas and data that have come to maturity between 2005 and 2007. Although not all Research Units (RUs) performed at their best, we contend that no activity went astray, as they all contributed either to increase the project knowledge basis (Task 1, 2, 3), or to assess the feasibility and limitations of the statistical calculations (Task 4).

Project S2 was seen by some as too big, or too vague in scopes. Although we admit that Year 1 of the project was very difficult and that we ourselves were rather concerned with how things appeared after we completed the first annual report, we believe during Year 2 most of the RUs worked really hard for converging towards the expected results. With is 40 RUs the project was and remained rather big, but its scopes became evident as we hope are its results. It was initially conceived as an extension of a the project "Probable Earthquakes in Italy between 2000 and 2030: guidelines for Determining Priorities in Seismic Risk Mitigation", funded within the 2000-2002 agreement between INGV and the Italian Civil Defence (DPC). Both coordinators of S2 and several of the scientists involved in it also participated in this parent project, which was even wider in scopes than S2 and indeed generated a large amount of basic data, some of which were to become fundamental cornerstones for our project. Yet it produced only one elaboration that pointed directly to the proposed target, namely a time-dependent map of probabilities associated with the repetition of damaging characteristic earthquakes. The main reasons for this limited performance were that (a) the different ingredients that should go into the calculation of earthquake probabilties were not mature yet, largely for reasons independent from the quality of the science being done in the project; and (b) the links among such ingredients had not been identified or clearly focused. At the end of Year 1, S2 faced the same condition, as some of the links between different parts of the project were late in being created or understood by the scientists involved. Things improved substantially at the beginning of Year 2, and we think the diversity and the quality of the deliverables of the project will prove that.

S2, however, was not simply an updated version of its parent project; in fact, one of its main goals was to challenge some of the key decisions made in 2000: *Is geology-based hazard a realistic goal? Is it realistic in Italy, or perhaps in some portions of the country? What data does it require? And what about time-dependent hazard? How complete is the geological record? Are slip and strain rates from GPS comparable to those evaluated from geological or seismological data? And how do these various ways*

of assessing tectonic and earthquake rates compare with each other? S2 attempted to give an answer to most of these questions. In short:

1) the geological record of active faulting can be made reasonably complete if we accept to step back and give up the systematic search for individual potential earthquake sources. In conjunction with historical and instrumental earthquake data, geological observations are most successful at delineating trends and outlining deep geometries and discontinuities, but in many areas their resolving power is simply insufficient to delineate presumable rupture ends, and hence to relate historical earthquake ruptures to actual fault segments. This does not imply that characteristic earthquakes do or do not exist, but simply that it is extremely difficult to devise the segmentation of many blind, deep or otherwise difficult-to-locate faults. The record is probably 95% complete in better known portions of the country, 70% complete in others, 50% complete or less in the offshore;
2) the above conclusion implies that geological data can fully constrain a detailed, country-wide seismogenic model for hazard assessment, but also that time-dependent hazard may only work for selected portions of the country and for the largest magnitudes;
3) reliable slip and strain rates supplied by geology are limited – and are not likely to increase drastically in the next few years - though well distributed over Italy. Strain rates from GPS can be very accurate, but currently only for limited portions of the country. The data that will be made available in the next few years by the new INGV national GPS network will improve things substantially, but geological and seismological data will still be fundamental for localizing strain onto discrete (seismogenic) faults. Localizing strain (i.e. identifying individual fault trends) with GPS data alone in a country that exhibits the structural complexity of Italy is simply irrealistic unless the spacing of GPS stations is reduced by a factor of two or more (currently is 20-25 km in selected target areas, about 50 km countrywide);
4) there are many possible ways of representing seismic hazard and earthquake probabilities, each one responding to a specific question by planners, administrators, and structural engineers. Each individual problem must use a suitable set of input data and a specific technique that maximizes the most robust characteristics of the information content of the data;
5) no matter what technique we are using, the quality of the results will always be as good as the uncertainties in the input data;
6) Finite Elements Models may play a fundamental role in reconciling observations at different time scales, extracting the best from each of the available datasets and effectively reducing global uncertainties by binding together independent datasets;
7) none of the datasets used by S2 – starting with the geological data - are expected to improve fast enough to become the reference dataset for seismic hazard in the years to come. *Data diversity* and *interdisciplinarity* are therefore the keywords for any successful approach to calculating earthquake probabilties.

During its 26-month duration, S2 accomplished several important results, some of which should have a "structuring effect" for future research efforts. Many results have already been proposed in meetings, some have been already published or are in the process of publication. The section of this report *Papers published or submitted during the project* lists 76 papers, a good portion of which have already appeared or are expected to appear on major refereed journals. Tangible results are presented in the *Deliverables* section, which ended up being substantially richer than envisioned at the beginning of the project. The elaborations presented in this section are described in detail in the RU reports and sometimes supplied along with raw data in tabular form.

Following is a brief summary of the main accomplishments of the different tasks. The reader is encouraged to refer to the RU reports for further details, illustrations and references.

Task 1 – During the project, scientists of Task 1 developed three releases of the DISS database. Version 3.0.2., that was made available in September 2006, has been used by most RUs for their respective calculations, so that by using the same input data the differences in their results

could be more reliably evaluated. Task 1 also distributed data and provided support to projects S3 and S5.

A new version of DISS that has been made available at the end of the project (v3.0.3) was used only by specific RUs for improving the quality of their estimates. This latter version includes some of the findings of the RUs of Task 2, but obviously not all. To overcome this limitation scientists of RU 1.1 have agreed to include most of the findings from Task 2 in a new version of the Database (v3.0.4) to be made available through the web by 30 September 2007.

DISS v3.0.2 was validated using available independent instrumental estimates of the stress and strain fields and was analyzed for completeness. The results of this analysis show that the balance geological vs seismological and GPS strains is rather satisfactory in over 50% of the seismogenic areas.

Scientists of Task 1 also worked extensively on the quantification of historical earthquakes. A new release of the Boxer code has been elaborated and extensively tested and is currently at the stage of a beta-version.

Finally, scientists of Task 1 gathered from the literature over 3,300 focal mechanisms that were entered in a new version of the EMMA database, the largest such compilation in Europe.

Task 2 – The numerous RUs involved in Task 2 gathered a significant number of new observations and made new important inferences on seismogenic processes in the Italian peninsula. Interestingly, some of the activities planned in Task 2 were not aimed at identifying new faults but rather at reorganizing and strenghtening existing information. In at least two cases scientists were specifically asked to confirm or disprove existing models that were weakly supported by experimental data.

As mentioned earlier, the wealth of new information generated in Task 2 could only partially be incorporated in the version of DISS that is being released at the end of the project (v3.0.3). Most of this information will be analyzed and formatted immediately after the end of the project to become part of a new DISS release (see above).

An especially valuable part of the research conducted in Task 2 dealt with tsunami scenarios and tsunami effects in peninsular Italy. The work done is both experimental, as tsunami deposits have been identified and dated at various sites in Sicily and Apulia; and analytical, as tsunami scenarios for the Italian coasts have been calculated using simplified models of the most important tsunamigenic sources of the Mediterranean.

Task 3 – This task attempted to take the most out of the instantaneous strain record represented by GPS velocities. Unfortunately this record is still rather patchy and its accuracy is highly variable for different parts of the country. Although geodetically derived strain rates for Italy have been extensively published in the past decade, their use in the context of seismic hazard assessment requires a deep understanding of their significance and limitations.

In view of these drawbacks Task 3 also attempted to predict crustal velocities through a geodynamic model blending a large set of experimental data into a single deterministic scheme. Task 3 scientists hence developed a Finite Elements Models based on a large variety of geologic and tectonic data, including fault geometries, the orientation of P and T axes from earthquake focal mechanisms, thermal, rheological and frictional properties of crustal rocks, the Moho depth, estimates of the heat flow, and kinematics at the plate scale. The model allowed crustal velocities and strains and fault slip rates to be estimated. Slip rates have then been used for calculating fully geology- and geodynamics based seismic hazard maps.

Task 4 – Although some years have passed since time-dependent models were proposed for hazard computation, they still find sporadic applications. This circumstance is motivated by the detailed information needed, and rarely available, concerning source kinematics and timing of occurrence. Moreover their application to seismic zonation is questionable, while their value for risk reduction is evident.

It is only based on these awareness that the utility of such a kind of studies for Italy could be addressed, and we hope our considerations on the challenging nature of this project fully answer this question. Task 4 suffered perhaps more than the other tasks from the actual limitations for a satisfactory applicability of time-dependent approaches in Italy. The results obtained span in a rather large range of values and, consequently, cannot be immediately useful

for civil defence purposes. Nevertheless, they offer a clear and honest view of the present state-of-the-art.

To sum up: *what did we expect from S2*? We expected it to be able to illustrate what can be realistically done in Italy in the assessment of earthquake probabilties. *Did we succeed*? We believe we did, at least partially. We threw in so many ingredients that even summarizing the project's main accomplishments has been rather difficult. The project collected interesting and innovative results on specific and perhaps marginal aspects, such as earthquake triggering in the northern Apennines. Some of the results, such as the transient effects due to slip on adjacent faults, are rather controversial and suggest that the impact of such effects on earthquake probabilities is always negligible, especially if compared with the other uncertainties. GPS data alone have shown to be too sparse to feed accurate earthquake probabilities, not even in northeastern Italy; a substantially denser network associated with reliable knowledge on the location of the main active faults are needed to retrieve meaningful strains. Based on its capacity to combine highly diverse data in a single – though necessarily simplified – scheme, geodynamic modeling may represent an alternative to the lack of direct strain observations.

Perhaps due to its intrinsic nature, the project does not offer a single cutting-edge result, but rather a set of good quality results that help understanding where we stand in the quest for reliable probabilities to be assigned to future damaging earthquakes in Italy. Some of the results can be of immediate interest for DPC officials, some will perhaps be of interest for planners and for the insurance industry, others will remain as scientific advancements that will not be pursued further. All of these issues were thoroughly discussed during the meeting *Earthquake and Shaking Probabilities*, that was held in Erice (Sicily) from 18 to 24 October 2006 (www.ingv.it/primopiano/erice2006/indice.html). The meeting created an opportunity for comparing the current seismic hazard practice in Japan, USA, New Zealand and Italy, with special emphasis on specific topics such as the creation of fault databases, the use of historical information, the use of GPS data, and statistical techniques for calculating earthquake probabilties.

As a result of the Erice meeting we invited Steven Ward (University of California at Santa Cruz) to take part in the activities of S2. In addition to being an added value for the project, this exchange represented a fertile area for future cooperative work and cross-breeding, and materialized in a number of elaborations. Ward has recently produced and compared a wide range of independent, well documented and physically defensible hazard models for California that produce identically formatted output. The comparison is aimed at finding the best way to deal with the full uncertainty in earthquake hazard estimates. To this end Ward generated testable time-independent earthquake potential maps based on geodesy, geology, and historical seismicity. The results in terms of earthquake potential are expressed as the logarithm of the annual rate of events exceeding some magnitude threshold. Ward applied the same procedure to Italy, obtaining extremely interesting and thought-provoking results.

The next section contains a description of activities accomplished under each of the four tasks of S2:

Task 1 - Organizing a unitary georeferenced system for the description of seismogenic processes, *coordinator Roberto Basili (INGV-Roma 1)*
Task 2 - Defining the location and geometry of the main seismogenic sources in the Italian peninsula, *coordinator Fabrizio Galadini (INGV-Roma 1)*
Task 3 - Geophysical characterization of the main seismogenic structures, *coordinator Alessandro Caporali (University of Padova)*
Task 4 - Characterizing the behavior of seismogenic sources and assigning probabilities of activation, *coordinator Laura Peruzza (INOGS, Trieste)*

Each activity is described with reference to the individual RU that contributed to it (see full list below) and illustrated with original images or with images taken from the RU reports. An

Appendix describes the contribution given to the project by Steven Ward. The report is completed by the list of the deliverables and by the list of paper published or submitted during the project. Full RU reports are supplied through the Internet at the web-page http://www.ingv.it/progettiSV/Progetti/Sismologici/S2/Task_1[2, 3, 4].pdf .

Summary of Research Units and funding assigned

Task/RU	Scientist in charge	Funding* *Year 1*	Funding* *Year 2*	Funding* *Total*
1.1	Basili	46.0	36.0	82.0
1.2	Gasperini	6.0	6.0	12.0
1.3	Albini	10.2	8.2	18.4
2.1a	Brancolini	33.5	33.5	67.0
2.1b	Argnani	14.5	14.5	29.0
2.2a	Barbano	38.0	40.0	78.0
2.2b	De Martini	15.0	13.0	28.0
2.3	Barchi	27.8	23.1	50.9
2.4	Burrato	25.3	18.3	43.6
2.4	Catalano	34.0	32.0	66.0
2.5	Doglioni	24.0	26.0	50.0
2.6	Favali	18.0	15.0	33.0
2.7	Galadini	11.8	15.2	27.0
2.8	Italiano	40.0	40.0	80.0
2.9	Lavecchia	30.0	30.0	60.0
2.10	Mastronuzzi	6.0	6.0	12.0
2.11	Mucciarelli	10.0	1.5	11.5
2.12	Neri	20.6	19.6	40.2
2.13	Pizzi	19.0	19.0	38.0
2.14	Scandone	20.0	20.0	40.0
2.15	Siniscalchi	38.0	38.0	76.0
2.16	Pettenati	8.0	12.0	20.0
2.17	Solarino	15.0	15.0	30.0
2.19a	Tinti	2.5	2.5	5.0
2.19b	Piatanesi	5.5	2.5	8.0
2.20	Zuppetta	16.0	14.0	30.0
3.1	Barba	9.0	8.5	17.5
3.2a	Caporali	18.5	18.5	37.0
3.2b	Braitenberg	13.5	13.5	27.0
3.3	Guerra	15.0	0	15.0
3.4	Sepe	15.0	21.0	36.0
4.1	Akinci	16.0	16.0	32.0
4.2	Di Giovambattista	15.0	15.0	30.0
4.3	Cinti	12.0	10.0	22.0
4.4	Garavaglia	17.0	18.5	35.5
4.5	Godano	34.0	18.0	52.0
4.6	Mantovani	24.0	24.0	48.0
4.7	Murru	12.8	12.8	25.6
4.8	Peruzza	33.0	32.0	65.0
4.9	Rotondi	25.0	25.0	50.0
		794.5	733.7	1,528.2**

* Funding is given in KEuros
** of which 513.0 (34%) assigned to INGV RUs, 1,015.2 to non-INGV RUs (66%)

Task 1

Organizing a unitary georeferenced system for the description of seismogenic processes

Coordinator Roberto Basili, INGV-Roma 1

This Task includes three Research Units (RUs) which carried out several activities that are logically intertwined and operatively independent. Its main objective was the realization of an organic reference system to be used as a source of input data for the project. This objective was mainly pursued by increasing and updating the content of two databases, namely DISS and EMMA, and by providing support, either by consultancy or through dedicated software, for their usage.

Achievements

Database of Individual Seismogenic Sources (DISS)

The Database of Individual Seismogenic Sources has been improved both in terms of contents and user interface (Fig. 1.1). For a complete account of the activities and for the definition of the various source types please consult the report of **RU 1.1**. Following is a summary of the main achievements of the current version 3.0.3 with respect to DISS 3.0.0 (Fig. 1.2):

- Individual Seismogenic Sources: net increment of 15 sources (+15%).
- Composite Seismogenic Sources (also referred to as Seismogenic Areas): net increment of 43 sources (+100%).
- Macroseismic Sources: new version based on intensity data from DBMI04 and Boxer v. 3.3.
- Support data: ~400 references (+20%), 244 images (+44%), ~50 texts (+20%) added.

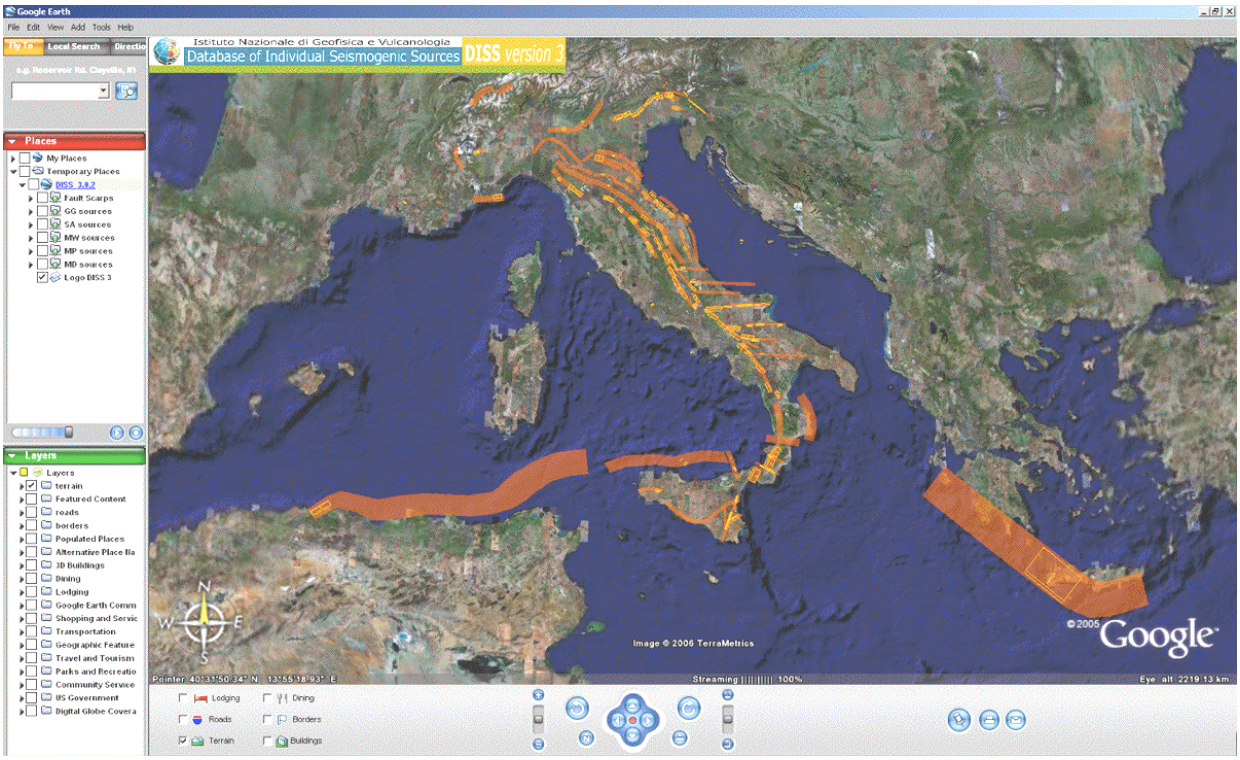

Figure 1.1 – The improved DISS 3 user Google Earth interface provides interactive navigation through the free Google Earth software.

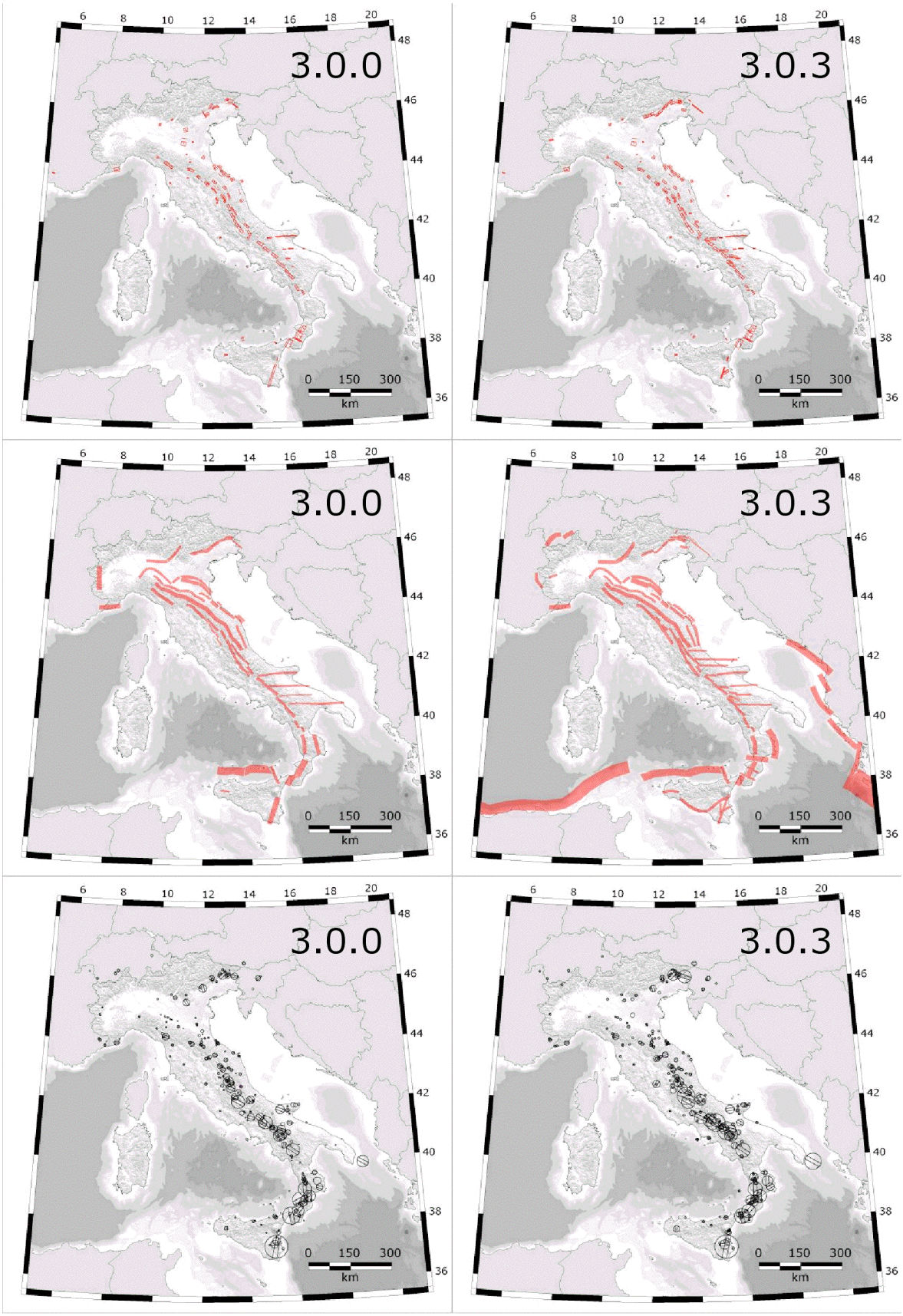

Figure 1.2 – Increment of DISS data during the project. Version 3.0.0 was available at the onset of the project (June 2005). Version 3.0.3 is the main deliverable of RU 1.1. Top to bottom: Individual Seismogenic Sources based on geological/geophysical data; Seismogenic Areas based on geological/geophysical data; Macroseismic Sources (this layer developed in collaboration with RU 1.2 and RU 1.3).

Figure 1.2 shows the increment of data incorporated in DISS during the project by comparing in map view the content before the project (DISS v3.0.0) with that of today (DISS v3.0.3). DISS was expanded by carrying out original investigations at a number of sites; DISS compilers will also incorporate the latest results from Task 2 in a dedicated issue of the database (DISS v3.0.4) by September 30, 2007 (Fig. 1.3). DISS compilers have also started a novel procedure for the validation of its content that strengthens the results of all elaborations made using it.

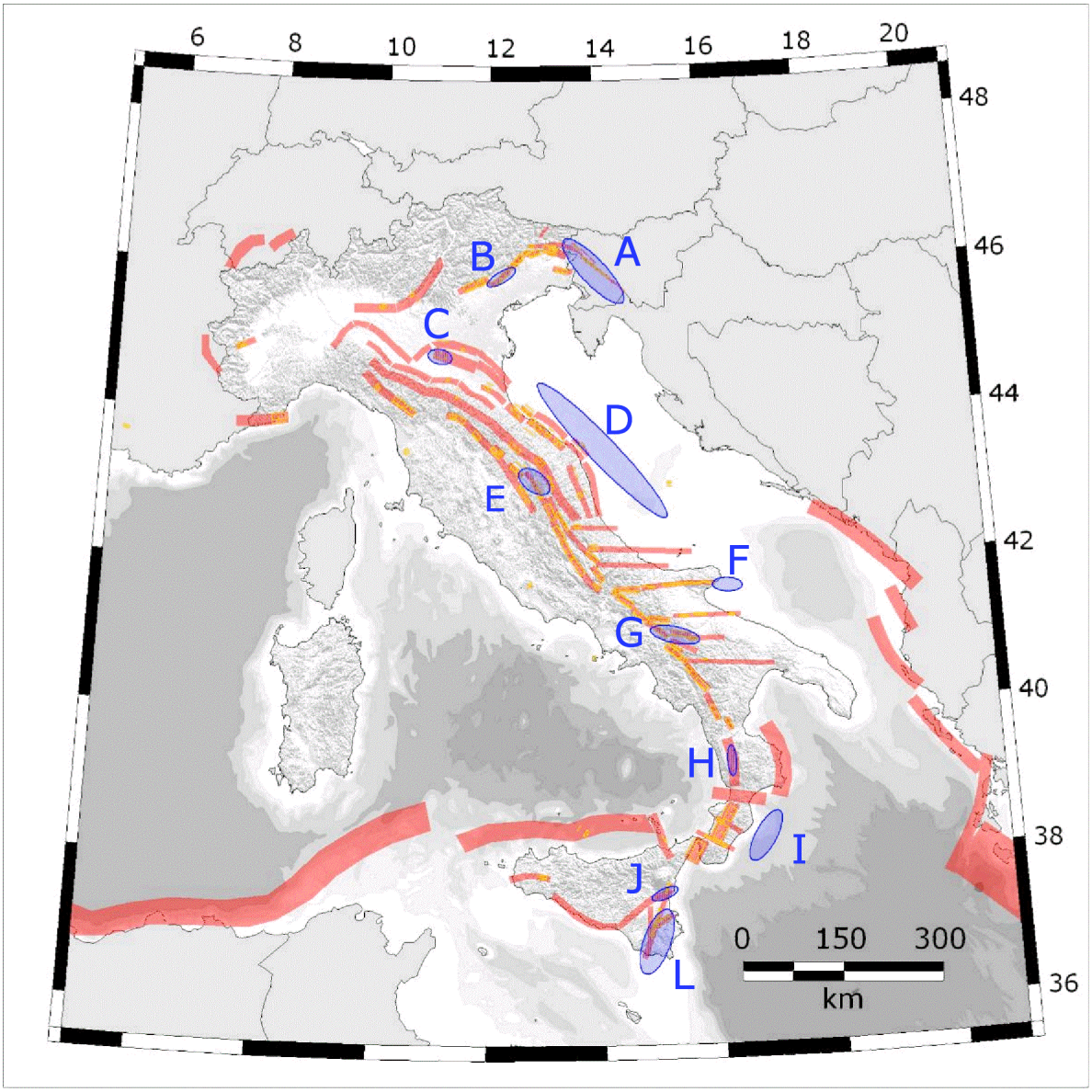

Figure 1.3 – Map showing areas (in blue) where the RU1.1 carried out original investigations during the project with DISS v3.0.3 in the background. A: Slovenian area; B: Montello-Conegliano thrust; C: Mirandola anticline; D: Mid-Adriatic Outer Front; E: Gubbio-Gualdo Tadino area; F: Mattinata-Gondola shear zone; G: Ufita River Valley-Vulture area; H: Crati River Valley; I: Southern Calabria Ionian Front; J: Terreforti anticlines; L: Hyblean area. These analyses will contribute in enriching DISS v3.0.4 (to be released by September 30, 2007).

Database of Earthquake Mechanisms of European Area (EMMA)

- Focal Mechanisms from literature: 3,355 focal mechanisms added; 54% increment with respect to the previous database version.

Figure 1.4 shows the increment of data incorporated in EMMA during the project by

comparing in map view the content before the onset of the project with that of today. This increment was obtained by scrutinizing the literature of the past 15 years and cross-examining the focal mechanism and earthquake parameters of 9,511 events.

Software

- Boxer: development and extensive testing of version 4 to be made available shortly.
- DISS tools: series of routines for (1) updating the database on both the standalone and online versions; (2) converting data tables to different GIS formats for seamless distribution; (3) generating the Google Earth version which further extends the capabilities of consulting the database; (4) generating thematic layers made up by DISS tables and other geophysical data.

In addition to the above material results, all RUs have provided each other with mutual assistance in using their own products or testing them against possible flaws or inaccuracies.

RU 1.1 assisted several RUs of other Tasks and other S projects in using DISS and by supplying original elaborations or in-depth analyses. **RU 1.1** also developed a research program in close collaboration with **RU 2.19b** to estimate the maximum water elevation expected on Southern Italy coastlines generated by tsunamigenic earthquake sources in the Mediterranean Sea (see description of Task 2 results).

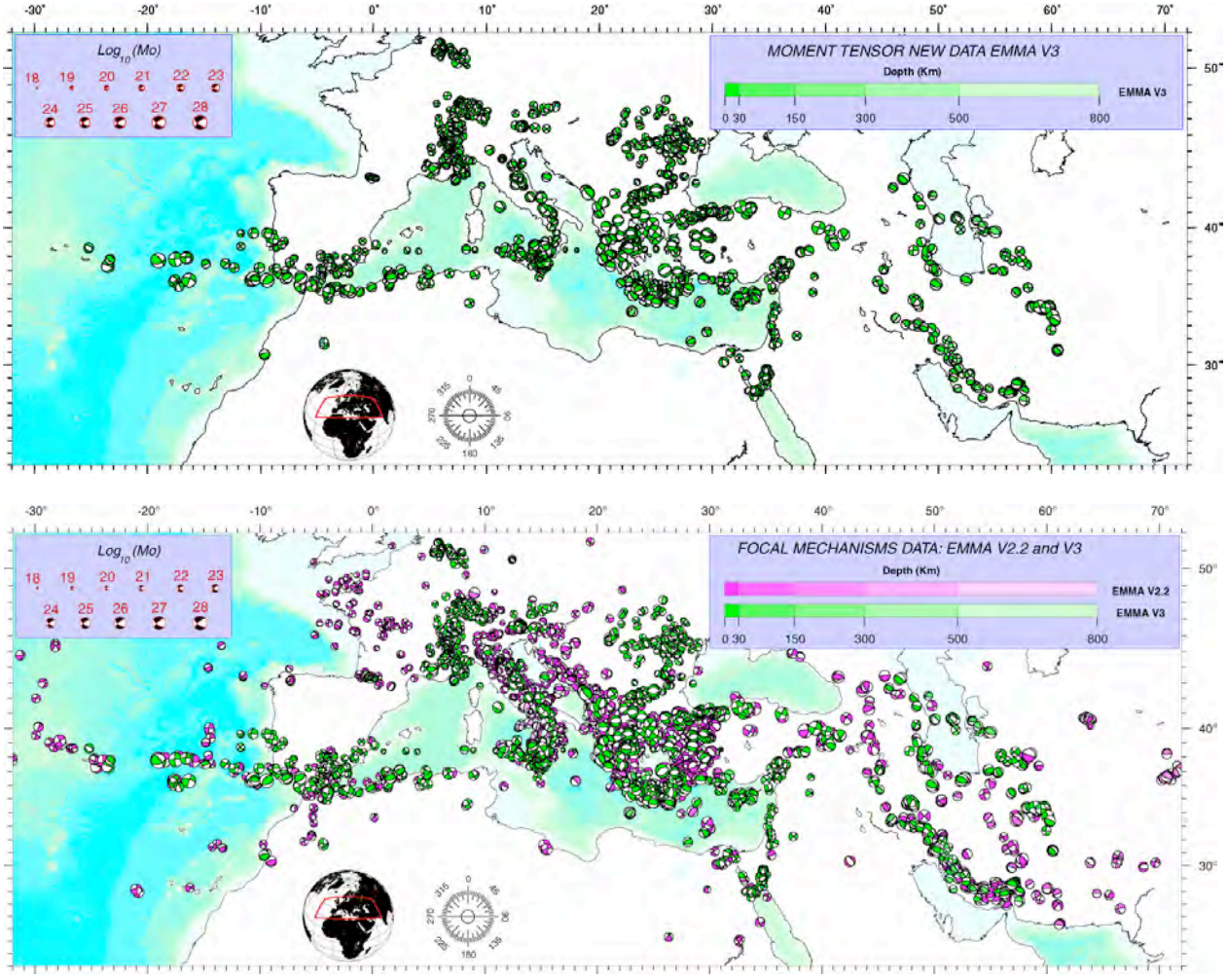

Figure 1.4 – Maps showing the increment of data incorporated into EMMA during the project. Green: mechanisms added during the project; pink: mechanisms already included in the version available at the begininng of the project.

Data validation

One of the outstanding issues in the realization of a reference database of seismogenic sources devised for SHA applications - and hence necessarily shared by a large community of scientists - is the validation of the data it contains. Other major such databases in the world are the Quaternary Fault and Fold Database of the United States (USGS: http://earthquake.usgs.gov/regional/qfaults/), the New Zealand Active Faults Database (GNS: http://data.gns.cri.nz/af/) and the Behavioral Segment-Based Active Fault Database of Japan (AIST: http://www.aist.go.jp/RIODB/activefault/cgi-bin/index_e.cgi). As of today, there is not a common strategy, not to mention an error-proof method, to declare the reliability of these types of data. In most cases, validation is implied by the effort of putting together large amounts of data and generally warranted only by the quality of the science behind each record. Unfortunately, this form of implied validation fails whenever the compilers of the database are faced with contrasting - but equally published - evidence or interpretations concerning the same aspect of seismogenic processes (e.g. the mere existence of a fault, its location or extent, its kinematics, its slip rate, etc.).

We tackled the validation issue in two ways: (1) by looking at individual database entries and (2) by looking at the whole database.

As for point (1) we propose, and are still testing, a conceptual model to assess the quality of the database entries by scoring both epistemic and stochastic uncertainties; the first being inherent with the declaration of existence of a seismogenic source, the second being associated with its characterization. This method provides an effective way to compare different database records, address areas of lack of knowledge, and make sensitivity tests to the applications that use them.

As for point (2) we propose two types of validations, tectonic and seismic, carried out by comparing geological data with independent datasets.

Tectonic validation was carried out by looking at major regional tectonic trends outlined by seismogenic sources grouped by faulting types (Fig. 1.5A) and their slip vectors in map projection (Fig. 1.5B). The sources illustrate the lateral continuity of the normal fault system along the backbone of peninsular Italy and the different styles of compression in the outer parts of the mountain belt: thrusts in the south-eastern Alps, northern Apennines, Calabrian Arc, and Sicilian-Maghrebian chain; predominant strike-slip east of the southern Apennines axis and in southeastern Sicily. The change in slip vector direction shows the continuous tectonic flow that extends through zones with different tectonic regimes. These two views facilitate the comparison between the information on faulting contained in DISS and other types of geophysical data. Kinematics and tectonic flow predicted by DISS can be compared with the results of moment tensor summation of a few decades of seismicity located within the Seismogenic Areas of DISS in terms of average focal mechanisms (Fig. 1.5C) and P and T axes (Fig. 1.5D). Normal faulting in the inner Apennines is well represented. Conversely, and apart from the southern Tyrrhenian and eastern Alps, compression is less well documented, with the exception of the thrust faulting earthquakes in the outer northern Apennines and the strike-slip faulting earthquakes in the Apulia foreland. In addition, we have analyzed borehole breakout [*Montone et al.*, 2004] and GPS data [*Serpelloni et al.*, 2005, 2007], both of which improve the picture of the stress field in areas where focal mechanism data are rare. For instance, the characterization of the compressional stress field in most of the areas previously mentioned is strongly improved. If taken alone, GPS and borehole breakouts mainly help with defining the geometrical properties of the stress field and tell little, if not nothing at all, on the potential for large earthquakes. This is where the knowledge about active faults illuminates the picture.

All these analyses show that the kinematic view based on geophysical observations agrees very well with that obtained from the DISS seismogenic sources. Comparing fault data, such as those contained in DISS, with other geophysical data may look inappropriate at times because the different datasets are not strictly independent. However when they are all put together, one gets at least two immediate benefits. The first is the enhanced capability of exploring the information from geographically scattered point data (focal mechanisms, borehole breakouts, GPS measurements) over the spatial domain. The second is the longer time window that can be analyzed; few years to few decades for geophysical data compared to thousands of years for geologic data on active faults.

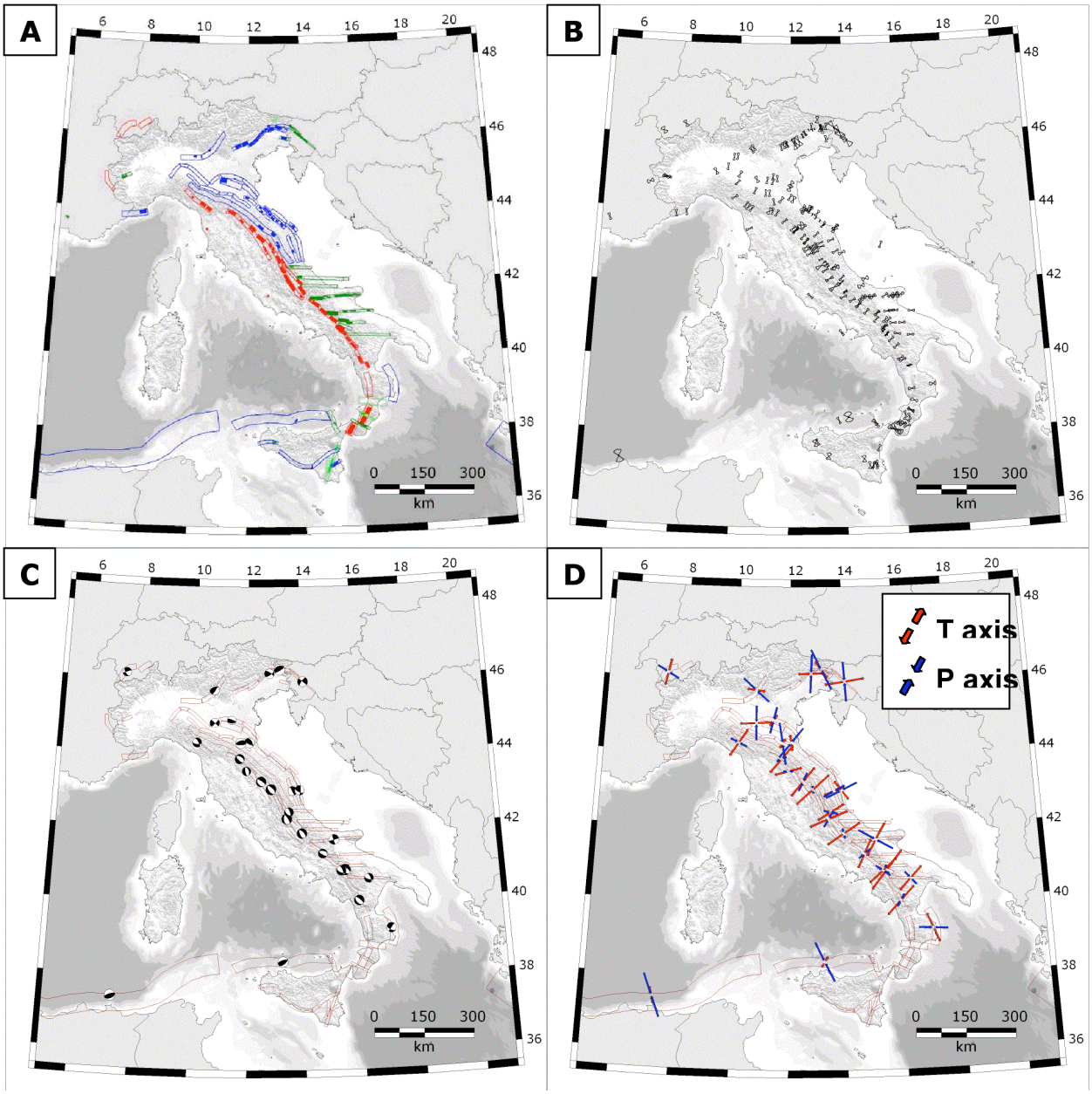

Figure 1.5 – (A) Individual Seismogenic Sources and Seismogenic Areas shown by color-coded faulting mechanisms. Blue: reverse or thrust; red: normal; dark green: right-lateral strike slip; light green: left-lateral strike slip. (B) Slip vectors with angular variability from Individual Seismogenic Sources and Seismogenic Areas projected on horizontal plane. (C) Average focal mechanisms and (D) P and T axes from earthquake moment tensor summation within Seismogenic Areas (elaboration by RU 1.2 using the EMMA database by *Gasperini and Vannucci* [2003] and *Vannucci and Gasperini* [2003]).

Seismic validation was carried out by assessing the database completeness. Completeness, in turn is given by balancing the seismic moment rate produced by the seismogenic sources with that produced by historical earthquakes. To do so we first subdivided the Italian territory into eight regions. Each region being dominated by a well characterized geodynamic process, containing the least possible number of faulting types, and a significant number of historical earthquakes. We then found the time window within which the earthquake Moment Rate Production MRP is stationary by recursively fitting a straight line to the curve of cumulative seismic moment over time and analyzing its statistic parameters. The slope of the best fitting straight line is the MRP. Figure 1.6 shows that in six regions (#1, #2, #3, #4, #5, #8) the MRP falls within the range of geological MRP predicted by the Seismogenic Areas and in only two regions (#6, #7) the earthquake MRP is higher than the geological MRP. This picture tells us

that in some regions we may have either failed to map all possible geological sources, or have underestimated the geological slip rates. However, at the scale of the entire country the completeness level of the database is well addressed. This is a very encouraging result that gives strength to all applications that use this dataset. It also confirms the good choice of introducing the category of Seismogenic Areas into DISS.

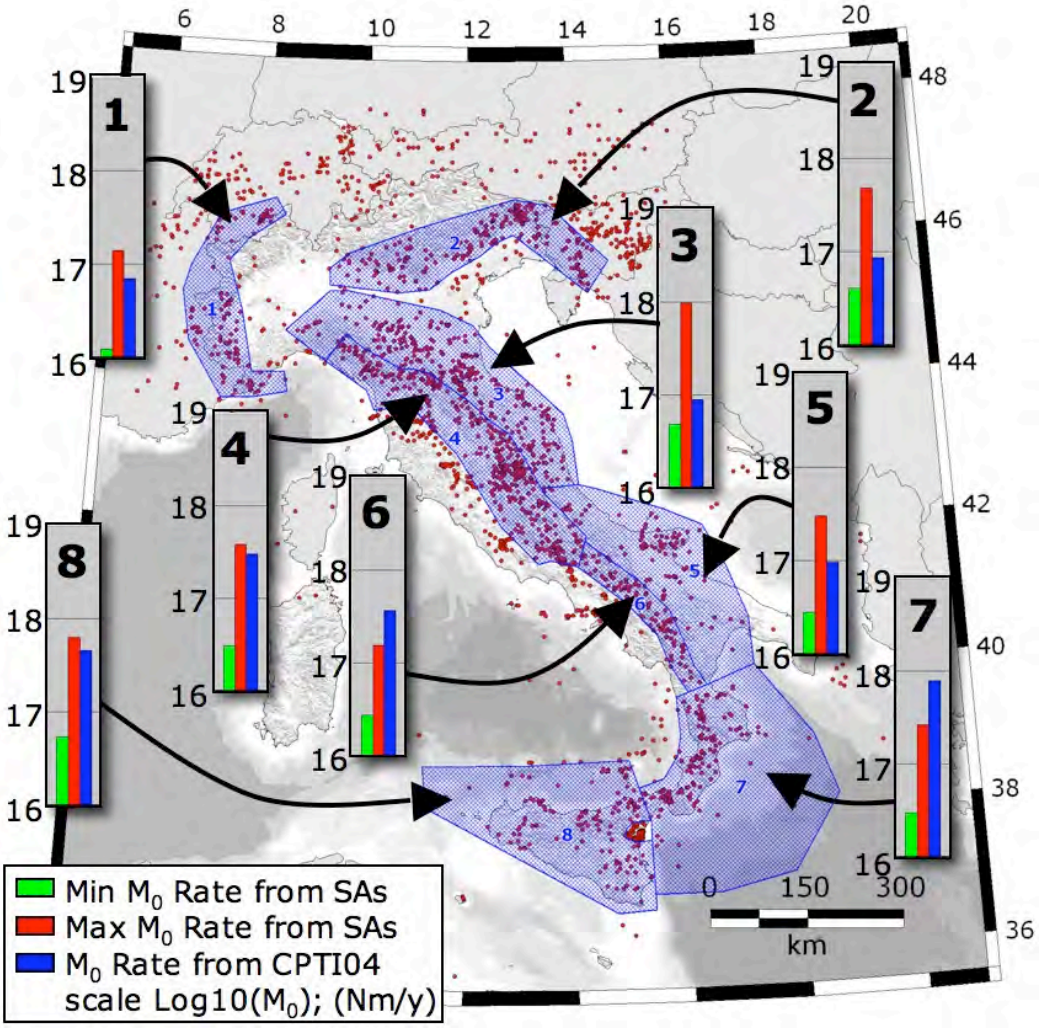

Figure 1.6 – Map showing the comparison between earthquake and geological moment rate productions in eight tectonically coherent regions.

Task 2

Defining the location and geometry of the main seismogenic sources in the Italian peninsula

Coordinator Fabrizio Galadini, INGV-MI

Introduction

Task 2 has produced the fundamental data needed to update and extend various layers of the reference database DISS. Figure 2.1 shows that the investigated areas are distributed throughout the entire seismically active Italian territory. The quality of the collected data, the importance of the results obtained in terms of seismogenic implications and the overall consistency of the final reports with the work proposed by each RU indicate that the all scientists involved in Task 2 have collected data that are directly suitable for the seismogenic characterization of the territory, thus fulfilling one of the fundamental guidelines of S2.

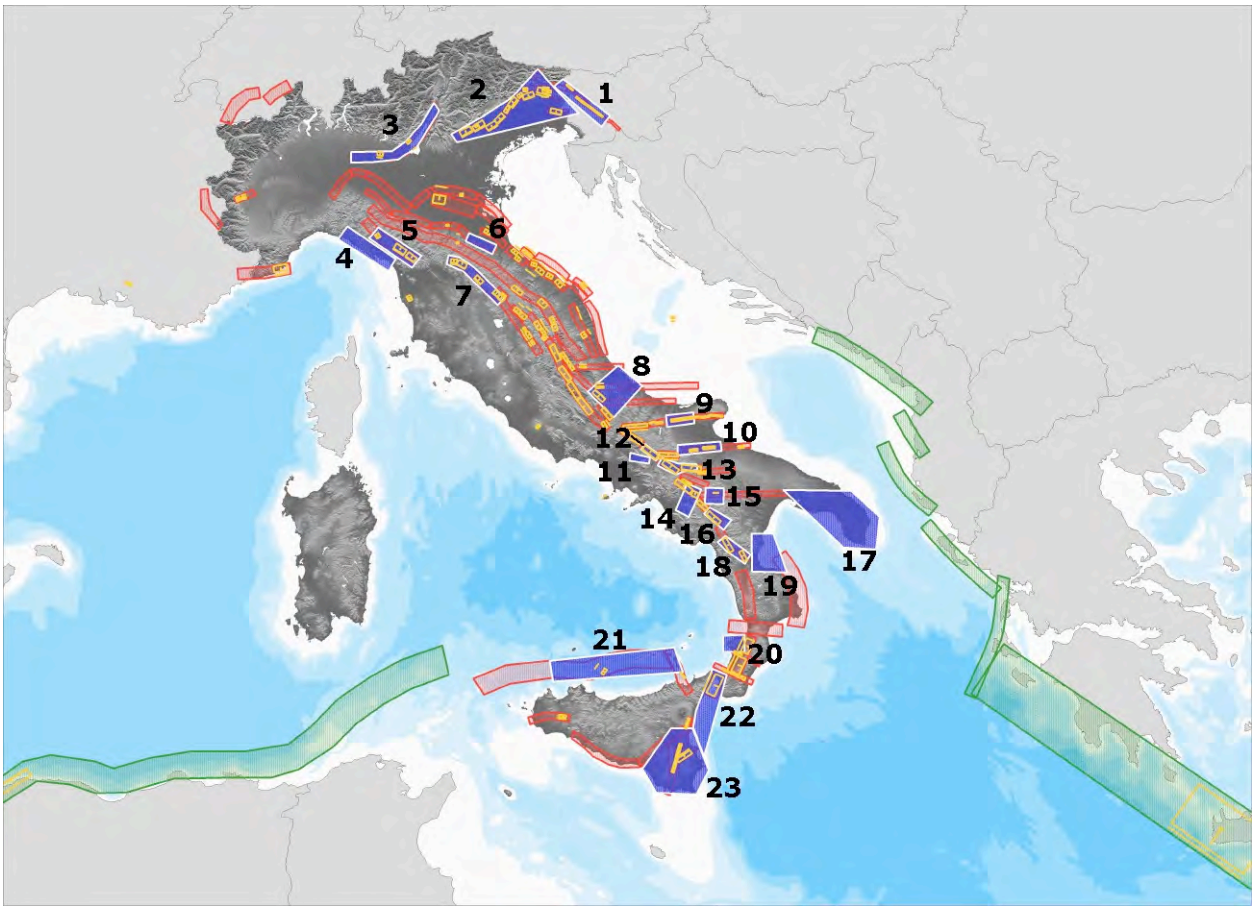

Figure. 2.1 - Summary of areas investigated in the project (in blue), superimposed on Individual Sources (in yellow) and Seismogenic Areas (in red and green) from DISS v3.0.3. The Seismogenic Areas outlined in green were investigated by RU 1.1 largely based on literature data. They were used as realistic - in some case even rather accurate - source zones for the calculation of tsunami scenarios by RU 2.19b.

The next sections summarize the most significant investigations and the open problems derived from the research performed in Task 2. Given the large number of RUs in Task 2 and the amount of data and materials they produced, this account will only briefly touch upon each individual finding, but will rather focus on the most outstanding results (shown in *italic*). the reader is encouraged to refer to the reports of individual RUs for a complete account of research accomplishments. Notice that due to the timing of the project these findings will be

implemented in a forthcoming version of the DISS database (v3.0.4, to be released Sep. 2007).

The following scheme outlines the main findings for a more rapid and effective appreciation of the Task results:

1) all damaging historical earthquakes of NE Italy have been associated with seismogenic sources; some silent sources (and related seismic gap areas) have been defined; as a whole, 15 sources responsible for strong earthquakes have been defined in NE Italy;
2) the major earthquakes of the Mugello and Sansepolcro basins have been related to NE-dipping major seismogenic faults, whose surficial expression is represented by faults bounding the basins to the SW; the intervening Casentino basin has been identified as underlain by a major fault and, due to its quiescence, as a seismic gap;

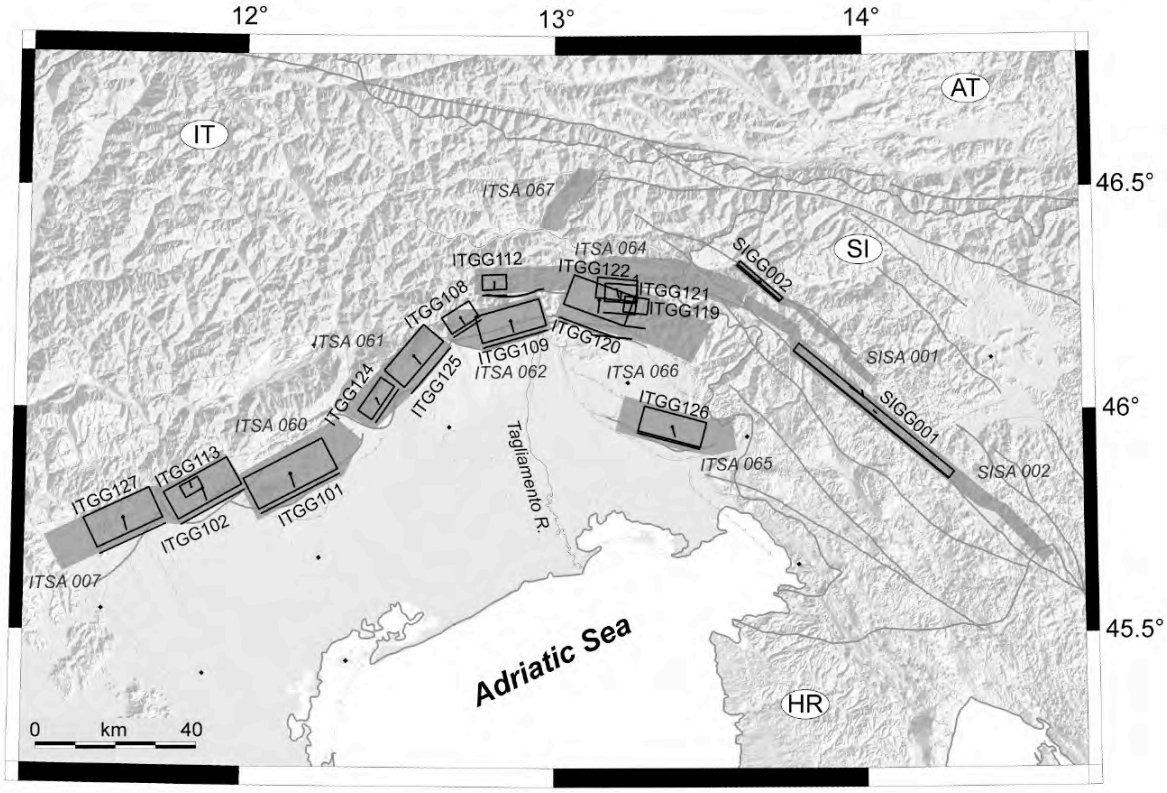

Figure 2.2 - Summary of Individual Seismogenic Sources and Seismogenic Areas identified in northeastern Italy during the project by joint work of RU 2.4 (Burrato) and RU 2.8 (Galadini). The scheme is based on a re-elaboration of geological and tectonic data and fits satisfactorily the most recent seismological and GPS data (see Figure 1.5 and RU 3.2b Braitenberg).

3) the 1881 and 1933 earthquakes in eastern Abruzzi may result from the activation of thrust-fault (Casoli thrust), while the 1706 earthquake may have been generated by a large normal fault (Maiella-Porrara) comparable to other intermontane seismogenic sources;
4) the large 1857 earthquake in the southern Apennines may result from the nearly simultaneous activation of two adjacent faults underlying the Pergola-Melandro and Val d'Agri basins;
5) new hypotheses have been put forward concerning seismogenic sources of Apulia. A NW-SE trending normal fault has been discovered in the Cerignola-Foggia area (source region of the 1731 earthquake). An E-W fault of unknown kinematics may represent the seismogenic source of the 1361 Ascoli Satriano earthquake;
6) the E-W trending southern Tyrrhenian active belt has been structurally characterized using exploration data: it is made of NE-SW to WNW-ESE thrust and reverse faults that, given their state of fragmentation, should not generate earthquakes larger than M 7;

7) the growing folds of the northern Catania Plain probably represent the surficial expressions of a major seismogenic source that may have ruptured during the January 1693 seismic crisis in southeastern Sicily;
8) original offshore multi-channel seismic surveys south of the Messina Straits have revealed no evidence for the Taormina fault hypothesized during two decades of geological literaure. This finding has profound seismological and geodynamic implications.

Main results and open problems

Eastern Southern Alps

The geometric and kinematic characteristics of the seismogenic sources of northeastern Italy (zones 1 and 2 in Figure 2.1) defined within the framework of the project "Scenarios of seismic damages in Friuli and Veneto" (part of the GNDT activities 2000-2002, ended in 2004) have been the object of further investigations. This region hosts the most significant seismogenic sources of all northern Italy and has been the locus of the catastrophic earthquakes that struck northern Friuli in 1976. The merger of geological and seismological information has produced a dataset consisting in *10 seismogenic sources potentially responsible for events with M≥6.0, located at the northern border of the Venetian-Friulian plain and 5 minor sources responsible for earthquakes with M between 5 and 6, located both at the margin of the plain and in the inner sector of the Alpine edifice*. In addition to the Individual Seismogenic Sources, also 10 Seismogenic Areas have been defined.

Northern Apennines

A reassessment of subsurface data allowed the definition of the whole structural framework of the Garfagnana and Lunigiana basins (zone 5) to be substantially improved (**RU 2.15**). The basins are bordered by a NW-SE striking, NE-dipping low-angle master fault and by a number of antithetic high-angle faults dipping towards the SW. A NE-SW to ENE-WSW transfer fault at the northern margin of the Alpi Apuane accommodates the sinistral offset of the faults.

Similarly to the Lunigiana and Garfagnana basins, also the Mugello, Casentino and Sansepolcro basins (zone 7) have formed through the activity of major NW-SE trending faults bordering the depressions along their SW flank and of secondary parallel faults along their NE flank. The surface and subsurface data available for the Casentino and Sansepolcro basins and the surface data from the Mugello basin allowed **RU 2.3** to draw structural geological sections showing the main role of the NE-dipping faults in the recent evolution of the depressions. The new evidence is especially important for the Casentino basin, a historically quiescent basin were the existence of a major fault and of a significant earthquake potential is here documented for the first time (Figure 2.3).

All the evidence described above supports the existence of a major, NE-dipping low-angle seismogenic fault from the northwestern tip of Lunigiana to central Umbria, referred to as Etrurian Fault System in the literature. Along the northern portion of this major lineament the SW-dipping faults root into the master NE-dipping fault at shallow depth (3-4 km). We infer that along this stretch of the Apennines seismogenic backbone *the major seismicity is due to the activation of the low-angle NE-dipping faults* (Figure 2.3), whereas more to the south (Umbria) both shoulders of the system seem to be able to generate significant earthquakes (e.g. the 1997 Umbria-Marche earthquakes, that were generated by a set of SW-dipping faults rupturing down to a depth of 7-8 km). This scheme, that had already been put forward in earlier versions of DISS, can now be confirmed on a sounder geological basis.

RU 2.18 relocated 953 instrumental earthquakes and obtained Vp/Vs tomographic sections in the Garfagnana area (zones 4 and 5). This work also confirmed that the recent seismicity occurs along a NW-SE fault plane dipping 40-50° towards the NE. The kinematics of these earthquakes is generally transtensional. The elaborations also indicate the presence of a high-angle discontinuity corresponding to the SW-dipping fault system.

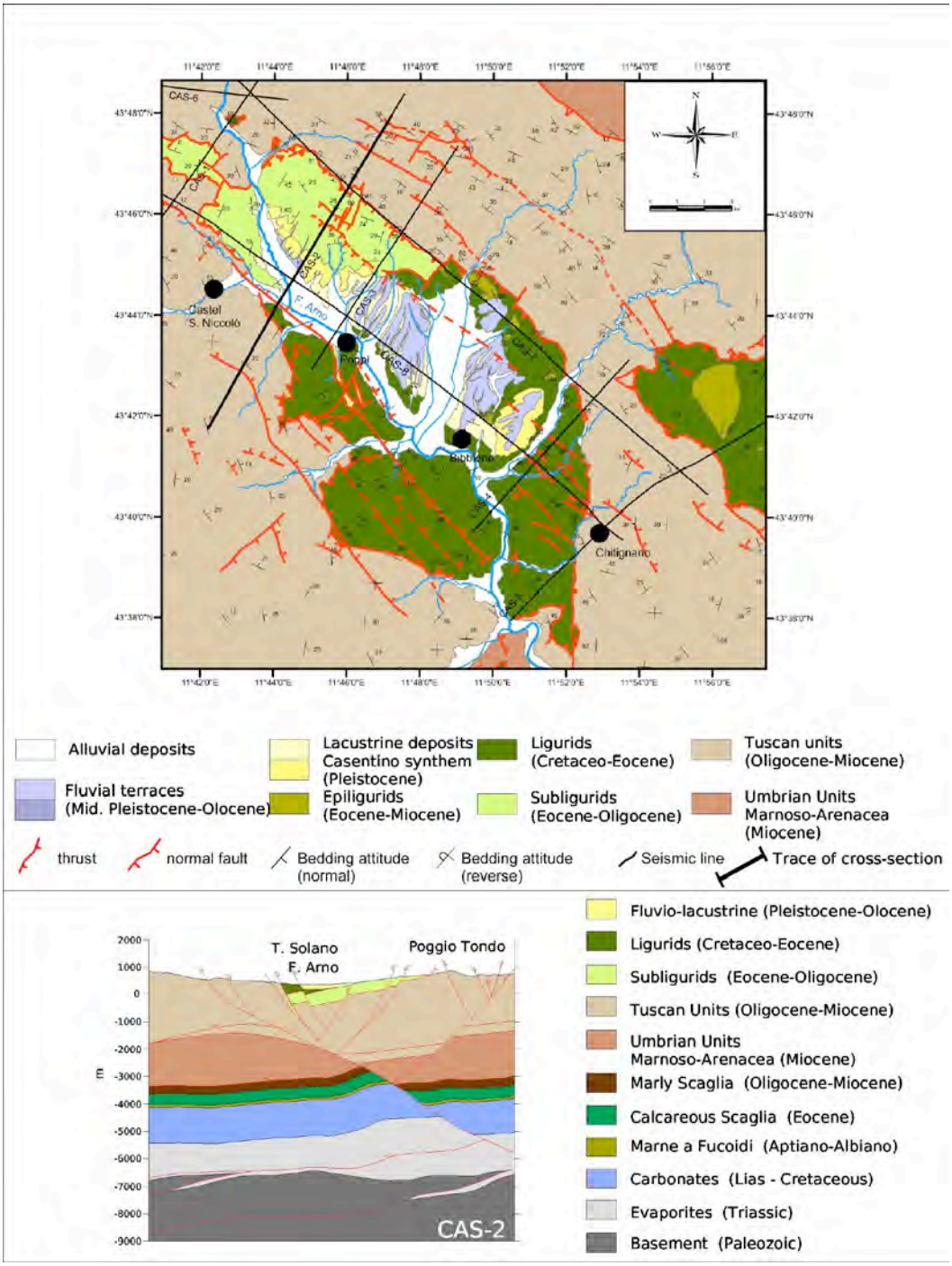

Figure 2.3 - Geological map and cross section (bottom) of the Casentino basin elaborated by RU 2.3. The section results from a new interpretation of a commercial seismic profile. The large fault dipping to the NE (to the right in the section) that underlies the Casentino basin was only hypotesized prior to this work, is coherent with the structural setting of this stretch of the Apennines and is not associated with any significant historical earthquake. The new work hence confirms the existence of a seismic gap in the Casentino area hypotesized in previous releases of DISS.

Central Apennines

Two RUs (**RU 2.8 and RU 2.14**) investigated the eastern margin of the Abruzzi Apennines, an area characterized by a complicated and almost unknown active tectonics framework, where numerous destructive earthquakes (2nd century AD, 1456, 1706, 1881, 1933) have occurred (zone 8). Investigations in the Maiella massif-Mt. Morrone area have revealed a previously unknown Late Pleistocene-Holocene NW-SE to WNW-ESE trending normal fault system having

a total length in excess of 20 km. The displacement of Late Quaternary slope deposits has been observed at several locations along bedrock scarps detected between Campo di Giove, Palena and Mt. Porrara. *Scientists of the mentioned RUs consider this fault system as the surface expression of the seismogenic source responsible for the 1706 earthquake*.

Historical investigations of the 1881 earthquake which struck Orsogna, Lanciano and Guardiagrele allowed a better definition of its damage pattern, with an increase of the information in the order of 50% (**RU 2.8**). New evidence on the structural framework of the eastern Abruzzi domain *has also suggested the association of the 1881 earthquake to the Casoli thrust*. Based on this framework, the damage distribution associated with *the 1933 earthquake appears consistent with the activation of a lateral ramp of the Casoli thrust* and of the whole "Struttura Costiera" thrust. If confirmed by investigations that are still ongoing, these conclusions support the seismogenic potential of the Abruzzi external thrusts, that were previously considered inactive or too shallow to generate significant earthquakes.

Southern Apennines and Apulia

Investigations of the southern Apennines (**RU 2.4**) have produced new hypotheses on the sources of the 1732 and 1857 earthquakes (zones 11, 12, 13, 14, 15, 16). As for the former, **RU 2.4** has refuted the tectonic origin of a scarp and related triangular facets along the right flank of the Ufita Valley. Based on the 1732 damage pattern, the same RU *has proposed an E-W seismogenic source close to the similarly oriented source recently hypothesized for the 1930 earthquake*. Its surface expression is faint, as usual for E-W sources also because they are generally deeper than standard large NW-SE normal faults. By contrast, based on an inversion of intensity data for the 1732 using the KF kinematic function **RU 2.17** has proposed for this earthquake a 1980-type NW-SE trending mechanism. The same RU obtained a similar source trend also for the 1694 earthquake. These solutions are different from those obtained for the 1962 (NE-SW) and 1930 (E-W) earthquakes. The latter result confirms previous hypotheses on the geometry of the 1930 seismogenic source.

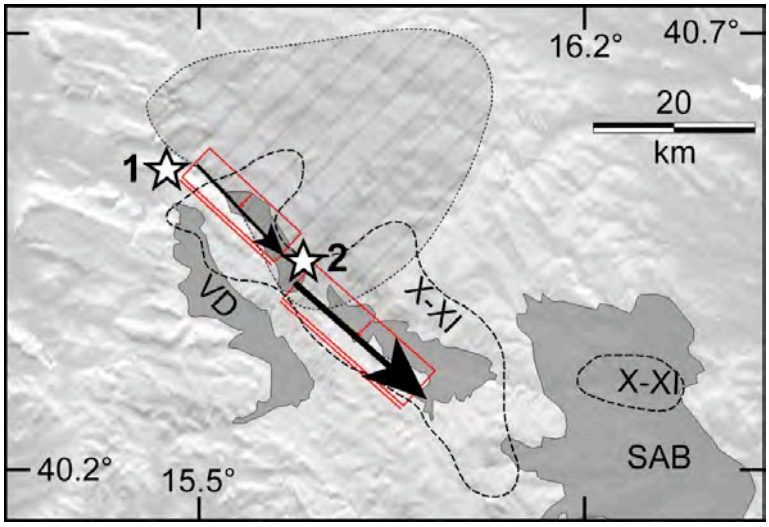

Figure 2.4 - Source complexity of the 1857 earthquake according to an hypothesis put forward by RU 2.4 based on a joint reinterpretation of tectonic and historical data and on similarity with instrumental earthquakes. The 1857 earthquake would have nucleated at the NW end of the Melandro-Pergola basin and then propagated SE-ward towards the Agri Valley proper.

The precise identification of the 1857 source in the Val d'Agri area (zone 16) has benefited of paleoseismological trenches along the Maddalena Mts., of the analysis of disrupted speleothems, of geomorphological investigations along the Mt. Aquila fault (**RU 2.4**) and of electric resistivity tomography (**RU 2.16**). Based on the historical information, the investigators believe that the earthquake as actually made of two independent shocks. This should be the reason for a magnitude (M_w 6.9 in CPTI Working Group, 2004) larger than that expected from the activation of the Val d'Agri fault proper. The new hypothesis holds that *the 1857 earthquake*

comprises two independent shocks two minutes apart: the first shock was caused by the activation of the Pergola-Melandro seismogenic source, while the second shock originated by motion of the Val d'Agri seismogenic source (Figure 2.4).

Other investigations in the southern Apennines returned interesting results, but due to the inherent limitations of field evidence must be considered less conclusive. Different hypotheses are still available on the source of the 1688 earthquake (zone 11). **RU 2.20** interpreted traces of recent activity in the Calore river valley (tilting of terraces) as the result of the activity of the Calore fault system, considered as the surficial expression of the causative source of the 1688 earthquake. In contrast, the analysis of minor seismicity for the interval 1990-1997 in the area of the Tammaro valley allowed **RU 2.4** to define a 40-km-long lineament that may be considered as the surface trace of a major seismogenic source. Geomorphologic investigations only found faint traces of this lineament for a length of about 24 km. As a whole, this semi-blind fault is considered as the possible source of the 1688 earthquake.

As for the structural framework related to the present tectonic regime, **RU 2.10** has investigated a WNW-ESE trending system of normal faults, dipping towards NNE between Mt. Cervati and the Alburni Mts. (zones 14 and 16). All surface evidence referes to fault planes detaching on a single low-angle fault at about 10-15 km of depth. The mechanism envisioned by **RU 2.10** is somewhat similar to that characteristic of the Etrurian Fault System mentioned earlier, and *supports the commonly accepted view that major normal faulting along this stretch of the Apennines is dominated by NE-dipping faults, as seen in the 1980 Irpinia earthquake*. The depth of the system increases towards the NNE, i.e. where the Irpinia and Mt. Paratiello faults are located. The Vallo di Diano depression is considered as the result of the coalescence of smaller Quaternary depressions formed along NW-SE and WNW-ESE trending faults dipping towards the SW and SSW representing the antithetic splays of the main Mt. Cervati fault.

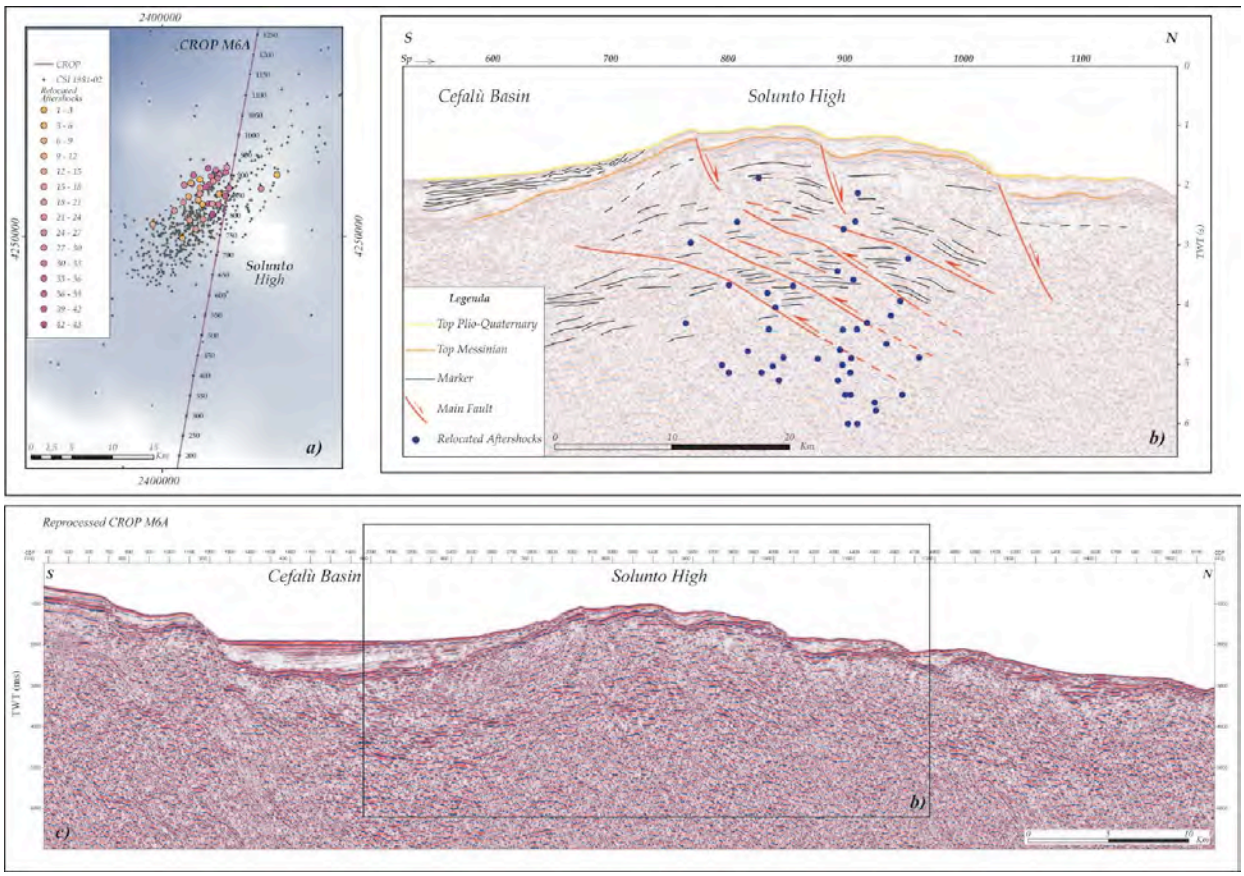

Figure 2.5 - Reprocessed CROP M6A seismic section and interpretation of the Solunto high off the northern coast of Sicily by RU 2.6. The relocated aftershocks of the September 2002 seismic sequence can be associated with the reactivation of inherited thrust structures, which were likely generated during the build-up of the northern Sicilian Maghrebian Chain. The section provides living evidence for the activity of compressional structures in the very active seismogenic belt of the southern Tyrrhenian.

The investigation of the Mt. Pollino-Castrovillari area by **RU 2.10** (zone 18) allowed the activity along the western portion of the Mt. Pollino fault to be defined in detail. The same investigation conclusively confirmed that its eastern portion is inactive, in contrast with previous hypotheses. The two faults (Pollino and Castrovillari) must hence be considered as structurally linked. During large magnitude earthquakes, the seismogenic Castrovillari fault may activate the favorably oriented western portion of the Pollino fault while locking its eastern portion.

As for the Apulia region (zones 9 and 10), **RU 2.15** supplied evidence for a NW-SE trending normal fault in the Cerignola-Foggia area, dipping towards the SW, with evidence of recent activation. The fault falls in the source region of the 1731 Foggia earthquake, currently assumed to have been generated by a deep E-W strike-slip fault. Further investigations will be needed to understand whether the extensional fault is a shallow, secondary structure associated with deeper strike-slip faulting, as commonly observed in other parts of Apulia, or if these is an alternative explanation for this evidence. The same RU has hypothesized the *association of the 1361 Ascoli Satriano earthquake with a E-W trending, N-dipping normal fault detected in the subsurface of the Castelluccio dei Sauri-Stornarella area*. This blind fault is seen as responsible for the gentle flexural deformation of the whole Quaternary sequence filling the foredeep. Finally, **RU 11** supplied evidence for gentle NW-trending compression in the Salento (zone 17), possibly interpreted as the far-field evidence of the shortening of the Albanides thrust system.

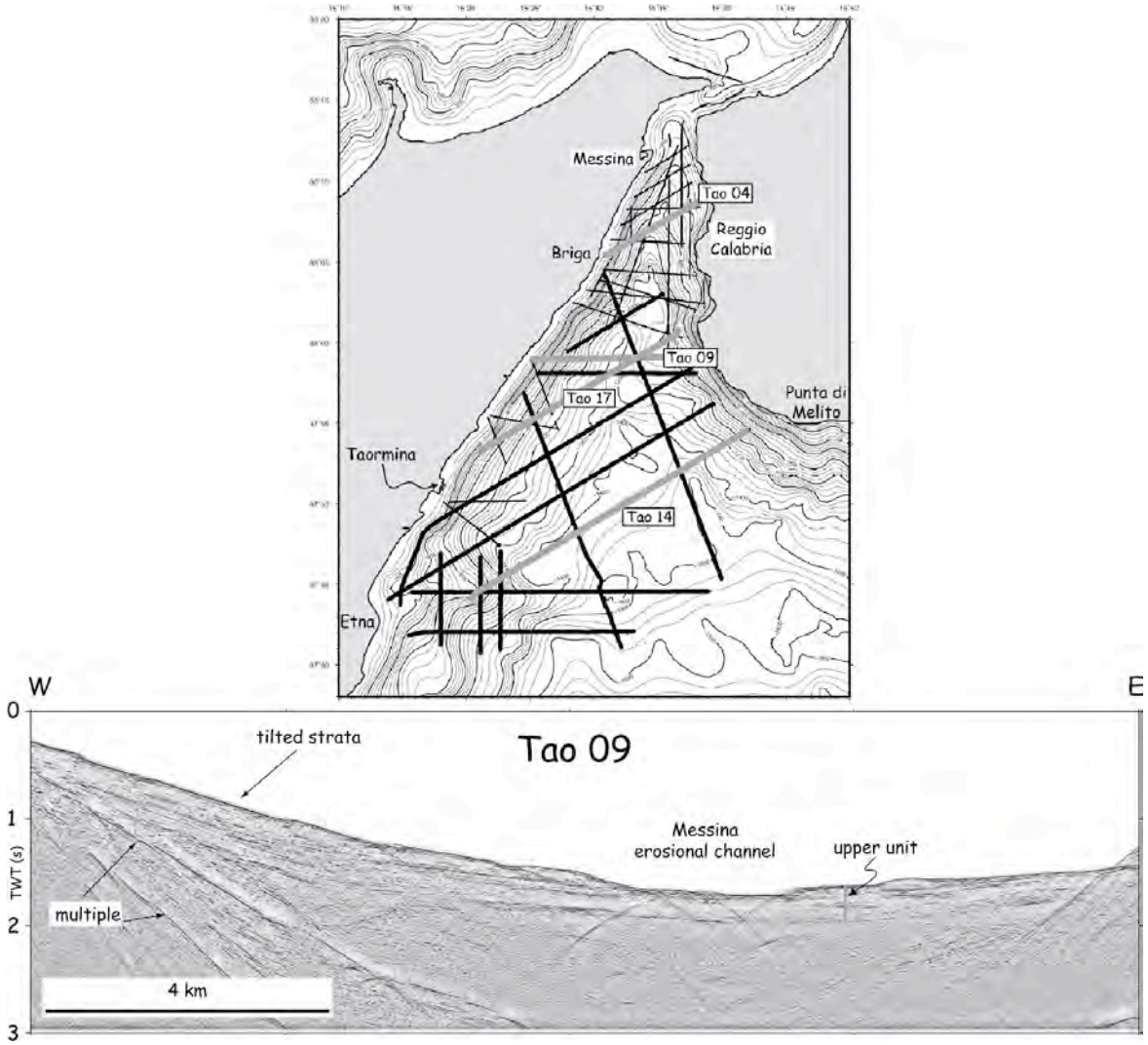

Figure 2.6 - Seismic profile TAO09 shot by RU 2.1a/RU 2.1b across the presumed trace of the Taormina fault (see above for location). Notice the thick package of almost parallel strata dipping to the E at 0.4-0.5 s (TWT), suggesting that the Taormina fault does not exist as an active tectonic feature.

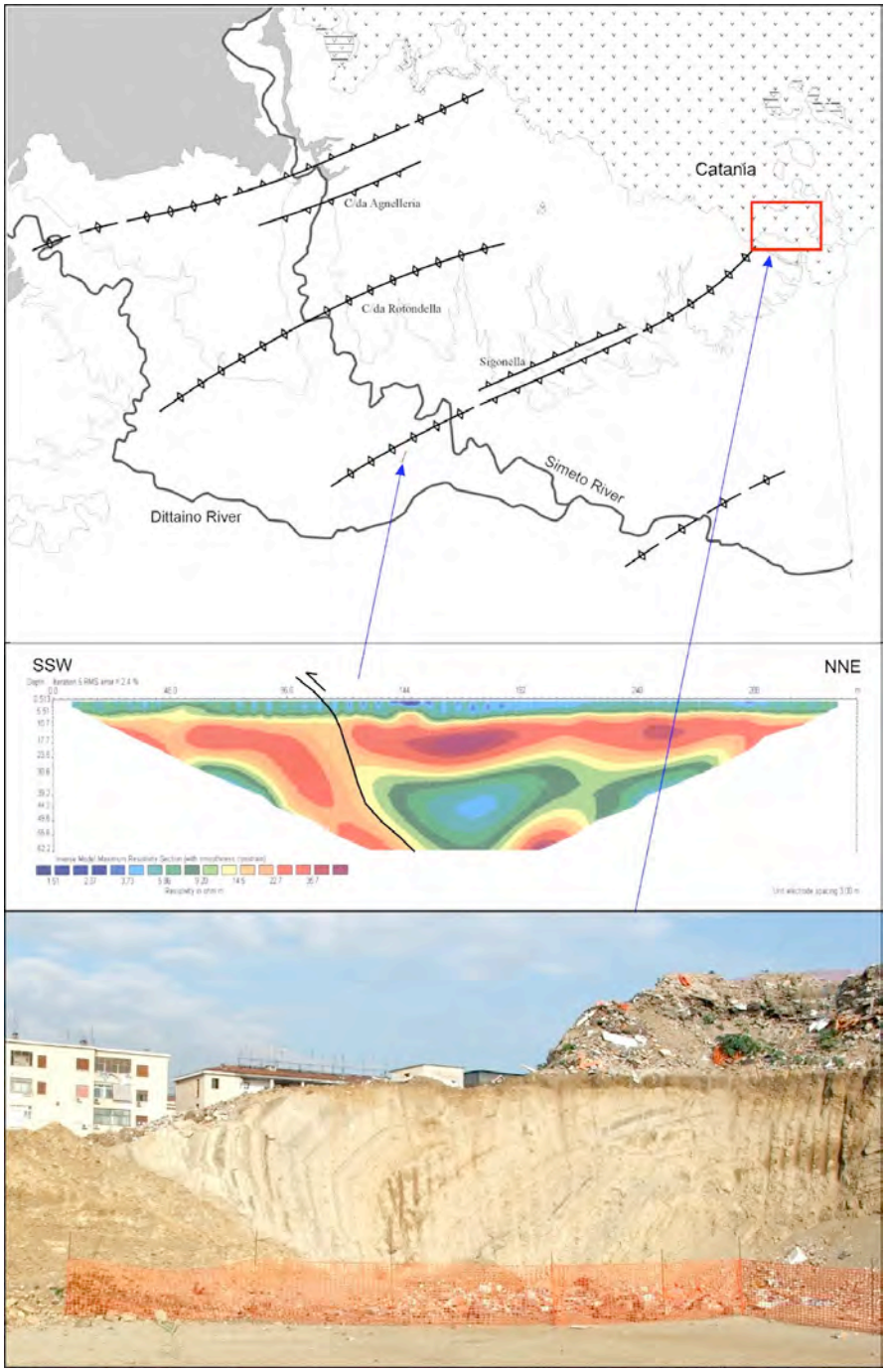

Figure 2.7 - Tectonic sketch-map of the fold system underlying the Catania Plain (top panel), inverse model of maximum resistivity measured at the forelimb of the Sigonella fold (middle) and a thrust-ramp exhumed at a construction site in downtown Catania (bottom), all by RU 2.5. The location and wavelength of the observed compressional features are compatible with the generation of one of the subevents of the January 1693 earthquake sequence in eastern Sicily.

Southern Tyrrhenian area and eastern Sicily

Using data available from existing seismic surveys (single-channel "Sparker" profiles, public and INOGS multi-channel profiles, CROP reflection profiles), **RU 2.6** has defined the tectonic history of the E-W seismically active belt located off the northern coast of Sicily (Figure 2.5; zone 21). The widespread Late Pliocene-Pleistocene tectonic reactivation is indicated by growth strata, titlted onlaps and the anomalous thickness of the Plio-Pleistocene units associated with

NE-SW trending structural highs. Tectonic reactivations have also been observed along WNW-ESE fault systems and along inherited E-W faults that were positively inverted. As a whole, tectonic uplift and folding are consistent with a roughly NNW-SSE oriented compression. The September 2002 Palermo earthquake occurred close to the Solunto high area and may have reactivated inherited thrust structures related to the formation of the Sicilian-Maghrebian chain (Figure 2.5). Very recent faulting along NE-SW or E-W structures has been observed, particularly in the eastern sector of the investigated area (e.g. Cefalù basin), both on NE-SW and E-W trending structures.

The already published instrumental seismicity and that processed by **RU 2.13** seem consistent with these structural inferences. According to this RU, the M>1.5 earthquakes which characterized the entire belt in the past 10 years show two main epicentral trends oriented NW-SE and NE-SW, respectively. Reverse faulting is common on E- to NE- striking planes.

Polar plots of the P- and T- axes indicate a NNW-SSE oriented compressive stress. The inherited Late Miocene structural framework is evidently segmented along the entire, about 200 km-long structural domain. *The length of the segments appears consistent with M ≤ 7. The energy associated with seismogenic sources composing this E-W belt is, therefore, lower than that previously proposed, but significant earthquakes may be rather frequent and hence pose a significant hazard to the coastal population* (**RU 2.6** and **RU 2.13**).

Multi-channel seismic surveys performed by **RU 2.1a/RU 2.1b** in the area where the presumed Taormina fault should be located (zone 22) have imaged a tilted sequence of marine layers (Figure 2.6). Traces of the fault have not been identified and the tilting may simply result from known regional uplift. On this basis, *the lack of seismicity in this area (see for example **RU 2.13**), previously interpreted by some workers as evidence of a seismic gap, should instead be related to the lack of a seismogenic source*. The same seismic surveys (**RU 2.1**) have uncovered an interesting structural feature at the SW tip of the Calabria peninsula, represented by a 25 km-long fault scarp trending NW-SE on the sea floor. Future investigations will cast further light on the issue and clarify the tectonic role of this fault.

A system of ENE-WSW folds at the front of the Maghrebian thrust belt between Mt. Etna and Catania (zone 23) shows evidence of Late Quaternary activity (**RU 2.5**: Figure 2.7). The folds formed in alluvial deposits dated at 40 ka in the area of the Simeto river. A thrust ramp is exposed in an outcrop along the Sigonella anticline. The fault puts sands and conglomerates older than 200 ka in contact with conglomerates of about 80 ka. Deformation due to the activity of the Sigonella anticline has been responsible for the 4-m-growth of the Holocene alluvial plain and for a clear signature on the drainage pattern of the entire region south of Mt. Etna. *The identification of this system of thrust-related growing folds as the surface expression of crustal-scale shortening is fundamental for a better understanding of seismogenic processes in the Catania area, particularly in relation with the catastrophic 1693 and 1818 earthquakes.*

Tsunami

Numerous investigations have been devoted to tsunami effects. The importance of these investigations is twofold: i) they allow the assessment of tsunami hazard, as discussed in the dedicated section below, and ii) they shed light on the cause of the tsunami on the basis of the distribution of their effects. Within this perspective, the activities of **RU 2.2a RU 2.19a** *are important for the definition of the seismogenic source responsible for the 1693 tsunami*. **RU 2.2a**, for example, used run-up amplitudes and distribution along the shore of the 1693 tsunami in an application of the *Okal and Synolakis*' [2004] method for discriminating between a truly tectonic and a submarine landslide-induced tsunami (zone 23). Their conclusion is that *the 1693 tsunami was generated by a genuine tectonic source, i.e. by actual displacement of the sea floor*.

RU 2.19a and **RU 2.19b** did a great deal of work on the estimation of tsunami hazard for the Italian coasts. Their analyses evaluated the effects of the activation of all seismogenic sources that may generate significant tsunami waves along the Italian coasts. They placed special emphasis on distant but large sources such as those located off the coasts of southern Dalmatia and Albania, or pertaining to the Cephalonia transform zone and the Western Hellenic Arc (zone 21 and Seismogenic Areas shown in green in Figure 2.1). **RU 2.19b** considered the tsunamigenic sources as floating within DISS v3.0.3 source zones (Figure 2.8). A maximum

credible earthquake has been attributed to each zone, based on the available knowledge of the seismogenic behavior. *The results indicate that expected wave heights on the Italian coasts do not exceed 0.6-0.7 m for most potential tsunamigenic sources*. However, a substantially larger impact may be expected from the activation of the Hellenic Arc source zone (responsible for the 365 AD earthquake and tsunami), with *wave heights along the coasts of southern Italy and Sicily exceeding 4 m*. As for the sources close to the Italian coasts, **RU 2.19a** modelled the effects of a tsunami generated by the Hyblean-Malta escarpment (considered as the source of the 1693 tsunami by this RU).

Apart from the different evaluations obtained by modelling the coseismic displacement of the sea floor, a quite important part of the research has been represented by the identification of stratigraphic-sedimentological evidence of tsunami at different sites of the eastern Sicily coasts (**RU 2.2b**). Evidence of tsunami at Capo Peloro has been attributed to the 17 AD and 1783 earthquakes (zone 22). Older traces of tsunamis have been found at other sites north of Catania. South of Catania (zone 23), tsunami deposits have been attributed to the 1693 and 1169 earthquakes. Further evidence of paleoinundations has been related to events that occurred in 570-122 BC (Priolo), 1000-800 BC (Augusta), 2100-1635 (Priolo). These data alone give an idea about the large frequency of tsunami waves in this region.

The fact that tsunami waves may have a strong impact on the coasts of southern Italy is testified by the numerous boulder fields found along the southern Apulia coast (**RU 2.11**; zone 17). The most interesting case is represented by the boulders distributed between Capo Santa Maria di Leuca and Torre San Leonardo (Ostuni, Brindisi) probably related to the 1743 earthquake. According to **RU 2.11**, this earthquake was caused by a source located in the Otranto channel.

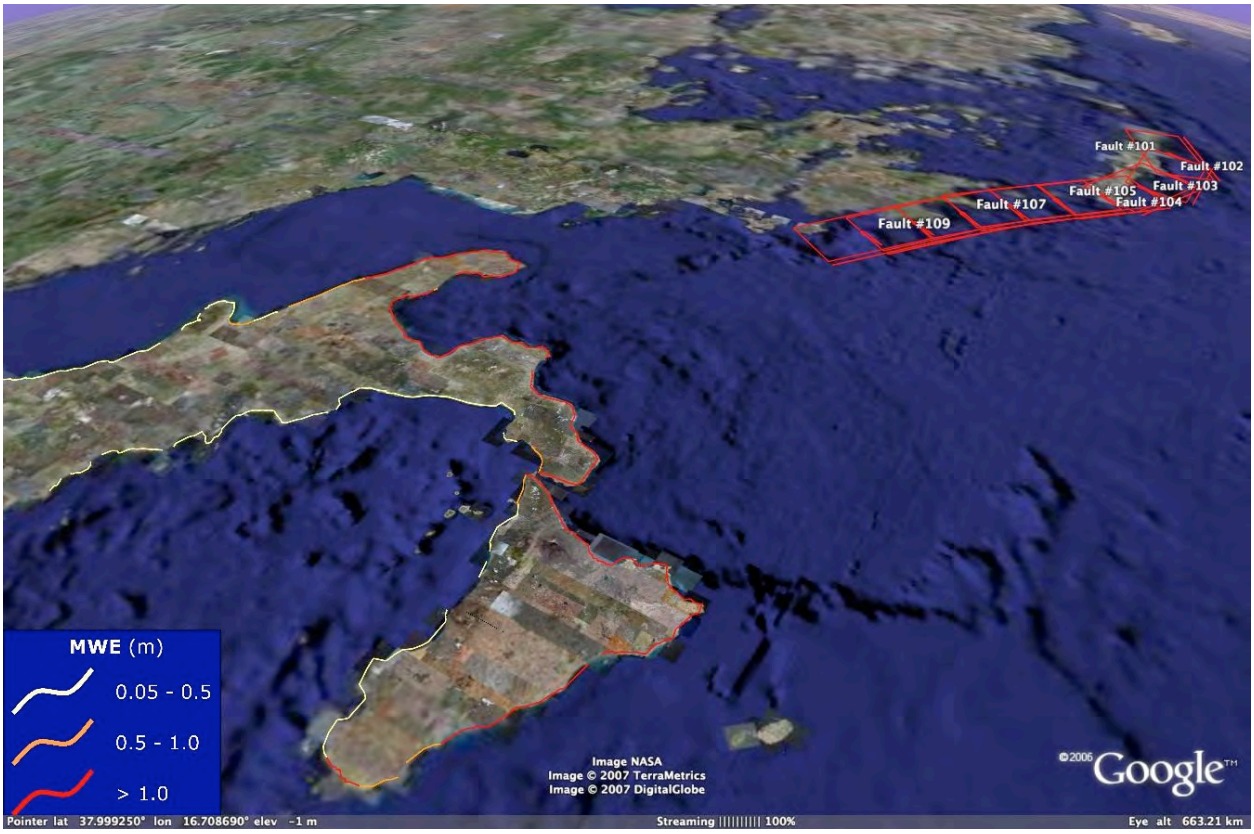

Figure 2.8 - Sample image of the Maximum Water Elevation (MWE) on the coasts of southern Italy induced by tsunami originating along the Hellenic Arc. The predicted MWE values represent the average of the maximum values obtained by letting the tsunamigenic source float along one of the Seismogenic Areas (see Task 1) and repeating the calculations for each new source position. The elaboration shows that wave heights up to 5 m are expected along the Ionian and southern Adriatic coasts. Conversely, the Tyrrhenian coasts of southern Italy are efficiently sheltered with respect to tsunami sources occurring in the eastern Mediterranean. For further information refer to the reports of RU 2.19b and RU 1.1 and to Deliverable D 1.4. (http://diss.rm.ingv.it/medtsunami/S2_D1.4.html).

Task 3

Geophysical characterization of the main seismogenic structures

Coordinator Alessandro Caporali, University of Padova

Introduction

With its exceptional accuracy in measuring relative positions over large distances, space geodesy has a profound impact on the definition of the surface strain of any tectonic province. However the spatial distribution of the measuring stations, and their uneven period of activity make the velocity estimates rather patchy and variable in accuracy. Although geodetically derived strain rates have been shown in several publications to define homogeneous areas of deformation in close agreement with results based on geophysical indicators of stress, the application of geodetic data to seismic hazard problems requires a thoughtful review of the data and of the data processing techniques. If the forces and the boundary conditions responsible for block interactions are, at least in part, responsible for the observed surface deformation, then one should be able to predict the velocities by means of a geodynamic model which blends the observational data, whether geodetic or geophysical or structural, into a unique deterministic scheme. A finite element model fitting the observational data may not be the answer to open questions in seismic hazard in Italy, as pointed out in the Year 1 review of Task 3. However we believe that a structural model is the only way to link together, and merge into a unique synthesis, observations of different kinds, such as fault geometry, geological and geodetic slip and strain rates, orientation of the PT axes, thermal, rheological and frictional properties of crustal rocks, Moho depth and heat flow, and kinematics at plate scale.

The main goals of Task 3 included:

1) collection and validation of geodetic data;
2) development of the Finite Element Model;
3) model tuning and final estimates of slip and strain rates along active fault trends.

The first year has been devoted to activities under a) and b). The second year focused on activity c). **RU 3.1** was primarily responsible for the model development. **RU 3.2** , **RU 3.3** and **RU 3.4** were responsible for the measurements and validation of previous data. Enrico Sepelloni of **RU 3.1** made available valuable campaign GPS data in areas of central and southern Italy, which would otherwise have been poorly covered by the network of permanent GPS stations. **RU 3.1** and **RU 3.2** closely collaborated on activity c) during the second year of the project.

The remainder of this section is devoted to an overview of the results achieved by activities under a), b) and c).

Collection and validation of geodetic data

Which data should be used, and how should they be processed to estimate the most reliable velocities to be used as constraints for the numerical model? The best way to proceed, in our opinion, is first to create a backbone network of top quality GPS stations. Then densify the backbone using campaign data, levelling/tiltmeter data, and GPS stations of lower quality, but still meeting high standards.

GPS data exist in two formats. One is the RINEX format, which contains raw data (phases and pseudoranges) from each station. The other is the SINEX format. This is the result of a data processing session, in which data from several stations are analyzed, the station

coordinates and their covariance being the result of this analysis. Clearly the SINEX data depend on the used software and processing scheme, including the applied constraints. However, processing standards have been developed within the activities of the IGS, which are accepted by the majority of the scientific community and implemented in their analysis by the most qualified Analysis Centers. Such standards include the use of final IGS orbits and clocks, antenna calibration, rigorous handling of ionospheric and tropospheric delays, ambiguity fixing and use of minimal constraints. It follows that SINEX files can conveniently replace the raw RINEX files: not only is the computational load considerably reduced, but there is also an increased confidence in such metadata because they have been validated by independent parties. For example, the SINEX files of the weekly adjustment of the European Permanent Network result from a combination of up to 16 SINEX files computed by 16 Local Analysis Centers and covering overlapping subnetworks, so that each station of the network is processed by a minimum of three Analysis Centers.

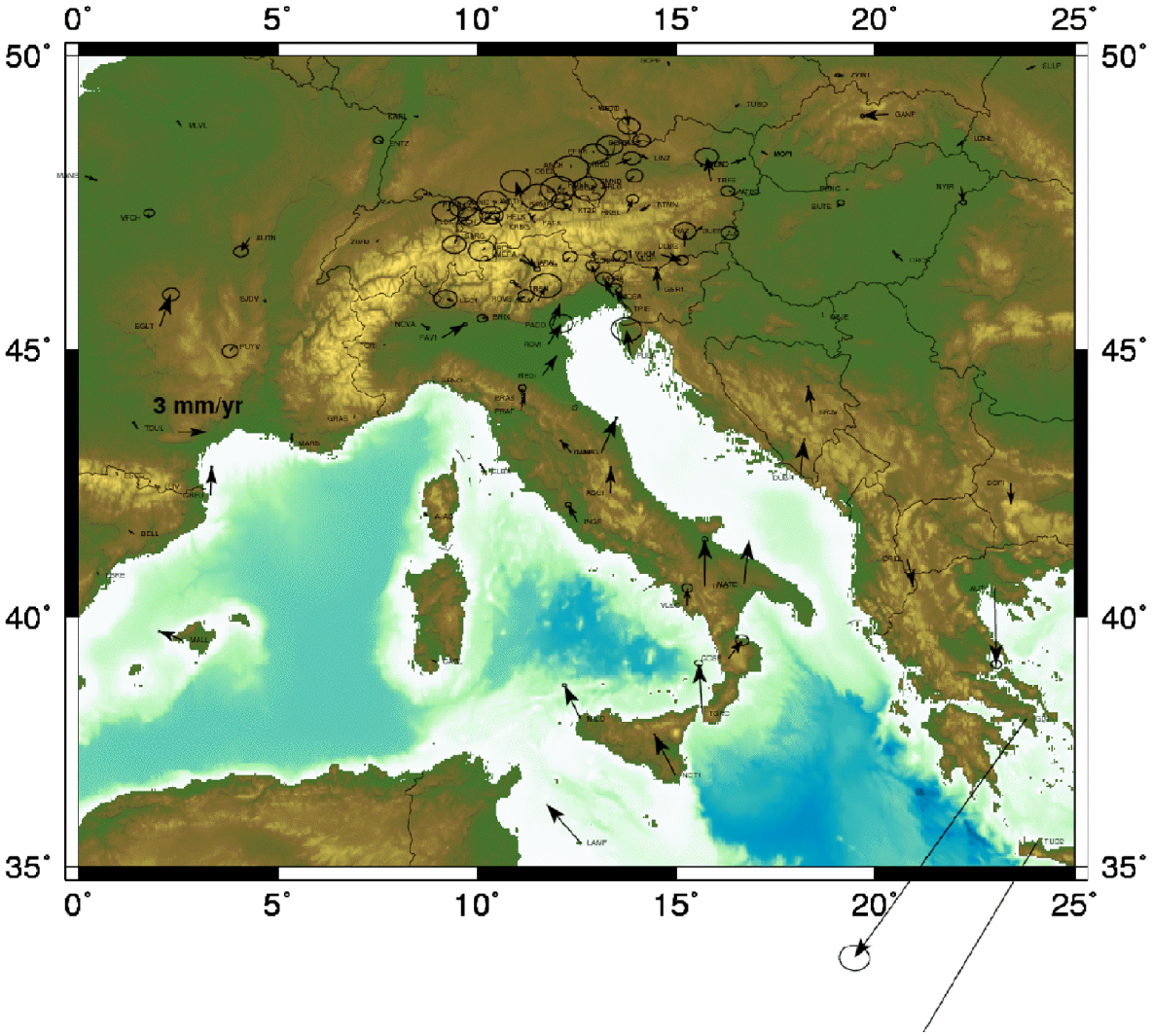

Figure 3.1 - Velocities of permanent GPS stations referred to the ITRF2000 Eurasian pole of rotation, computed by multiyear (1996-2006) normal equation stacking of the combined EUREF, Italian and Austrian networks. Error ellipses are at 2σ level.

The combination of the partially overlapping subnetworks is done by an independent center, the Bundesamt fuer Kartographie und Geodaesie in Frankfurt, which also validates the individual solutions of each contributing Analysis Center, on a weekly basis. Typical discrepancies in the estimated coordinates among different analysis centers are in the order of fractions of mm. Two of the 16 Analysis Centers, the Austrian and the Italian (Padova), generate additional SINEX files referring to national networks which locally densify the

EUREF network. The resulting SINEX files are fully compliant with the IGS/EUREF standards. It is important to stress that the SINEX files we have used are publicly available, and are detailed as follows:

EUREF : (EUR<GPSwk>.SNX) from GPSwk 860 to 1380 (~10 years)
(ftp://igs.ifag.de/EUREF/products)

Italian Network: (UPA<GPSwk>.SNX) from GPSwk 1000 to 1380 (~7 years)
(ftp://ux1.unipd.it/utenti/user1/ftp/pub/incoming/GPS-UPAD/upasinex)

Austrian Network: (GP_<GPSwk>.SNX) from GPSwk 995 to 1380 (~ 7 years)
(ftp://olggps.oeaw.ac.at/pub/products)

To define a backbone network of top quality permanent GPS stations we have chosen to combine on a weekly basis the EUREF, Austrian and Italian SINEX files using a state of the art software Bernese 4.2. As a result we have available for velocity computation a consistently defined time series of permanent GPS stations from GPS week 860 (June 30, 1996) to present. The reference system, datum definition and imposed constraints (ITRF2000) are such that the kinematics of the stations is consistent with plate kinematics at a global scale.

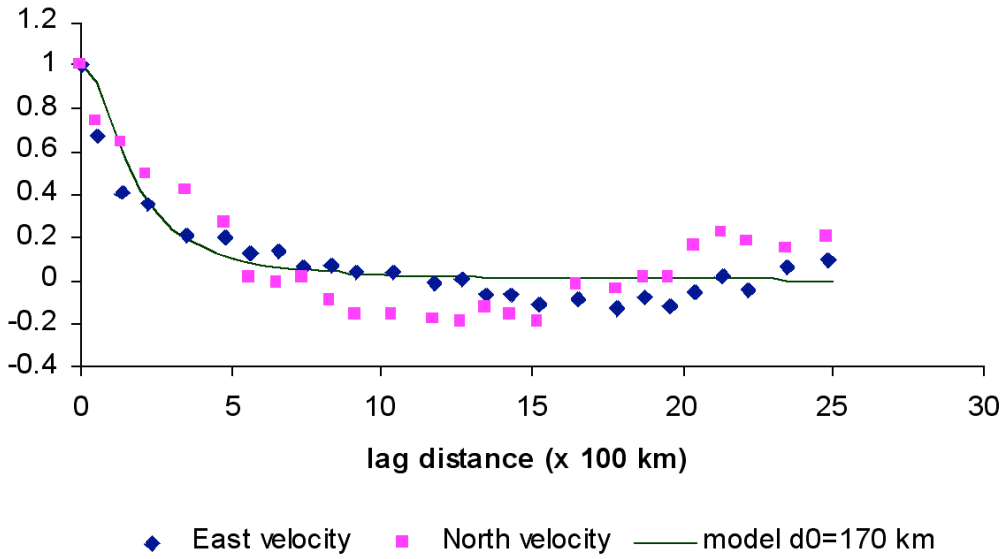

Figure 3.2 - Autocorrelation of the estimated horizontal velocities as a function of the lag distange between stations. This is a measure of the likelyhood of any two sites having the same velocity, as a function of their relative distance, and is expected to decrease with increasing lag. The scale distance is estimated to be approximately in the range 150 - 200 km.

Figure 3.1 summarizes the backbone velocity field for the Italian area based on the analysis of time series are given in the report of **RU3.2a**. Velocities in Figure 3.1 refer to permanent stations with two or more years of continuous tracking, and error ellipses are at 2σ confidence. At each site the corresponding velocity computed from the ITRF00 Eulerian pole of Eurasia has been subtracted. Hence the kinematics implied in Figure 3.1 can be considered as referred to a 'fixed' Eurasian plate. Details on the analysis of time series are given in the report of **UR3.2a**, where we also provide the validation of our velocities by comparing with an independent, publicly available solution using compatible constraints but different software (CATREF). Figure 3.2 provides the autocovariance of the estimated velocities, that is how the correlation coefficient of the east and north component of the velocities decays with increasing relative distance between stations. This decorrelation length is an important parameter for the estimation of the horizontal derivative of the velocities, and the understanding of the spatial resolution of the implied strain rate

estimates. Figure 3.2 shows that the scale length of decorrelation is in the order of 170 km, implying that our velocity gradients are averaged on areas of roughly this radius. In this sense we can speak in terms of regional strain rate measured by GPS, rather than local, and certainly not at fault scale.

The horizontal gravity gradient has been computed from the velocities of the backbone network using the method of Least Squares Collocation. The points at which the strain rate are computed are chosen to coincide with the position of those permanent GPS stations which are surrounded, within the correlation distance, by at least 4 permanent GPS sites, one per quadrant. In this way we could guarantee that the most reliable estimate has been obtained with the available data. Uncertainties are also obtained by the same algorithm and shown in Figures 3.3 for Northern Italy and 3.4 for Central Italy. Our rather strict criteria for strain rate computation did not allow us to carry out the corresponding estimates in Southern Italy and Sicily, where unfortunately the population of permanent GPS stations is not so dense as elsewhere. Conversely, data are absolutely necessary in these areas for the model to be completed, although in a preliminary form. Therefore we decided to incorporate an independent data set of velocities resulting from permanent and campaign sites provided by E. Serpelloni as part of the contribution of **RU 3.1** to the Task 3. The velocities were converted to strain using the same least squares collocation algorithm used in Figures 3.3 and 3.4, to ensure maximum consistency. The result is shown in Figure 3.5.

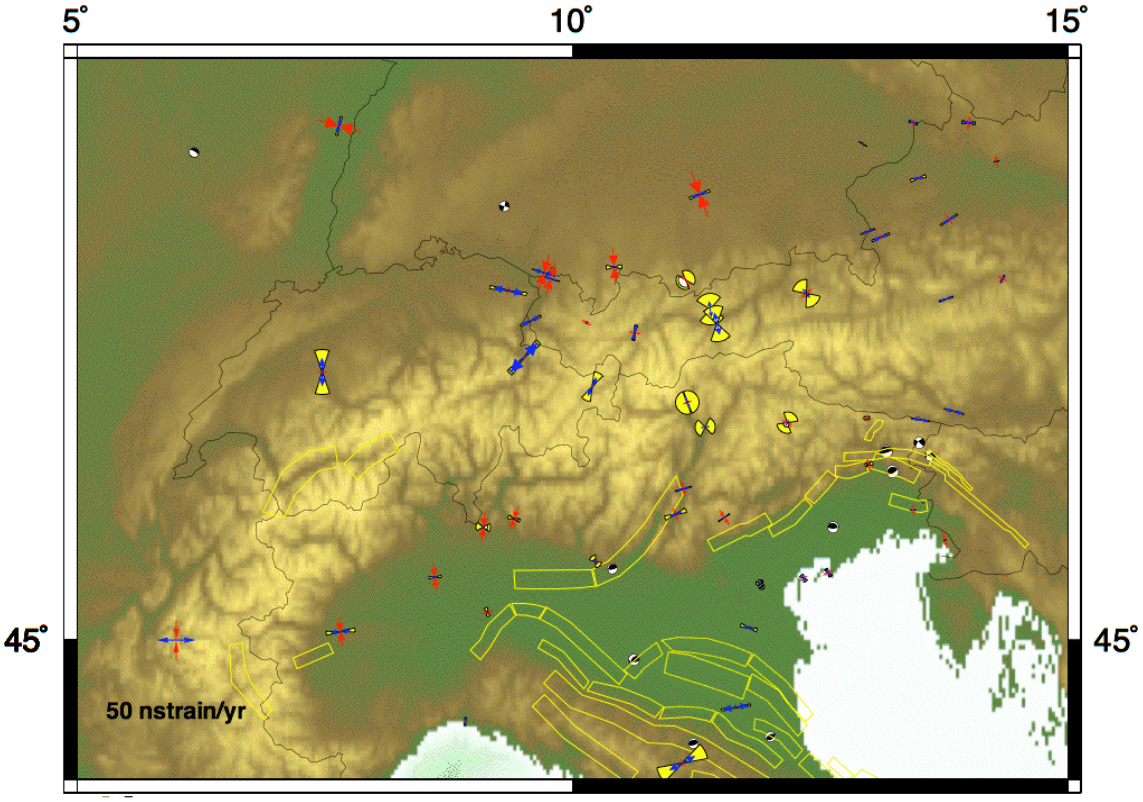

Figure 3.3 - Regional strain rates in Northern Italy and the Alps, computed at the center of clusters of permanent GPS stations and superimposed to the Seismogenic Areas of DISS v. 3.0.2 (outlined in yellow). The 2σ uncertainty is obtained by linear propagation of the velocity uncertainty.

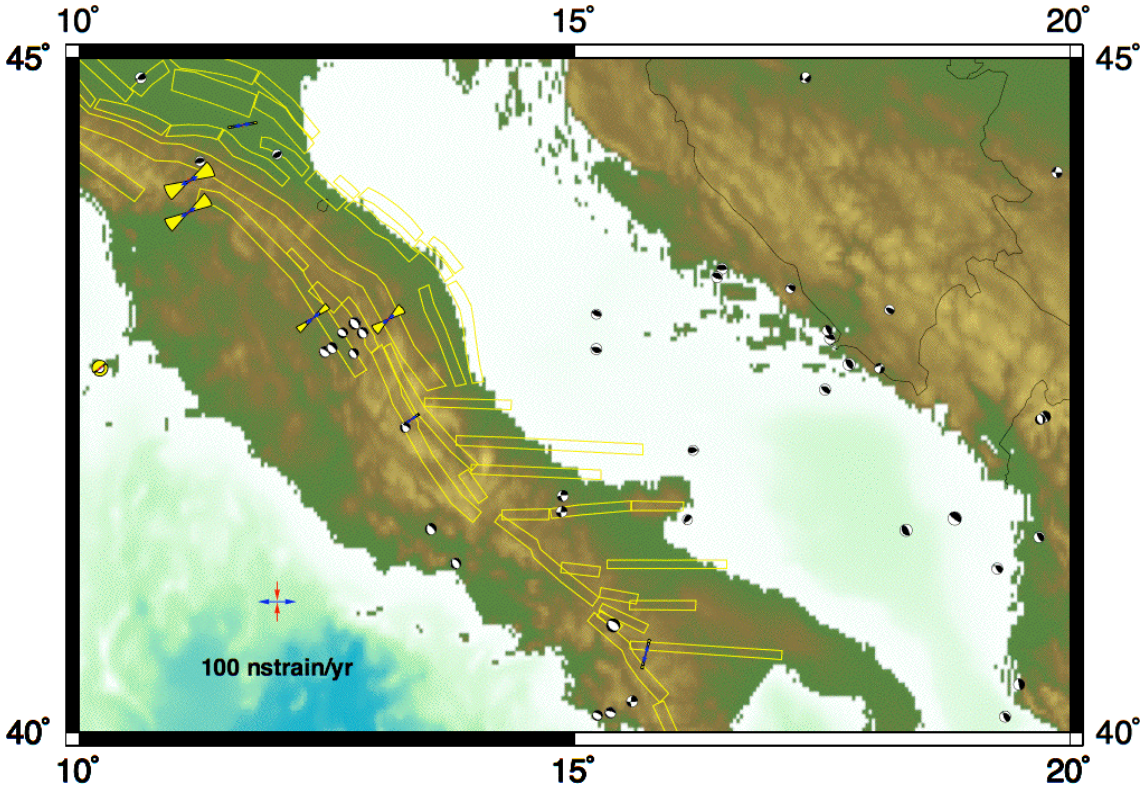

Figure 3.4 - Same as in Figure 3.3, for central Italy.

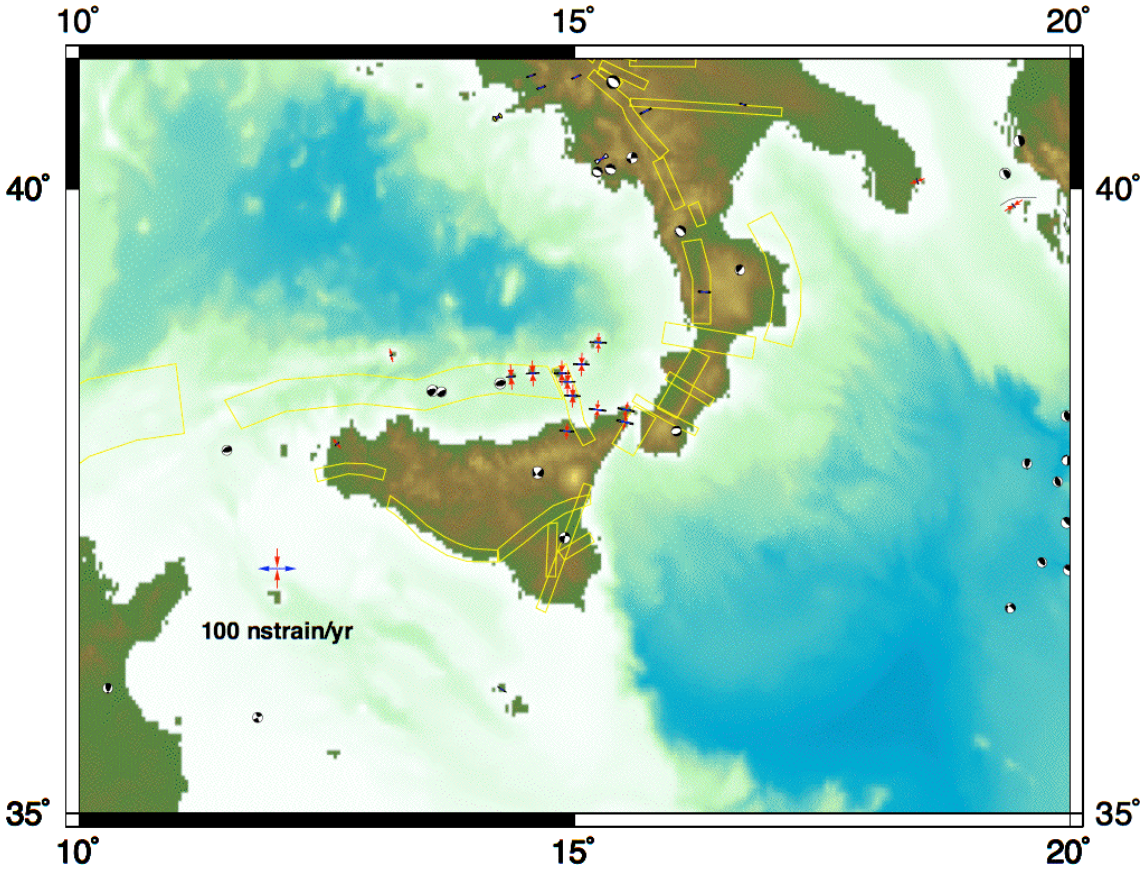

Figure 3.5 - Same as in Figure 3.3, for southern Italy. Notice that this elaboration also benefits from a number of non-permanent GPS stations (see report of RU 3.2a and RU 3.).

Development of the Finite Element Model

The goal of this part of Task 3 was to model crustal velocities, horizontal stress directions, anelastic (long-term) strain rates by integrating different datasets, such as GPS velocities, focal mechanisms, fault kinematics, each one weighted by its uncertainty. The model is based on a thin-shell finite element technique developed by *Bird* [1999]. Its main features are a 3D structure, 2 layers, 2D integrated strength. The procedure we follow to build a model can be decomposed into the following steps:

- Building the models (crustal and lithospheric structure, heat flow, rheology, faults, topography, etc.)
- Finite element mesh and faults
- Boundary conditions (plates, tractions)
- Solving (software SHELLS from *Bird* [1999])
- Computing direct and indirect quantities (anelastic "long term" velocities, "fault locked" velocities, stress, strain, tectonic regime, ...)
- Scoring models with data (RMS and average error)
- Analyzing the misfit (currently using GPS, stress azimuth, and tectonic regime)
- Choosing the "least arbitrary" good solution (if possible)

The setup of the geodynamic model is summarized in Figure 3.6.

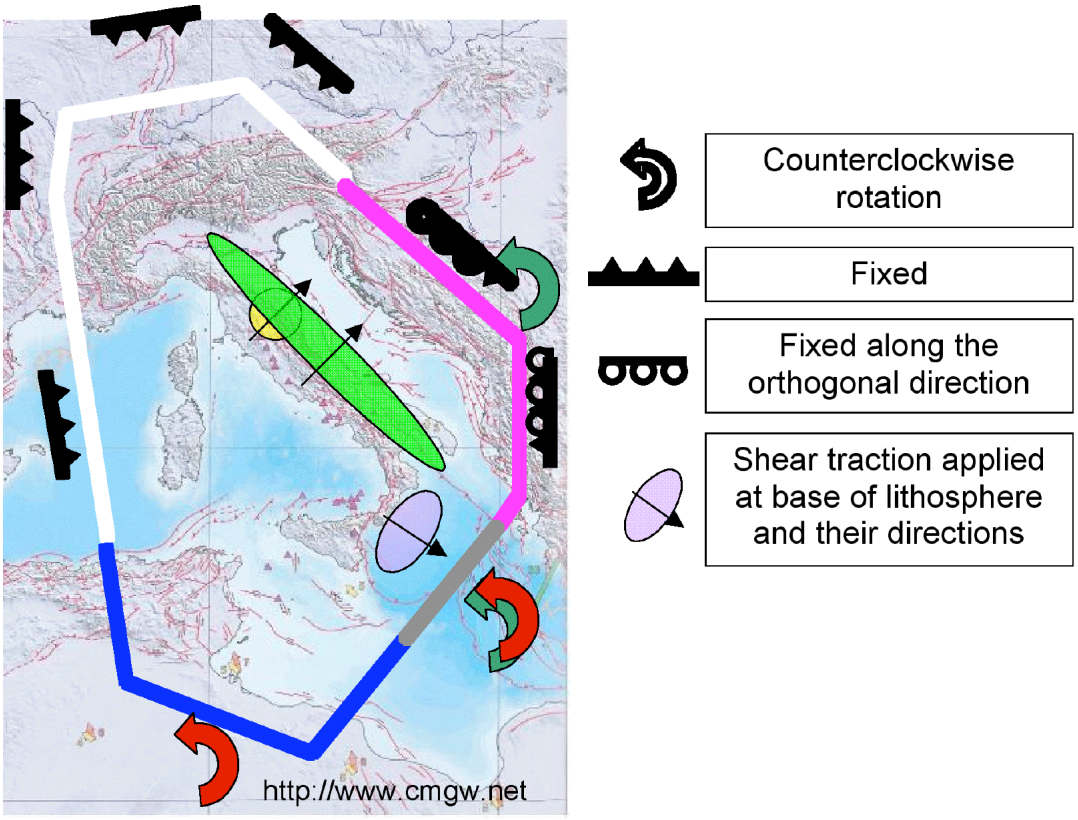

Figure 3.6 - Boundary conditions and body forces modelled in the 3D finite elements model.

In order to limit the spatial extent of the modeled domain, we set our boundaries where large geological structures exist and where we can infer from literature the range of possible boundary conditions. This approach allowed us to keep the region relatively small and attain a detail of few km in the analysis. We used Bird's definition of *orogen* for the Central Mediterranean, where his plate model is not expected to be accurate [*Bird*, 2003], and divided

such region into two partsseparated by the Cephalonia transform fault: a "fast" region to the East (~3 cm/y, Aegean Sea and Greece) and a "slow" region to the West (~3 mm/y, Thyrrenian Sea and Italy).

We applied boundary conditions reproducing the motion of surrounding plates in the Eurasia reference frame ETRS89 or representing geological information. Uncertainties in the interpretation of available data and the difficulties to delineate the model edges in the studied region led us to define different possible boundary conditions taken from the literature. Where information is weak, like in the Ionian Sea, we also tried boundary conditions from neighbouring areas and selected arbitrary conditions that were worthy of investigation.

The existence of low-angle active normal faults and the occurrence of compressional tectonics close to the large normal faults suggested to consider basal tractions below the Apennines and the Calabrian Arc. We applied shear tractions at a depth of 400 km that correspond to shear tractions at the base of the lithosphere of ~20 MPa; in addition to the effect due to other boundary conditions and lithostatic compensation forces, such tractions produce ~0.2 mm/y extension in the Apennines and the rotation of the σ_1 axes in compressional areas.

Model tuning and final estimates of slip and strain rates at seismic areas

The scoring datasets include the geodetic velocities and strain rates shown in Figg. 3.1, 3.3, 3.4 and 3.5 and the data schematically shown in Figure 3.7. We considered the azimuth of stress directions and the tectonic regime implied by fault plane solutions. The final model is summarized in Figures 3.8 through 3.12. Hence, to fine tune the Finite Elements Model we considered the azimuth of stress directions and the tectonic regime implied by fault plane solutions, in addition to the geodetic data.

For several subsets of conditions and/or parameters (Tables 1 and 2 of the final report of **RU 3.1**) we computed the misfit between the model predictions (corrected velocities and stress) and experimental data (GPS, SH orientations, and tectonic regime); we scored each solution with its RMS, and found a preferred subset of boundary conditions and a preferred subset of parameters (or a range of).

After the preliminary models produced during Year 1 of the project we improved the definition of the Moho depth by integrating more data derived from the literature and by reviewing velocities from the tomography of *Di Stefano et al.* [2006]. In addition, we regionalized the rheology in about 9 zones; by starting from 10 sets of rheological parameters, we chose the best set based on the least misfit with data, then improved the expected brittle to ductile transition based on instrumental earthquake depths. Specifically, because the Bird code assumes uniform rheology, we also assumed uniform "starting" parameters but sligltly modified the temperature field in order to better reproduce the maximum earthquake depths through the thickness of the brittle layer.

We evaluated the local misfit between the model and data (similarly to Figure 2 of **RU 3.1**, which shows the final misfits) and improved the definition of the Moho depth and the brittle layer thichness in areas where the misfit was possibly affected by such values.

Once the model was developed in its final form (more than 5,000 elements, ~850 fault segments) we "tuned" it; in other words, we choose the boundary conditions and set of parameters which produce the least misfit between model and data.

The slip rates (Table 3.1) have been obtained by averaging the slip rate over the DISS v3.0.2 Seismogenic Areas. Such slip rates have been validated by comparing them with geological values (in collaboration with the Task 1) and comparing the model predicted moment rate with that implied by the CPTI04 catalogue [*CPTI Working Group*, 2004]. We found that the model slip rates are nearly 30% smaller than geological slip rates, and that moment rate due to slip-rate only is nearly 50% of the CPTI04 rate. Although these values are possibly still underestimated with respect to our expectations, the pattern of slip rates seems to be realistic. At the moment, part of the permanent strain rate that may have some role in the total moment rate has been neglected. However, despite such discrepancies, the results showed that the model and the geodetic-geological data can be successfully integrated to give an independent set of results; discrepancies have been discussed. Sometimes they are believed to depend on the model implementation, that can be improved further; sometimes the model predicts slip-rate along

faults that were not incorporated in DISS yet; sometimes the model predicts permanent strain in areas where there are no sources at all. In collaboration with Task1 we highlighted the weaknesses of the models and/or data and proposed that slip at a significant rate must take place along two major fault zones (the Calabrian thrust and the Central Adriatic thrust) that may require further investigations. The final model is summarized in Figure 3.12.

Table 3.1 provides an example of model tuning: the different columns indicate the used data types; each line corresponds to a slightly different model. The best fitting model is defined as the one that yields the minimum weighted root mean square error across the different data types. Note that, in this example, GPS data from permanent and temporary stations are considered separately and are given the same weight.

For the final results, we took the 50 best models based on synthetic indexes, then averaged the calculated quantities to avoid falling in local minima.

Finally, Table 3.2 summarizes the estimates of slip and strain rates for all DISS Seismogenic Areas as predicted by the numerical model. They result from an optimal blending of all the available data. The slip rate and strain rate in the hypothesis of partial and full lock is shown for each Seismogenic Area where the model has been defined, along with the number of available observations in a 50 km radius from the Seismogenic Area itself. The reader is encouraged to refer to the report of RU 1.1 for further details.

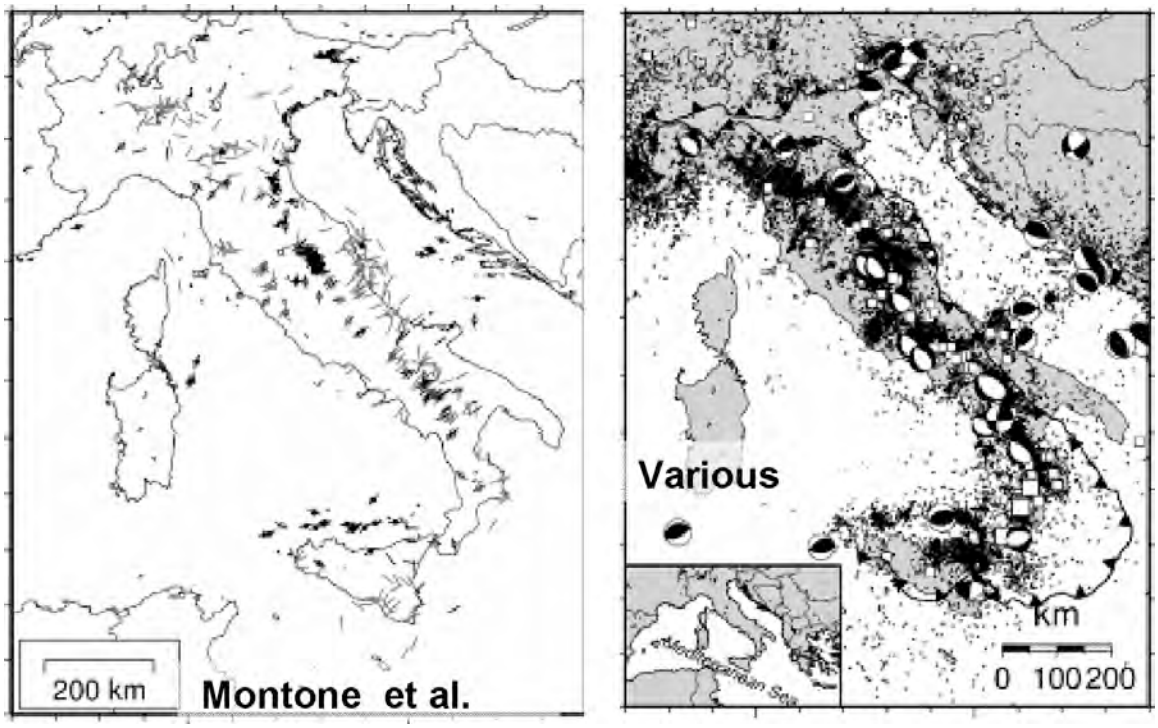

Figure 3.7 - Sample of geophysical data used to calibrate the 3D finite elements model. Left: stress-in-situ data from *Montone et al.* [2004]. Right: focal mechanisms from various sources.

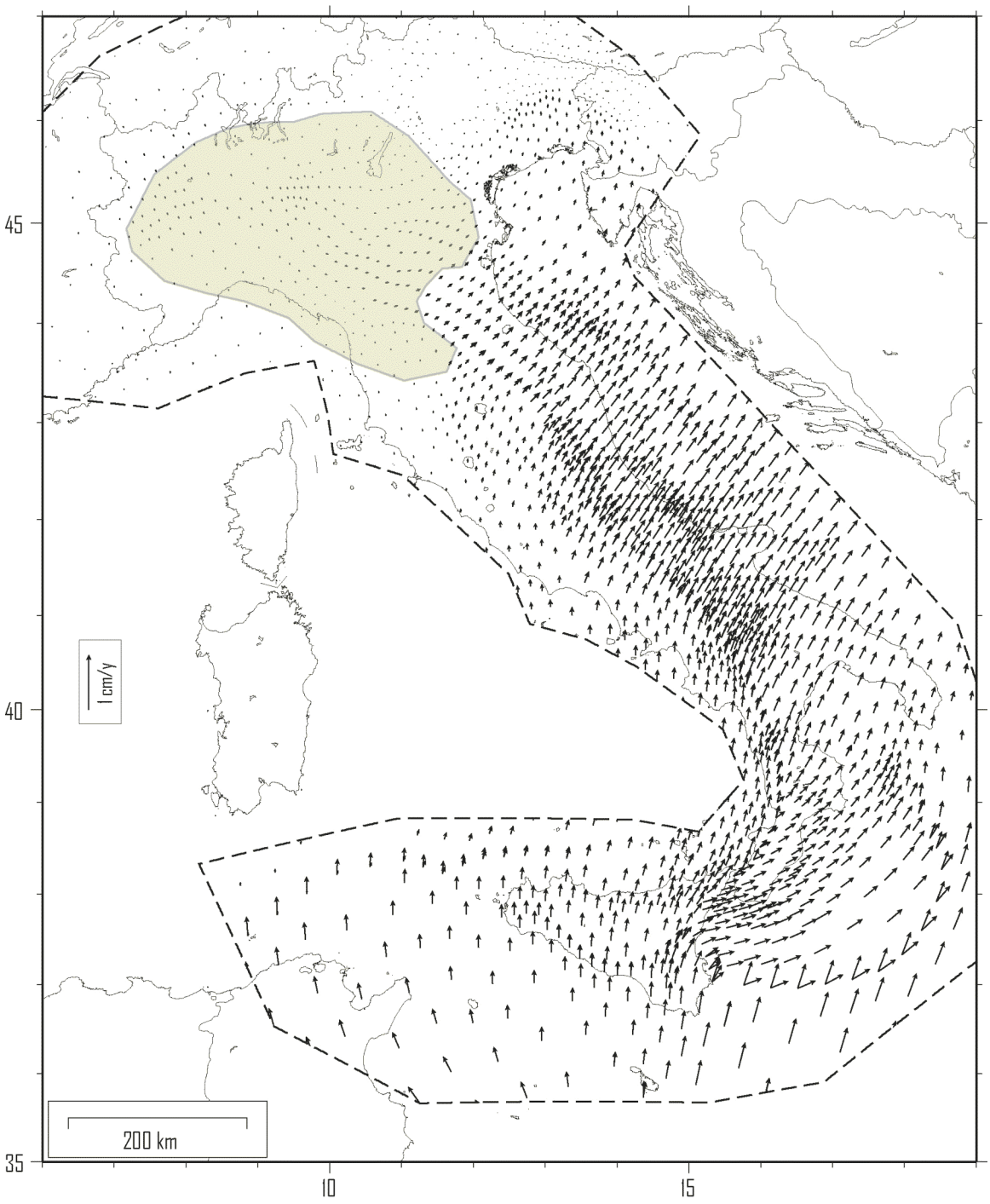

Figure 3.8 - Velocity field resulting from the numerical model, relative to a frame nearly aligned with the ITRF2000 rotation of Eurasia. The dashed line encloses the region for which there are observations available. The irregular gray patch over northern Italy indicates a portion of the model that is comparatively less resolved.

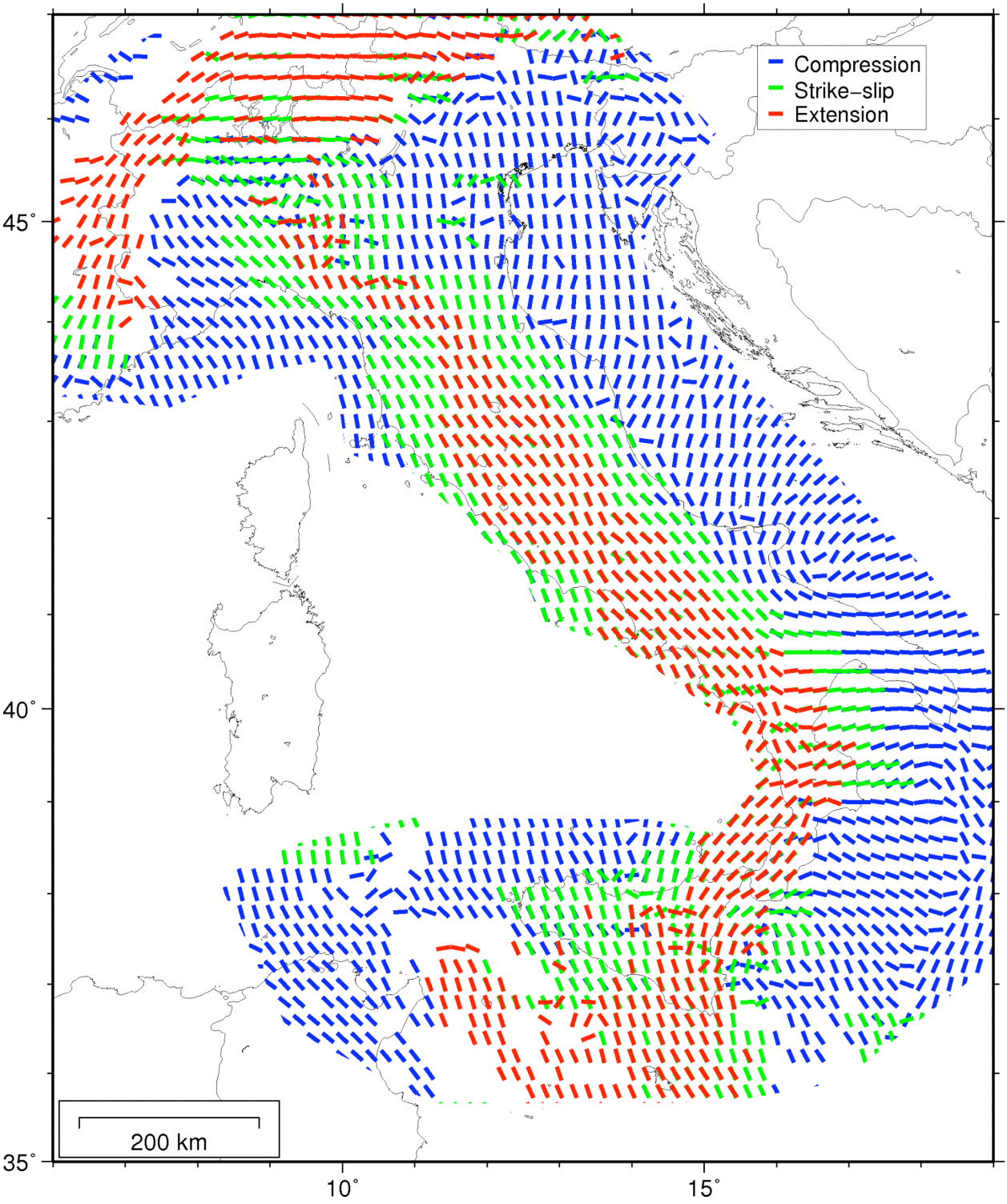

Figure 3.9 – Principal directions of strain resulting from the Finite Elements Model.

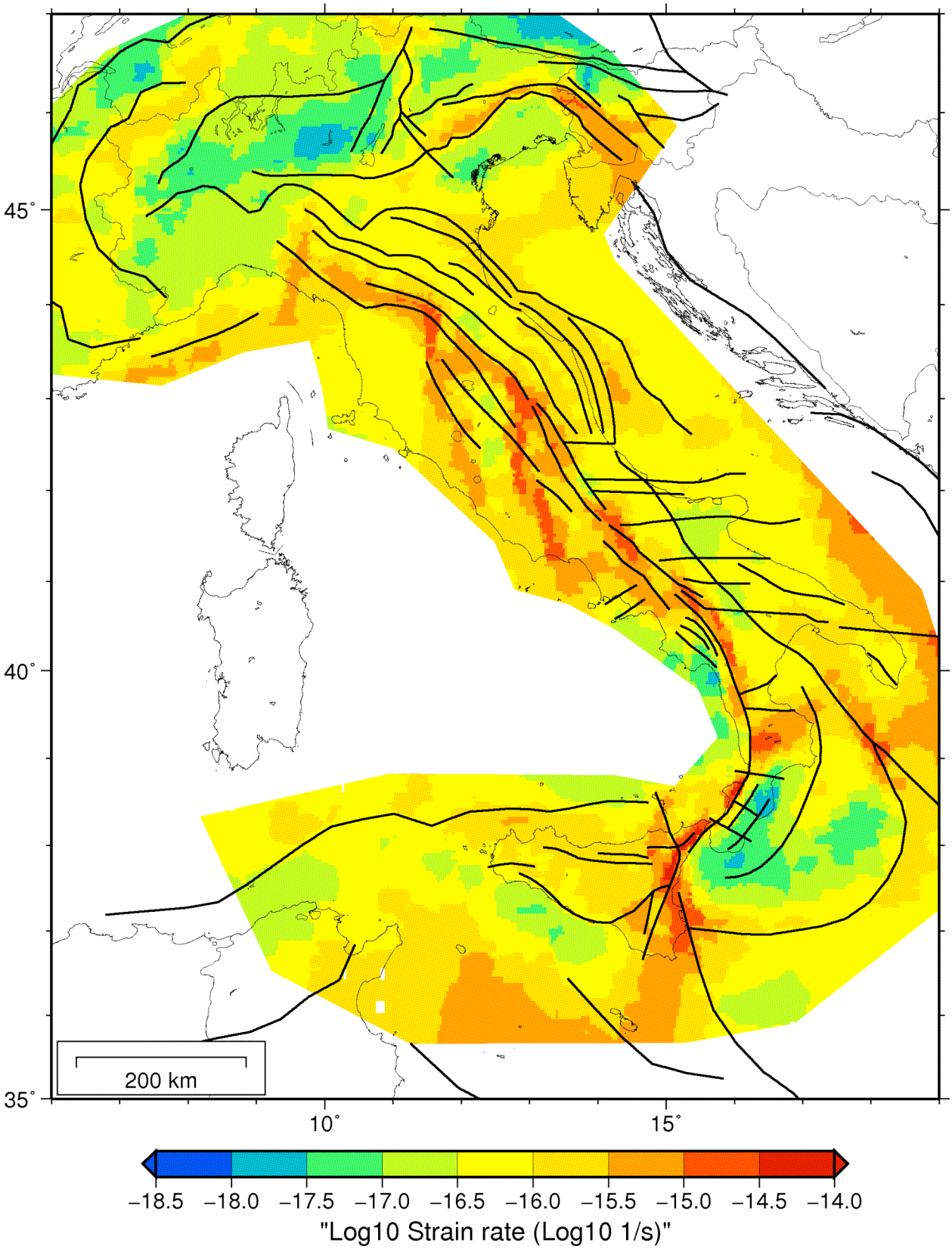

Figure 3.10 – Maximum shear strain rate contours predicted by the Finite Elements Model.

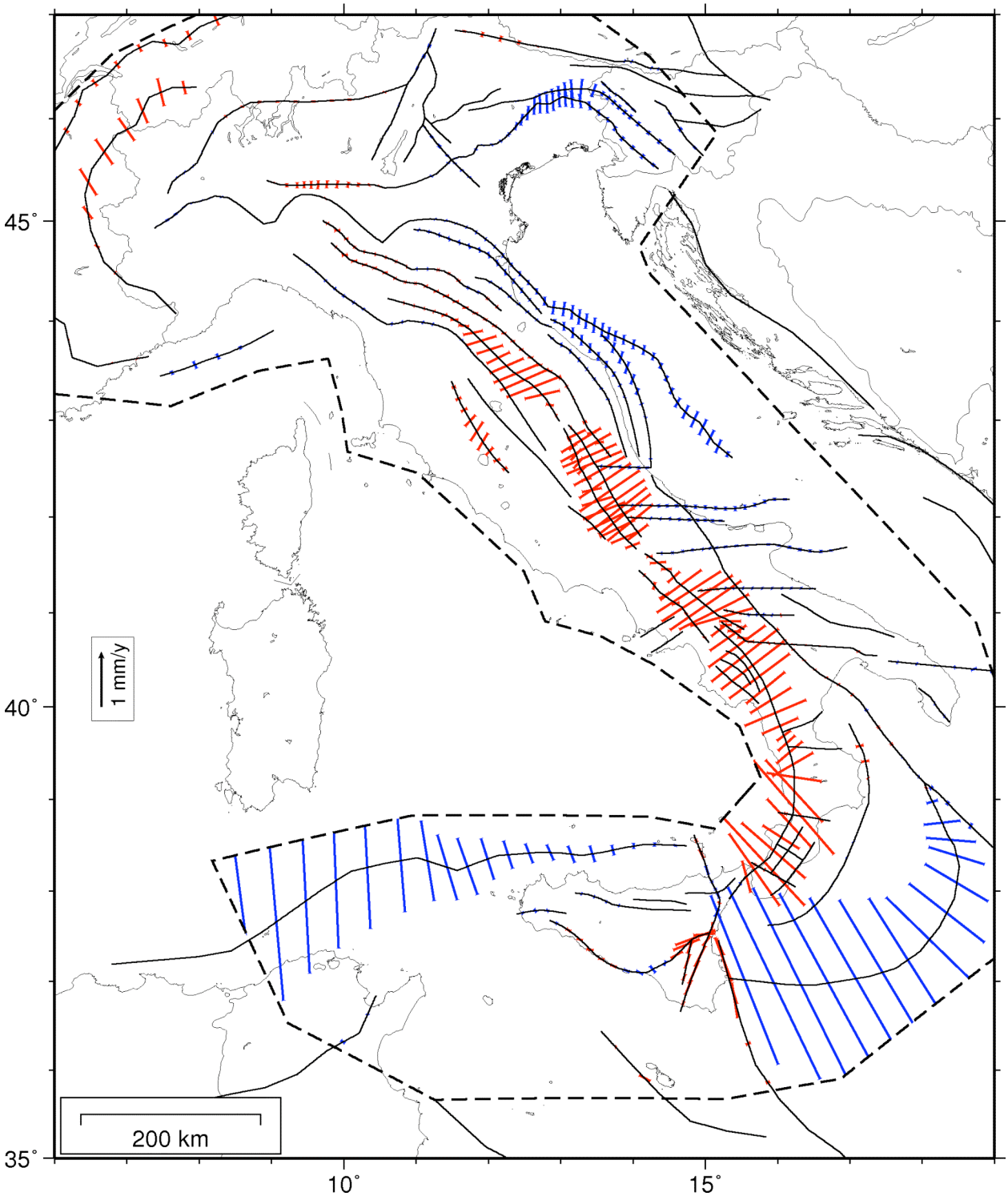

Figure 3.11 – Slip rate across a set of major active faults, including all Seismogenic Sources of DISS v3.0.2 plus a few additional tectonic trends offshore.

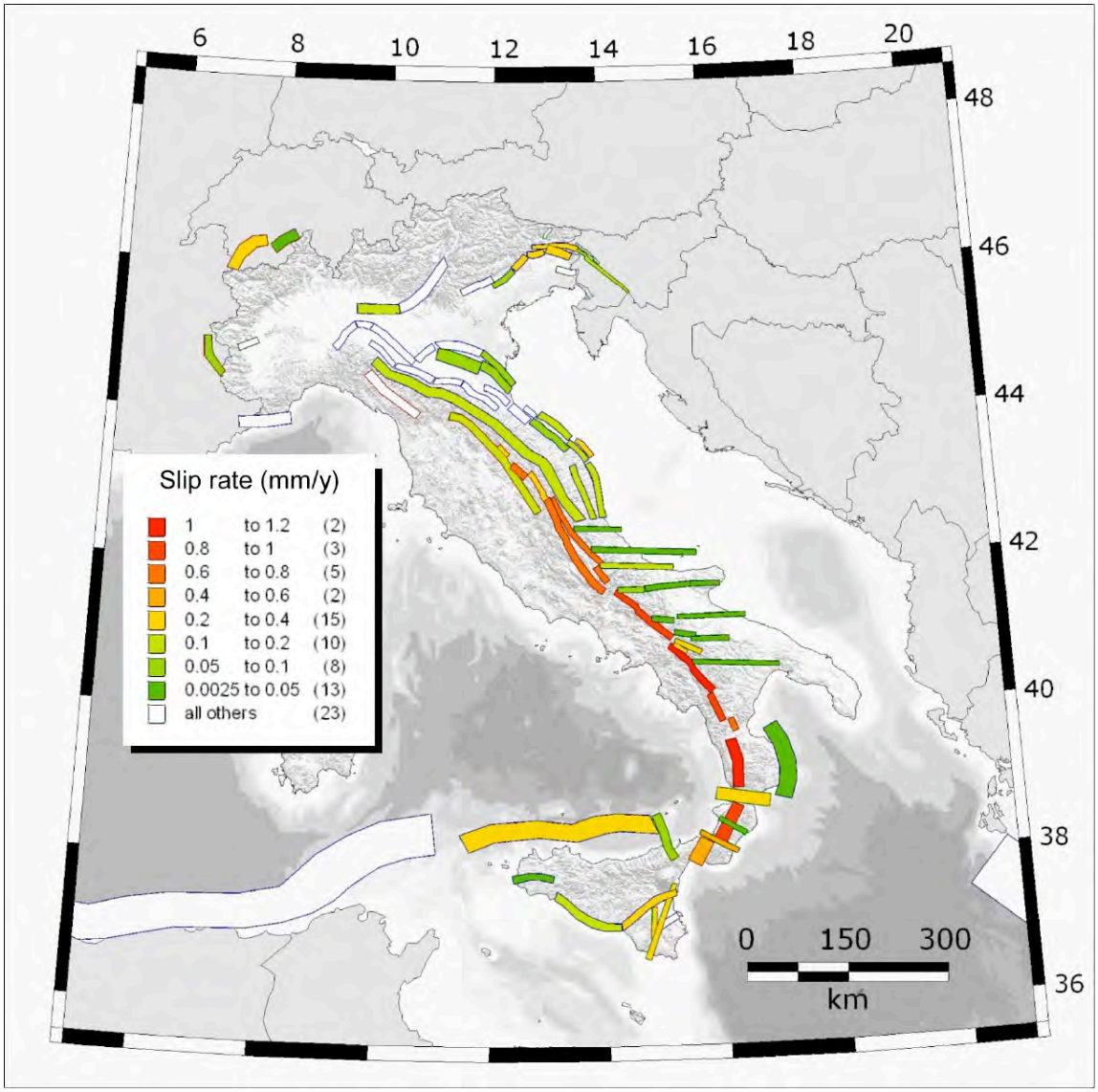

Figure 3.12 – Average slip rate in Seismogenic Areas of DISS v3.0.2 predicted by the Finite Elements Model.

Table 3.1 - An example of best-fitting models and their misfits. Notice that permanent and temporary GPS are dealt with separately and have been assigned the same weight. See report of RU 3.1 for further details.

No.	Boundary Conditions					Tractions				Main parameters			RMS					Synthetic	
	EU	AFT	AF	IO	AD	NA	CA	SA	ARC	V_{times} (a.u., 1E9)	effc	τmax (N/m, 1E12)	GPS1 (1) (mm/y)	GPS2 Euref (2) (mm/y)	SHmax (3) (DEG)	Regime misfit (3) (%)	Slip-rate (4) (mm/y)	Index1	Index2
1	1	1	1	3	2	36N	30N	24N	-	4	0.25	4	1.67	1.16	24.88	11.24	0.43	1.181	1.370
2	1	1	1	4	2	39N	36N	24N	140N	3.5	0.25	4	1.64	1.29	25.73	11.7	0.45	1.225	1.374
3	1	1	1	4	2	39N	36N	24N	140N	3.5	0.25	3.5	1.64	1.29	25.77	11.7	0.45	1.231	1.380
4	1	1	1	4	2	39N	36N	21N	140N	3.5	0.25	4	1.64	1.29	25.74	12.39	0.44	1.272	1.382
5	1	1	1	3	2	36N	24N	24N	-	4	0.25	4	1.67	1.16	25.29	11.47	0.42	1.264	1.383
...	...	...	...	...	...	...	...	...	...	...	...	...	...	...	...	...	...	...	...
50	1	1	1	4	2	36N	39N	21N	140N	3.5	0.25	3	1.64	1.3	25.84	12.39	0.44	1.324	1.439

Table 3.2 - Average results obtained from the best 50 models. Nf and Ne: Number of fault elements (nf) and finite elements (ne) in the model for each seismogenic area (Source ID and region name as in DISS); ZS: model-derived average seismogenic thickness in the hypothesis of major fault; Average strain rate under the assumption of full and partial lock (maximum strain rate in the seismogenic region gives a measure of uncertainities); average and maximum slip rate in the assumption of partial lock; geological minimum and maximum slip rates from DISS v3.0.2; Number of observations in a 50 km radius of each Seismogenic Area: Temporary GPS data [*Serpelloni et al.*, 2007]; Permanent GPS data (RU 3.2-Caporali, this project); SHmax data [*Montone et al.*, 2004]. ND = Not Determined.

Source ID	Region	Model								Geological		No. of Data		
		nf	ne	Z_S (km)	Strain rate (ns/y)			Slip Rate (mm/y)		Slip Rate (mm/y)		GPS temp	GPS perm	SH_{max}
					Full lock (Avg)	Partial lock (Avg)	Partial lock (Max)	Avg	Max	Min	Max			
DZSA001	Northern Africa Offshore	9	56	10.4	270.3	32.90	34.5	2.71	3.639	0.26	1.87	0	0	0
FRSA001	Brianconnais	2	10	12.7	26.7	25.10	26.5	0.06	0.09	0.1	1	0	0	0
GRSA001	Southwestern Hellenic Arc	1	9	8.8	29.0	ND	ND	ND	ND	1	5.3	0	0	0
ITSA001	Ozzano dell'Emilia – Mendola	6	30	9.7	4.7	ND	ND	ND	ND	0.1	1	2	2	15
ITSA002	Central Southern Alps	7	63	10.5	11.2	0.50	0.9	0.12	0.145	0.1	1	1	1	27
ITSA003	Ripabottoni – San Severo	7	35	8.7	2.2	1.10	1.6	0.03	0.041	0.1	1	0	0	20
ITSA004	Ascoli Satriano – Barletta	10	59	8.8	2.0	1.10	1.4	0.03	0.036	0.1	1	0	0	17
ITSA005	Picerno – Massafra	11	71	9.8	8.6	8.10	21.4	0.03	0.049	0.1	1	2	1	20
ITSA006	Sciacca-Gela	6	40	10.1	9.2	2.20	4	0.11	0.121	0.1	1	0	0	1
ITSA007	Thiene – Cornuda	1	15	7.7	8.5	ND	ND	ND	ND	0.1	1	0	2	4
ITSA008	Conero onshore	3	24	10.2	16.3	6.10	7.8	0.12	0.15	0.1	1	1	0	19
ITSA009	Codogno – Sant'Ilario d'Enza	7	42	9.1	2.2	ND	ND	ND	ND	0.1	1	0	0	14
ITSA010	Copparo – Comacchio	6	30	9.9	10.6	5.20	5.9	0.06	0.071	0.1	1	1	2	12
ITSA011	Lugo-Cesena	4	30	9.2	3.6	ND	ND	ND	ND	0.1	1	1	1	18
ITSA012	Portomaggiore – Ravenna	5	29	10.1	12.6	4.30	5.4	0.10	0.1	0.1	1	1	1	15
ITSA013	Aremogna – Cinquemiglia	2	17	12.4	48.0	16.50	30.6	0.75	1.047	0.1	0.6	3	0	6
ITSA014	Southern Tyrrhenian	11	70	6.3	57.2	3.60	6.9	0.37	0.69	0.2	1.5	2	0	8
ITSA015	Crati Valley	5	48	9.4	86.2	27.80	45.2	1.06	1.709	0.1	1	2	1	3
ITSA016	Aspromonte – Peloritani	5	52	6.8	122.0	67.80	118.9	0.44	1.129	0.9	2	2	1	4
ITSA017	Scicli – Catania	6	37	11.4	30.9	26.10	57.9	0.27	0.426	0.1	1	1	1	16
ITSA018	Rivanazzano – Villanterio	3	17	9.2	1.2	ND	ND	ND	ND	0.1	1	0	1	16
ITSA019	Crotone – Rossano	6	74	9.2	12.5	8.00	14.6	0.05	0.113	0.1	1	0	0	8
ITSA020	Southern Marche	6	29	8.9	22.8	12.60	13.5	0.12	0.124	0.1	1	2	1	23

Source ID	Region	Model									Geological		No. of Data		
		nf	ne	Z_S (km)	Strain rate (ns/y)			Slip Rate (mm/y)			Slip Rate (mm/y)		GPS temp	GPS perm	SH_{max}
					Full lock (Avg)	Partial lock (Avg)	Partial lock (Max)	Avg	Max		Min	Max			
ITSA021	Marsala – Belice	4	23	9.1	6.5	3.60	5.3	0.04	0.067		0.1	1	2	1	5
ITSA022	Imperia	3	29	8.3	5.1	ND	ND	ND	ND		0.1	1	0	0	1
ITSA023	Western Piemonte	1	18	10.7	2.0	ND	ND	ND	ND		0.1	1	0	1	0
ITSA024	Castelpetroso – UfitaValley	9	65	9.2	79.3	24.70	51.3	0.85	1.481		0.1	1	3	0	13
ITSA025	Inner Central Apennines	14	101	11.7	45.4	17.70	29.1	0.63	0.912		0.1	1.7	1	1	26
ITSA026	Lunigiana - Garfagnana	8	51	7.4	13.7	ND	ND	ND	ND		0.1	1	0	0	8
ITSA027	Outer Central and Northern Apennines	31	219	9.9	15.0	7.50	12.5	0.10	0.137		0.1	1	0	0	11
ITSA028	Colfiorito - Sellano	3	28	8.9	66.8	45.60	81.6	0.26	0.602		0.1	1	2	2	51
ITSA029	Gela - Catania	6	34	10.6	51.1	29.10	63.6	0.36	0.608		0.1	1	0	0	12
ITSA030	Riminese offshore	1	12	9.4	7.3	ND	ND	ND	ND		0.1	1	0	0	3
ITSA031	Conero offshore	3	19	10.5	23.2	5.40	7.5	0.21	0.225		0.1	1	1	0	17
ITSA032	Pesaro - Senigallia	4	28	9.8	7.6	3.30	4	0.06	0.073		0.1	1	1	0	5
ITSA033	Mt. Pollino South	1	6	9.4	53.1	13.70	22.4	0.72	0.715		0.2	0.6	0	0	6
ITSA034	Irpinia - Agri Valley	6	57	9.5	81.4	20.20	37.4	1.12	1.542		0.4	0.6	2	1	24
ITSA035	Ragusa-Palagonia	2	18	11.9	13.1	9.70	13.9	0.20	0.273		0.1	1	1	1	18
ITSA036	Monte Lauro	0	5	ND	ND	ND	ND	ND	ND		0.1	1	1	1	13
ITSA037	Mugello-San Sepolcro - Trevi	15	80	7	25.9	10.30	38.6	0.13	0.137		0.1	1	2	2	7
ITSA038	Mercure Basin	3	18	9.5	73.2	19.40	39.7	0.99	1.168		0.1	1	0	0	13
ITSA039	Riminese onshore	3	18	9.4	4.8	ND	ND	ND	ND		0.1	1	0	0	8
ITSA040	Castelluccio-Sulmona	13	99	12.1	42.0	16.00	28.4	0.63	1.048		0.2	0.7	1	1	22
ITSA041	Selci Lama	2	18	9.3	51.9	28.80	37.6	0.30	0.398		0.1	1	2	1	10
ITSA042	Patti - Eolie	5	29	6.7	15.9	13.20	30.4	0.09	0.159		0.1	1	5	0	3
ITSA043	Pesaro-Senigallia offshore	5	31	10.3	17.7	4.80	7	0.15	0.187		0.1	1	0	0	2
ITSA044	Sant'Angelo Lodigiano - Casalpusterlengo	3	22	9.2	1.2	ND	ND	ND	ND		0.1	1	0	1	28
ITSA045	Podenzano - Fornovo di Taro	4	25	10.2	7.9	ND	ND	ND	ND		0.1	1	0	0	11
ITSA046	Felino - Maranello	5	36	9.7	3.7	ND	ND	ND	ND		0.1	1	1	0	27
ITSA047	Castelvetro di Modena - San Lazzaro di Savena	3	23	9.5	3.7	ND	ND	ND	ND		0.1	1	3	2	25
ITSA048	Giudicarie	8	94	9.9	1.7	ND	ND	ND	ND		0.1	1	1	2	2

Source ID	Region	Model							Geological		No. of Data		
		nf	ne	Z_S (km)	Strain rate (ns/y)			Slip Rate (mm/y)		Slip Rate (mm/y)			
					Full lock (Avg)	Partial lock (Avg)	Partial lock (Max)	Avg	Max	Min	Max	GPS temp	GPS perm	SH_{max}
ITSA049	Cadelbosco di Sopra - Gonzaga	3	18	9	2.3	ND	ND	ND	ND	0.1	1	1	0	23
ITSA050	Quistello - Ferrara	6	41	9.2	4.4	ND	ND	ND	ND	0.1	1	1	1	14
ITSA051	Mirandola - Molinella	5	36	9.7	7.0	2.50	3.1	0.05	0.081	0.1	1	2	2	17
ITSA053	Southern Calabria	4	31	7.8	109.9	37.00	79.7	0.87	1.518	0.1	1	2	0	1
ITSA054	Porto San Giorgio	6	37	8.9	24.6	11.50	13.7	0.13	0.154	0.1	1	0	0	39
ITSA055	Bagnara - Bovalino	5	20	8.3	24.9	3.80	15.7	0.44	1.394	0.1	1	3	1	3
ITSA056	Gubbio Basin	2	24	9.7	89.7	40.70	59.4	0.66	0.71	0.1	1	3	2	48
ITSA057	Pago Veiano - Montaguto	4	23	9.4	5.3	4.60	7.3	0.03	0.043	0.1	1	1	0	28
ITSA058	San Marco in Lamis – Mattinata	7	39	7.2	1.7	1.10	1.3	0.04	0.047	0.1	1.2	1	0	2
ITSA059	Tocco Casauria - Tremiti	18	96	8.4	3.5	1.60	2.2	0.05	0.073	0.1	1	0	0	18
ITSA060	Montello - Conegliano	4	17	8.8	13.5	7.90	15.9	0.05	0.108	0.47	1.56	0	0	3
ITSA061	Cansiglio - Polcenigo	3	39	9.6	32.1	8.20	16.2	0.25	0.302	0.31	0.78	0	1	3
ITSA062	Maniago - Sequals	5	23	9.4	33.3	7.50	14.6	0.27	0.354	0.1	0.34	0	2	11
ITSA063	Andretta - Filano	2	24	8.8	32.5	22.90	49.1	0.23	0.395	0.1	1	2	1	29
ITSA064	Tramonti - Kobarid	5	25	8.9	25.3	6.40	11.7	0.22	0.321	0.1	1	0	4	12
ITSA065	Medea	0	14	ND	ND	ND	ND	ND	ND	0.1	1	0	3	12
ITSA066	Gemona - Tarcento	6	41	9.3	43.2	19.30	28.2	0.27	0.339	0.1	1.15	0	4	12
ITSA067	But - Chiarso	0	0	ND	ND	ND	ND	ND	ND	0.1	1	0	3	11
ITSA068	Catanzaro Trough	4	27	7.8	18.4	11.72	30.2	0.32	1.429	0.1	1	3	1	1
ITSA075	Pietracamela - Montesilvano	6	46	8.6	5.4	4.30	9.5	0.05	0.057	0.1	1	1	1	23
ITSA077	Pescolanciano - Castellino del Biferno	3	22	8.6	27.0	24.00	54.1	0.09	0.100	0.1	1	2	0	17
ITSA079	Campo di Giove - Campomarino	14	74	9.1	6.3	2.20	4.3	0.11	0.377	0.1	1	1	0	18
ITSA080	Nicotera - Roccella Ionica	2	19	8.4	13.6	13.50	45	0.00	0.004	0.1	1	1	0	2
ITSA084	Vallata - Monteverde	4	23	9.2	6.7	5.90	11.5	0.04	0.042	0.1	1	1	0	31
ITSA087	Conza della Campania – Tolve	3	20	9.1	50.4	39.10	67.1	0.28	0.381	0.1	1	2	1	26
ITSA089	Melfi - Spinazzola	7	29	9.5	1.9	1.20	1.7	0.02	0.036	0.1	1	2	1	15
SISA001	Bovec - Tolminka	6	29	9	3.3	ND	ND	ND	ND	0.1	2	0	2	4

Source ID	Region	Model								Geological		No. of Data		
		nf	ne	Z_S (km)	Strain rate (ns/y)			Slip Rate (mm/y)		Slip Rate (mm/y)		GPS temp	GPS perm	SH_{max}
					Full lock (Avg)	Partial lock (Avg)	Partial lock (Max)	Avg	Max	Min	Max			
SISA002	Tolmin - Idrija	9	60	7	22.2	16.90	29.7	0.18	0.195	0.1	2	0	2	1
SWSA001	Eastern Valais	1	6	13.7	11.5	10.20	13.8	0.05	0.05	0.1	1	0	0	0
SWSA002	Western Valais	3	13	14	15.1	4.91	7.306	0.39	0.407	0.1	1	0	0	0

Task 4

Characterizing the behavior of seismogenic sources and assigning probabilities of activation

Coordinator Laura Peruzza, INOGS, Trieste

Introduction

The goal of Task 4 was to parameterize the behavior of a given set of seismogenic sources by using the most updated results released within the project, and to assign each source a probability of generating a significant earthquake, possibly in a time-dependent perspective. These are very recent themes for the international literature, and usually only countries where there exists a record for repeated earthquakes on the same fault segment (Japan, California, New Zealand) have faced the time-dipendency problem. Nevertheless, Italy plays a role in this context for the originality in the approaches used in compiling and using source models derived from a combination of geological and seismological observation [*Various Authors*, 2006]. Time-dependent issues may play a critical role in seismic risk reduction strategies, by giving higher priority to earthquake-prone areas (e.g. *Grant et al.* [2006]).

As these are innovative topics and no "ready-to use recipe" is available, the Task collected different research proposals dealing with probabilities of earthquake occurrence. The 9 Research Units participating to Task 4 in the period 2005-2007 used different and sometimes contradictory methods and techniques, and our challenge was to gather pieces of evidence that could coexist and be merged in the more general framework depicted by the other Tasks.

After an initial tuning phase[1] for the critical re-evaluation of the RUs proposals and for the definition of the common data to be used and of products to be achieved, the Task goals and the research teams were subdivided into three Themes:

1) Occurrence of an impending earthquake based on instrumental seismological data (**RU 4.2**-Di Giovambattista, **RU 4.5**-Godano and **RU 4.7**-Murru);
2) Occurrence of a significant earthquake based on physical models (**RU 4.3**-Cinti, **RU 4.6**-Mantovani and **RU 4.7**-Murru);
3) Occurrence of a significant earthquake based on statistical analysis of earthquake and fault data (respectively **RU 4.4**-Garavaglia and **RU 4.9**-Rotondi for seismogenic areas; **RU 4.1**-Akinci and **RU 4.8**-Peruzza for individual sources).

During the project all RUs developed original elaborations using new or updated computational tools and sharing as much as possible common input data so that their final results could be easily compared. These results represent the methodological evolution of the preliminary results reported in the Year 1 report, and updated data or innovative elaborations have been proposed in this limited time period. This report summarizes the analyses performed by Task 4 and the most outstanding results, which are shown in italics; to encourage the reader to refer to the RU reports directly, original figures and tables are only referenced but not shown in this text. The figures shown in the following are only aimed at synthesizing and comparing the RU results.

Main results

Theme 1 - Occurrence of an impending earthquake based on instrumental seismological data

In the framework of implementing time-dependent probability models, *Theme 1 represents the term of including clustering characteristics using aftershock statistics* (see the implementation priorities given in the 2007 straw pool taken at the WGCEP Workshop: http://gravity.usc.edu/WGCEP/activities/workshops/March07/StrawPollResults.pdf). Two known models have been used: the Accelerating Moment Release (AMR, by **RU 4.2**), and the

[1] A table of "facts" of Task4 is reported in the final report of RU 4.8

Epidemic Type Aftershock Sequence (ETAS, by **RU 4.7** and ETAS modified by **RU 4.5**). The RUs considered several case studies and a 20-30 year long earthquake catalogue as the methodology requires using complete datasets (earthquake catalogue must not be declustered). The expected result is a short-term prediction, but what "imminent earthquake" means is controversial. **RU 4.7** released daily occurrence rate density maps for selected events (Fig. 5 and 6 of the report of **RU 4.7**) and backward probabilities values referred to a circular area of 100 km radius for all the events with M>=5.0 that occurred in Italy from 1987 to 2006 (see their Tab. 5, Fig. 4); **RU 4.2** estimates that the preparation process of a strong earthquake is 2-3 years, giving a table of measured/predicted magnitude for 9 events (Tab. 1 of the **RU 4.2** report); for homogeneity purposes with Theme 3, **RU 4.5** maps the logarithm of probability integrated in 30 years after the last events that occurred in a 40X40 km cell model (Fig. 1 and 2 of **RU 4.5** report).

The proposed backward prediction aims at giving a rationale regarding the predictability in the evolution of earthquake sequences, and therefore may play an important role in real-time seismic monitoring; *Figure 4.1 shows how only swarm-like sequences exhibit a good predictability using the ETAS method*. The most recent literature [*Hardebeck et al.*, 2007] is very critical with the AMR method. *Space and time analyses of the completeness represent by-products of these studies having important follow-ups on seismic hazard assessment*. Further applications and implementation of these studies have been developed in the frame of CSEP activities (http://www.scec.org/research/projects/CSEP/), and as far as Italy is concerned, they will certainly benefit from the possibility to access to certified, transparent and updated real-time instrumental datasets and procedures.

Figure 4.1 – The backward prediction for real-time seismic monitoring: only swarm-like sequences exhibit a good predictability using the ETAS method.

Theme 2 - Occurrence of a significant earthquake based on physical models

Theme 2 is the container for modelling faults interaction. At the beginning of the project, the expectations on this Theme were to obtain from physical modelling elements in favor of, or against the simplest assumption that sources behave independently. This simplification is implicit in nearly all the seismic hazard estimates done in the past, based on areal sources or individual faults, under stationary or time-dependent conditions (e.g. *Gruppo di Lavoro* [2004]; *Pace et al.* [2006]). Fault interaction is evaluated by two RUs by the Coulomb Failure Function ΔCFF, but each of them used a different technique and fault population. For the **RU 4.7**, the ΔCFF produces a permanent effect that induces a shift in the time elapsed since the previous earthquake; they also introduce a second term, that is called "transient effect" and is due to the rheological properties of the slipping faults. The probabilities of a future earthquake are given in Fig. 3 and Tab. 3 of the **RU 4.7** report.

Figure 4.2 shows a comparison of probabilities obtained in central Italy for Individual Seismogenic Sources from DISS v3.0.2, first considered to behave independently (**RU 4.8**), then adding the effect of fault interaction (**RU 4.7**). The values reported by **RU 4.8** entered in the computation done by **RU 4.7**; there is a significant variability in space. *Significant changes in mean recurrence times of individual sources due to fault interaction are recognized also by **RU 4.3***. This RU identified multimodality in the distribution of recurrence times or significant departures from the starting value imposed to each individual fault (see Fig. 4 of the **RU 4.3** report). An important feature obtained by the simulation of a very long synthetic earthquake catalogue tends to rule out systematic interaction conditions: minor faults may cause perturbations to nearby faults, and repeated "cascade" sequences are therefore excluded. *This modelling is somehow able to reconcile the evidence of clustering in time of the historical catalogue with the characteristic nature of earthquakes generated by individual faults* (see Fig. 3 of the **RU 4.3** report). Adding or deleting a single fault does not modify the regional behavior of the system, but may have a strong impact on the timing of adjacent faults; *the completeness of the fault catalogue is therefore a crucial issue*.

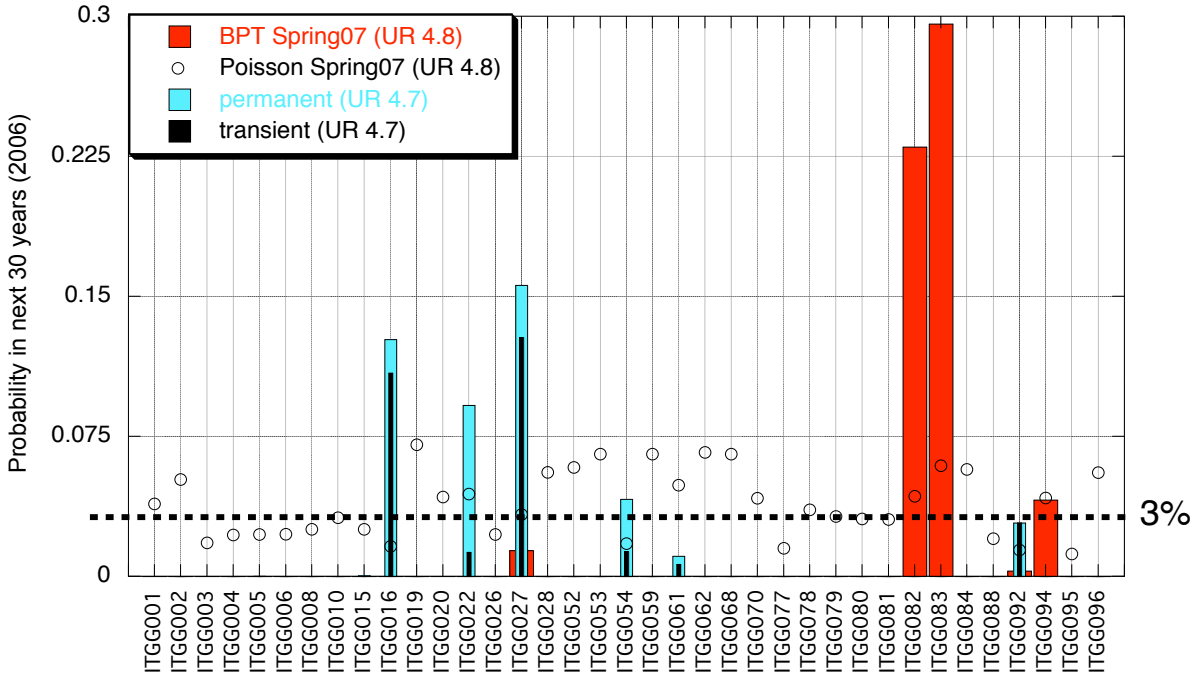

Fig 4.2 – Comparison of the probability of occurrence of a main earthquake in the next 30 years from 2006 resulting from forecasts obtained considering (RU 4.7) or not considering (RU 4.8) fault interactions. Probabilities not considering fault interactions refer to two models for intercurrence times: Poisson and BPT. Probabilities considering fault interactions separate the permanent contribution from the transient one.

The contribution of **RU 4.6** focused on large scale geodynamic modelling. Post-seismic relaxation modelling suggests interaction conditions between the Southern Dinarides and Apennines, and an hypothesis of Southern versus Northern Apennines interaction is proposed. The variation in time of velocities and strain rate obtained by numerical simulation (Fig. 7 of the report of **RU 4.6**) should be taken into consideration to properly interpret the experimental deformation data (e.g. GPS data).

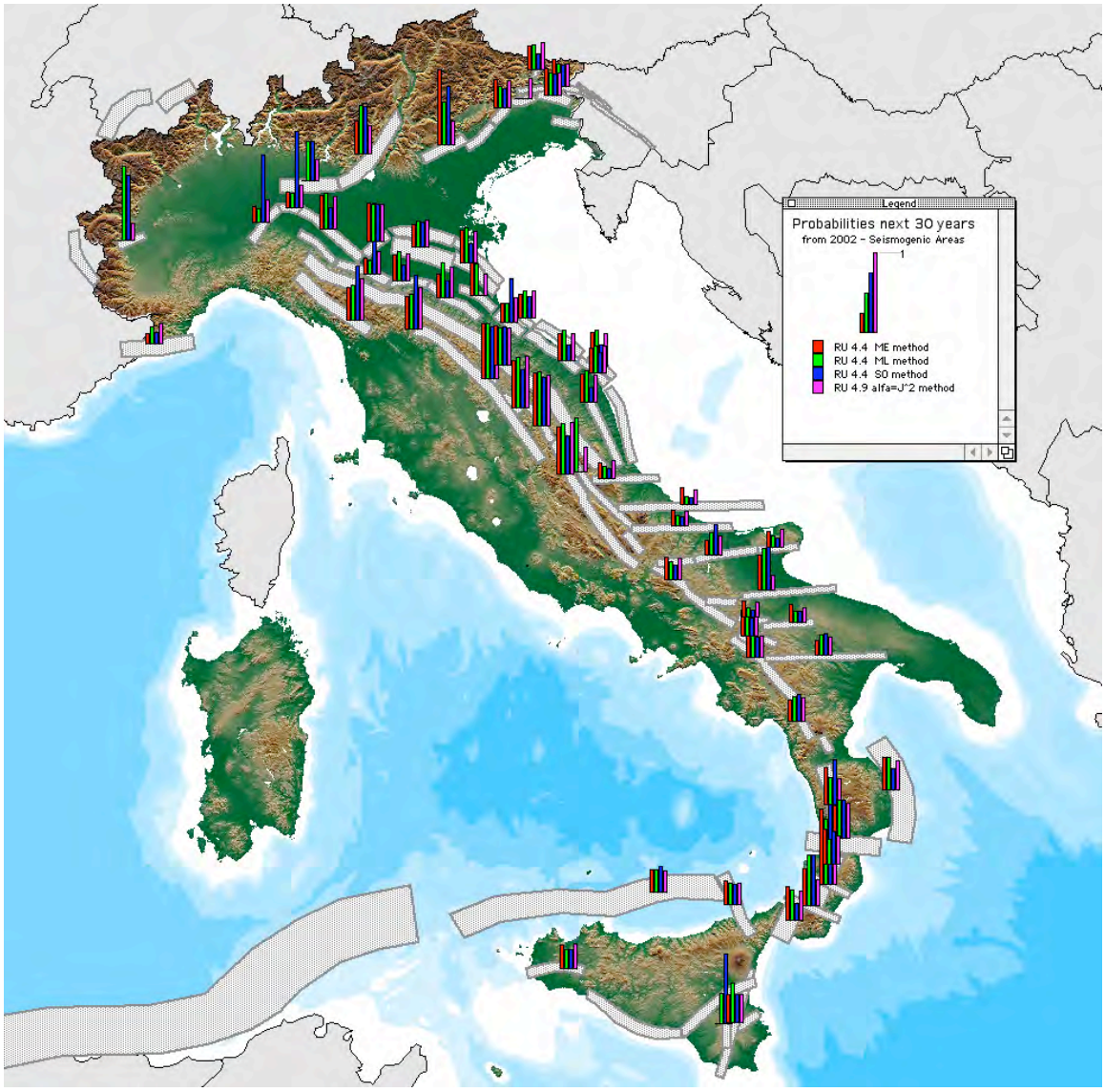

Figure 4.3 – Forecasts provided by RU 4.4 and RU 4.9 for the next 30 years (from 2003) for the Seismogenic Areas of DISS v3.0.2; details of the results in Fig. 4.4.

Theme 3 - Occurrence of a significant earthquake based on statistical analysis of earthquake and fault data

Theme 3 is expected to quantify the occurrence of a significant earthquake using statistical methods, and the RUs have been subdivided into two groups that produced estimates for Seismogenic Areas (SAs) and for Individual Seismogenic Sources (GG), respectively.

The statistical techniques developed independently by **RU 4.4** and **RU 4.9** during the project have been applied to the same population of interevent times. Eight macroregions (MR) have been identified by Task 1, and intertimes between earthquakes belonging to the same SA are now grouped in statistically acceptable samples.

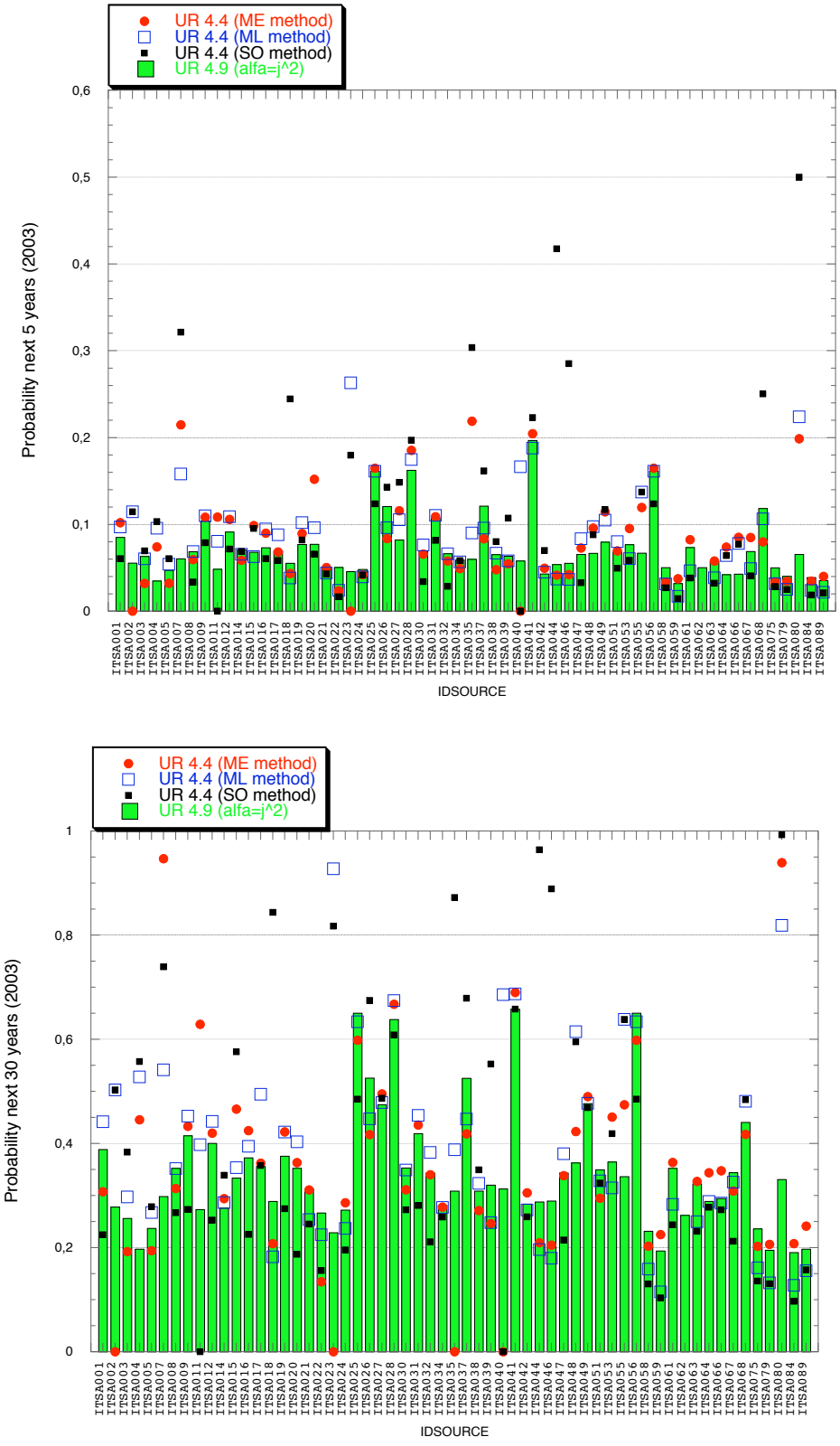

Figure 4.4 - Probability of occurrence of a main earthquake in the next 5 years (above) and 30 years (below) from 2003 in all Seismogenic Areas of DISS v3.0.2. The probabilities were computed by RU 4.9 using a nonparametric analysis of renewal processes, and by RU 4.4, modelling the renewal process by a combination of exponential and Weibull distributions. This latter computation was done according to three approaches (see the RU 4.4 report for more details) which led to different estimates.

RU 4.4 modeled the renewal process by a combination of exponential and Weibull distributions, parameterized on each MR with different techniques. **RU 4.9** used a nonparametric analysis of renewal processes and the distribution of intertimes is a continuos function having a certain probability assigned according to a stochastic process, called Polya tree, defined on a space of functions. Hazard rate defined as:

$$\lambda(t_0) = \frac{f_\tau(t_0)}{1 - F_\tau(t_0)}$$

and the probability associated with medium term prediction

$$P_{\Delta t_0 | t_0} = \frac{F_\tau(t_0 + \Delta t_0) - F_\tau(t_0)}{1 - F_\tau(t_0)}$$

are given in the extended report and in workshop proceedings for different time intervals [*Rotondi*, 2007; *Garavaglia et al.*, 2007]. The synthetic map of the results given in Figure 4.3 shows a generally good agreement between the forecasts provided by **RU 4.4** and **RU 4.9**; a snapshot of the probabilities referring to the next 5 and 30 years is given in Figure 4.4.

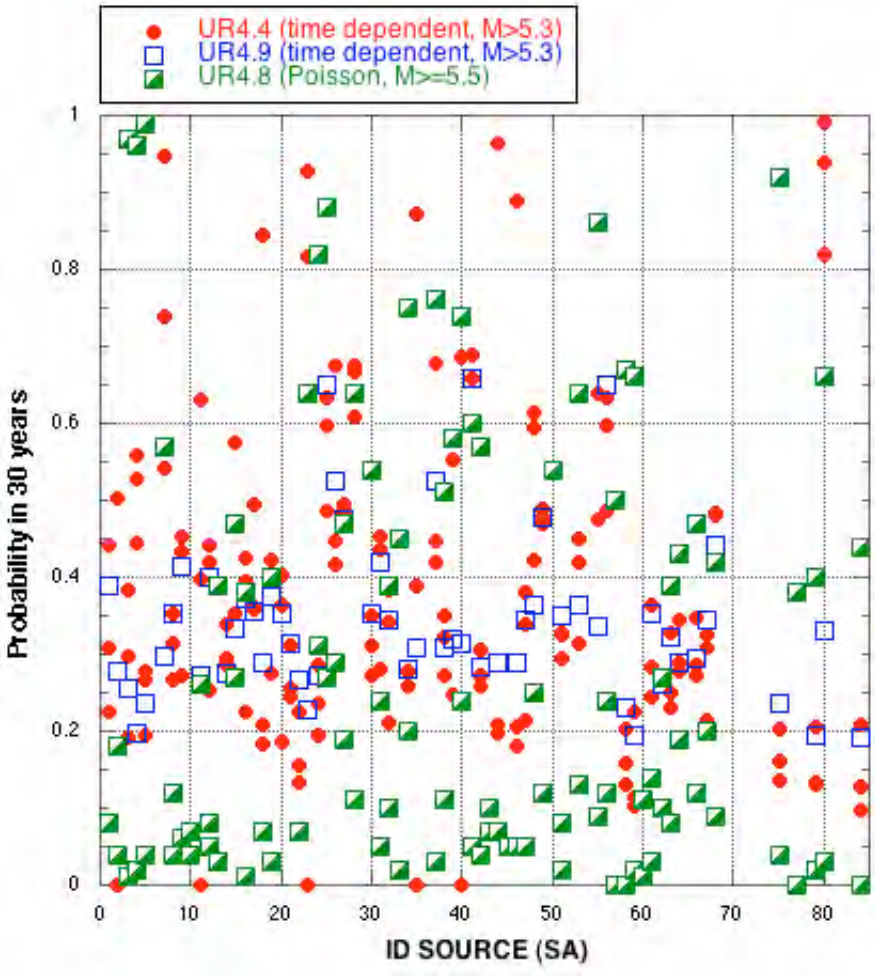

Figure 4.5 – Comparison between the time dependent forecasts referred to the Seismogenic Areas of Fig. 4.4 (RU 4.4 and RU 4.9) and the Poissonian estimates calibrated on the amount of moment rate derived from geodetic observations and geophysical modelling (see the report RU 4.8. for further details).

RU 4.8 attempted to apply geodetic constrains to the estimate of the probabilities of occurrence of large earthquakes. In this case the results of Task 3, in terms of moment rates computed over wide regions (from GPS measurements) and over the Seismogenic Areas (from geophysical modelling) were used as input data in the probability assessment. As pointed out

in the report of **RU 4.8**, this approach is innovative and the results must be considered preliminary and open to discussion. The agreement between the results from the two approaches is not satisfactory and the results from moment rates over DISS Seismogenic Areas are lower than those from moment rates over wide regions (see Fig. 6 of the **RU 4.8** report). Fig. 4.5 again shows this variability as well as the results obtained by **RU 4.4** and **RU 4.9**. It must be pointed out that the results of **RU 4.8** were obtained under a Poissonian earthquake occurrence model, while **RU 4.4** and **RU 4.9** applied a time-dependent model. Moreover, the forecasts refer to similar but not equal magnitudes (larger than 5.3 for **RU 4.4** and **RU 4.9**, larger than 5.4 for **RU 4.8**), and **RU 4.9** applied 3 different methodologies of computation, which led sometimes to a large variability of the estimates. In some cases the differences of the results according to the different approaches followed by the 3 RUs is quite large and the Poissonian estimates from moment rates over the Seismogenic Areas almost always represent the lowest values. Large Poissonian estimates should not be a surprise as it seems reasonable that using GPS-derived strains would result in forecasts that are somewhat larger than those obtained from the earthquake catalogue.

Comparable results were obtained by **RU 4.1** and **RU 4.8** using similar techiniques on individual seismogenic source data (GG sources). The conditional probability using renewal process and BPT distribution function is strongly influenced by the uncertainties on slip rate and on the date assigned to the most recent event. Different procedures have been developed to take into account the uncertainties, but if we do not consider earthquake sources for which the date of the last event is unknown (for which **RU 4.1** adopted a fixed elapsed time of about 1,300 years, while **RU 4.8** chose ~10,000 years), the estimates are rather similar (compare Fig. 9 of the report of **RU 4.1** and Fig. 5 of the report of **RU 4.8**). A comparison map is given in Figure 4.6.

Poissonian probabilities, given by both URs, also provide interesting elements to bridge the gap that exists between GG and SA sources. We consider therefore that the highest priority in data parametrization has now to be given to the definition of a reasonable – even if uncertain – elapsed time for all sources for which this information is not given at present.

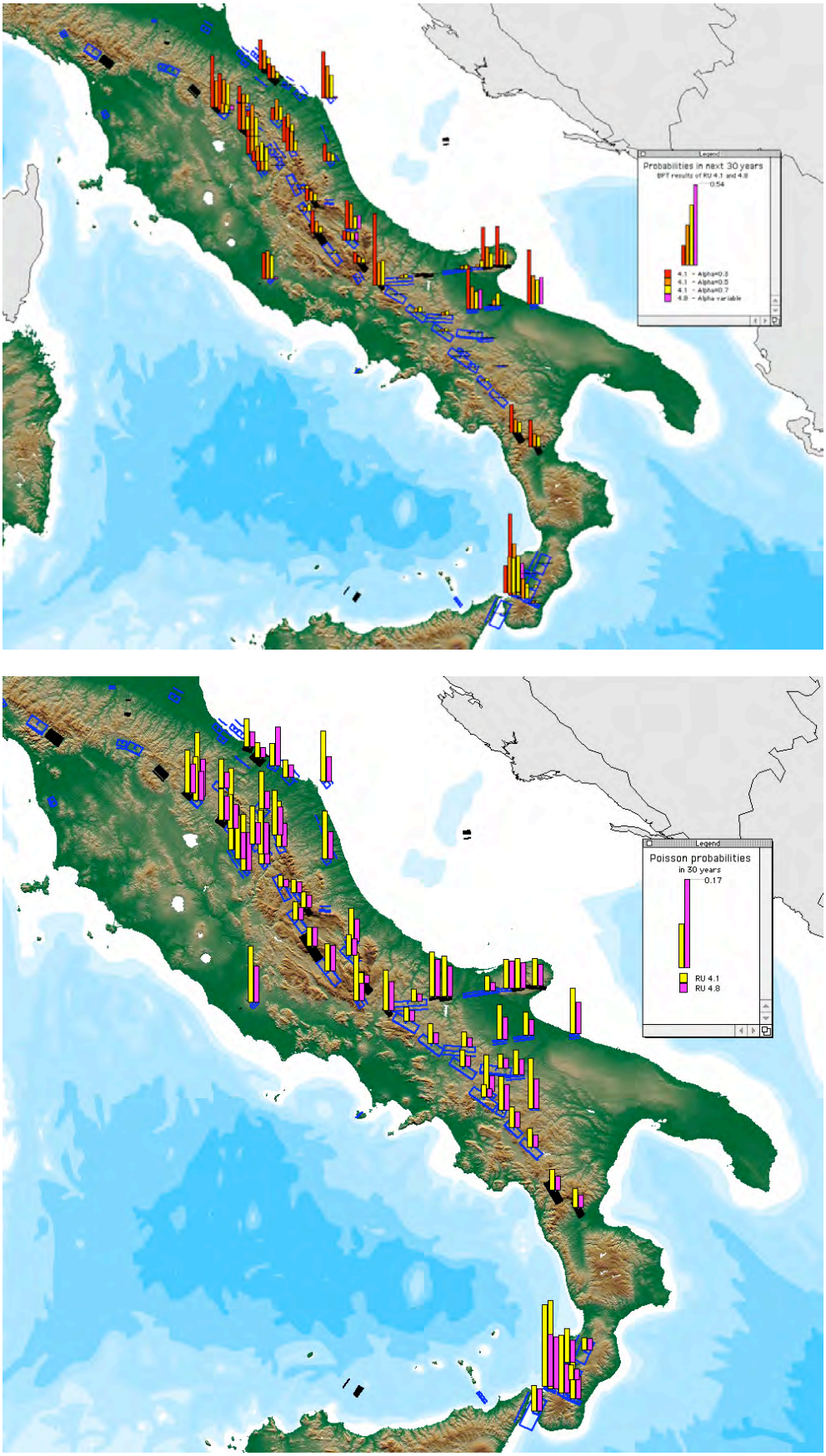

Figure 4.6 – Comparison of the results obtained by RU 4.1 and 4.8 for the sources treated by both RUs; above) probabilities of having a characteristic earthquake in individual GG sources of DISS 3.0.2 in the next 30 years (from 2006) based on BPT model; below) Poissonian probability of an event in 30 years.

Appendix A

Earthquake likelihood/earthquake hazard maps for Italy

by Steven N. Ward, University of California, Santa Cruz

Following the meeting "Earthquake and shaking probabilities" held in Erice (Sicily) in October 2006, the coordinators of the project "Assessing the seismogenic potential and the probability of strong earthquakes in Italy" asked me to produce several earthquake likelihood/earthquake hazard maps for Italy following similar procedures that I had used for California [*Ward*, 2007]. In response, I constructed five hazard models for Italy: three geologically-based, one based on historical seismicity, and one based on geodetic strain. These five models quantify time-independent or Poissonian hazard, and assume that earthquakes distribute in a Gutenberg-Richter fashion with b-value and Mmax fixed for the whole country. Potentially, future models might employ regionalized values of these parameters when they become available.

The geologically based maps employed INGV's "Seismogenic Areas" (SAs) from DISS v3.0.2. These several dozen areas purport to embody real faults, but ones with inferred and uncertain parameters. Even so, the computation of the earthquake density maps for the SAs was virtually the same as in California where fault information is more direct -- that is, fault slip rate to seismic moment rate, then seismic moment rate to earthquake rate density. The three geological maps differed only in the slip rates supplied by DISS for the SAs. Compared with historical seismicity, SA slip/moment rates on the lower end of their proposed range were definitely more appropriate.

All maps show 100 year probabilities are expressed as $\log_{10}$ rate of events per year M > 5.5 predicted in 100-km by 100-km boxes around each location. To get earthquake rates per km^2, multiply by 10^{-4}.

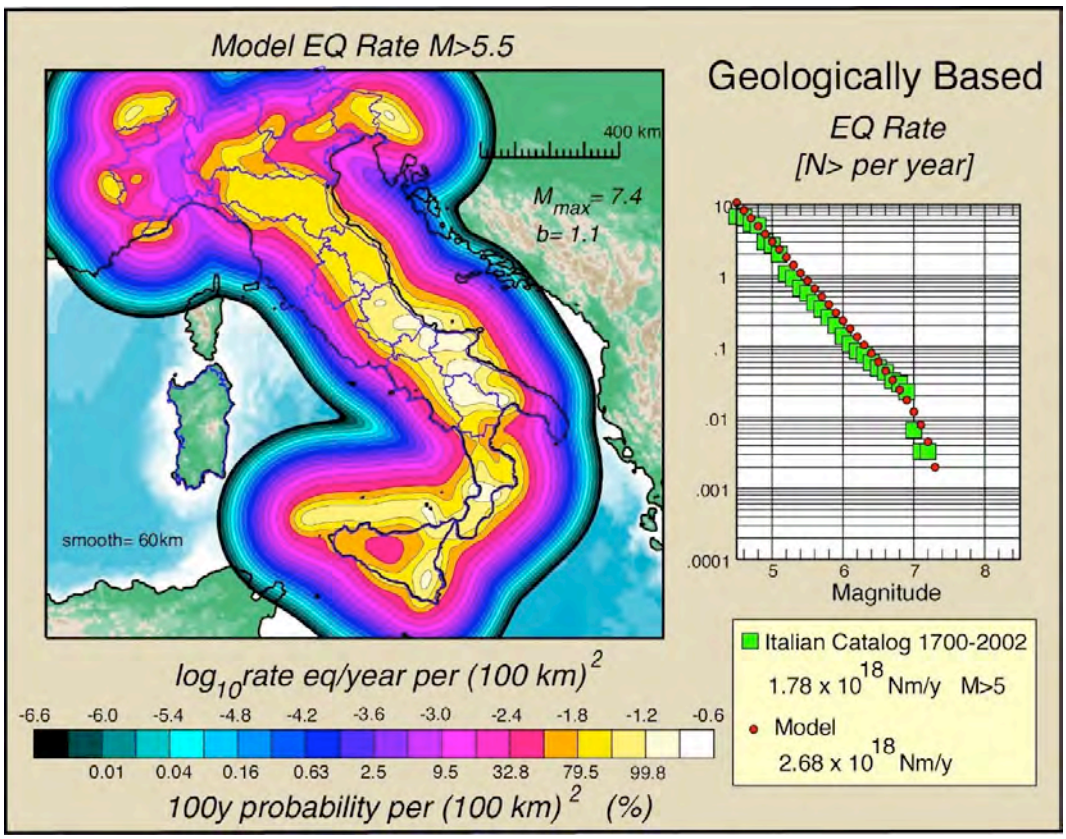

Fig. A1 – Model computed using mean slip rates from DISS v.3.0.2 ("Geological 1"). See also D 4.3.7 (map above).

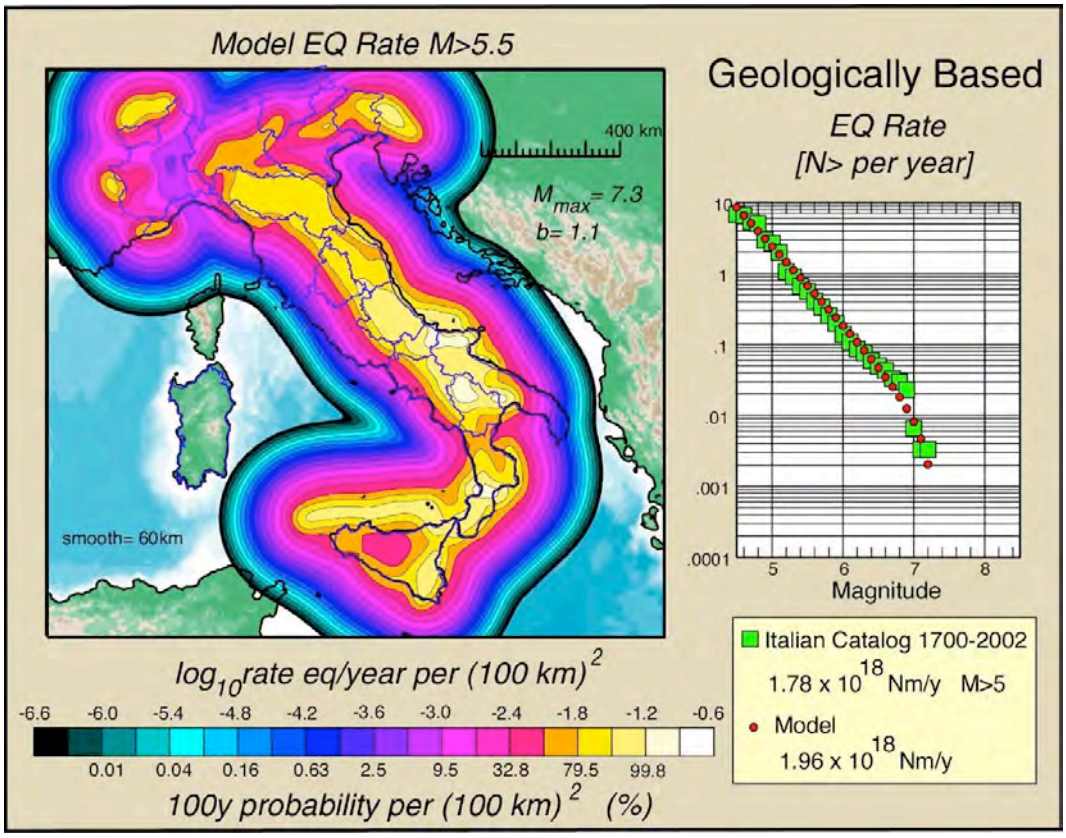

Fig. A2 –Same as A1 using slip rates 2/3 times mean ("Geological 2"). See also D 4.3.7 (map below).

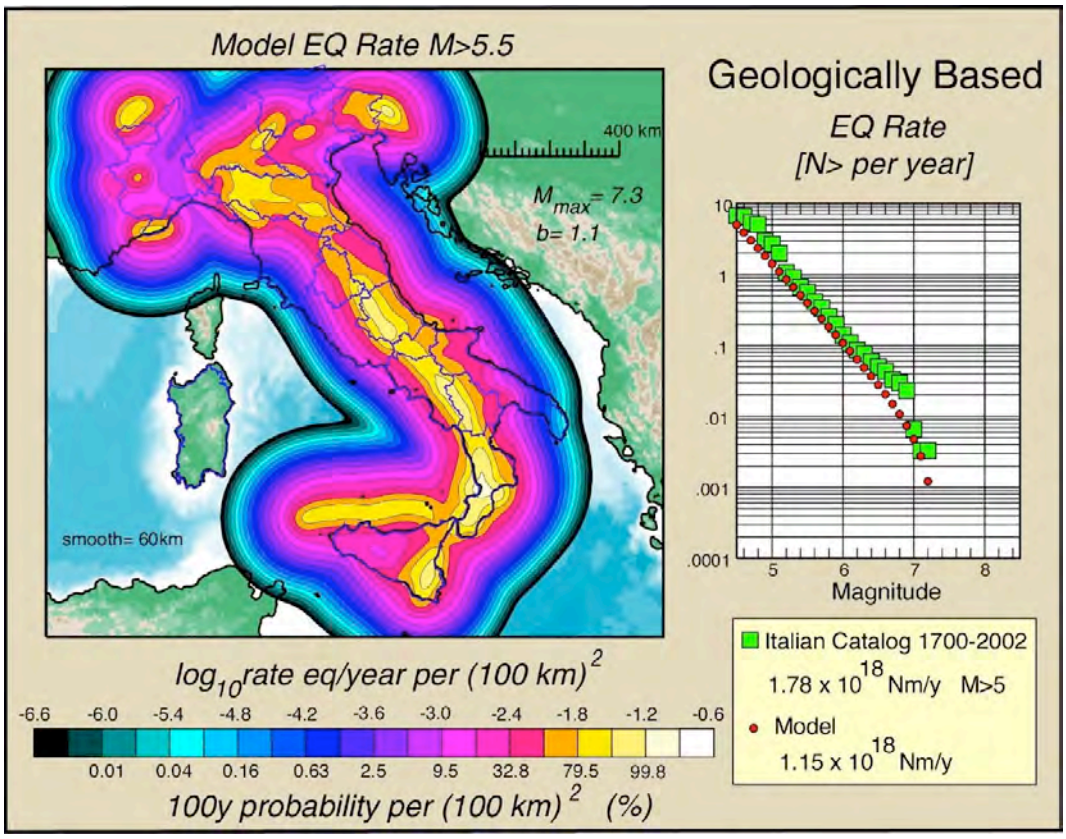

Fig. A3 –Same as A1 and A2 using slip rates derived from the Finite Element Model developed during the project ("Geological 3"). See also D 4.3.8.

The model "Geological 1" (Figure A1) took the mean rates, while "Geological 2" (Figure A2) took 2/3 times mean rates. The model "Geological 3" (Figure A3) took slips rates inferred from the Finite Element Model (FEM) described in Task 3 (slip rates are shown in Figures 3.11 and 3.1, and supplied in tabular form in Table 3.2). Slip rates from the FEM were even lower than "Geological 2" but still produced earthquake rates consistent with those observed historically.

Significant differences exist among "Geological(1/2)" and "Geological 3" that are reflected in the hazard maps. Future work might identify the most blatant differences in SA slip rates and attempt to narrow the gap. Also, compared with observed seismicity, I find several bands of earthquakes where no SA exists. Either the SAs need to be increased, or additional background seismic zones must be quantified and included with the SAs if direct comparison/validation of predicted and historical (and future) seismicity patterns are to be meaningful.

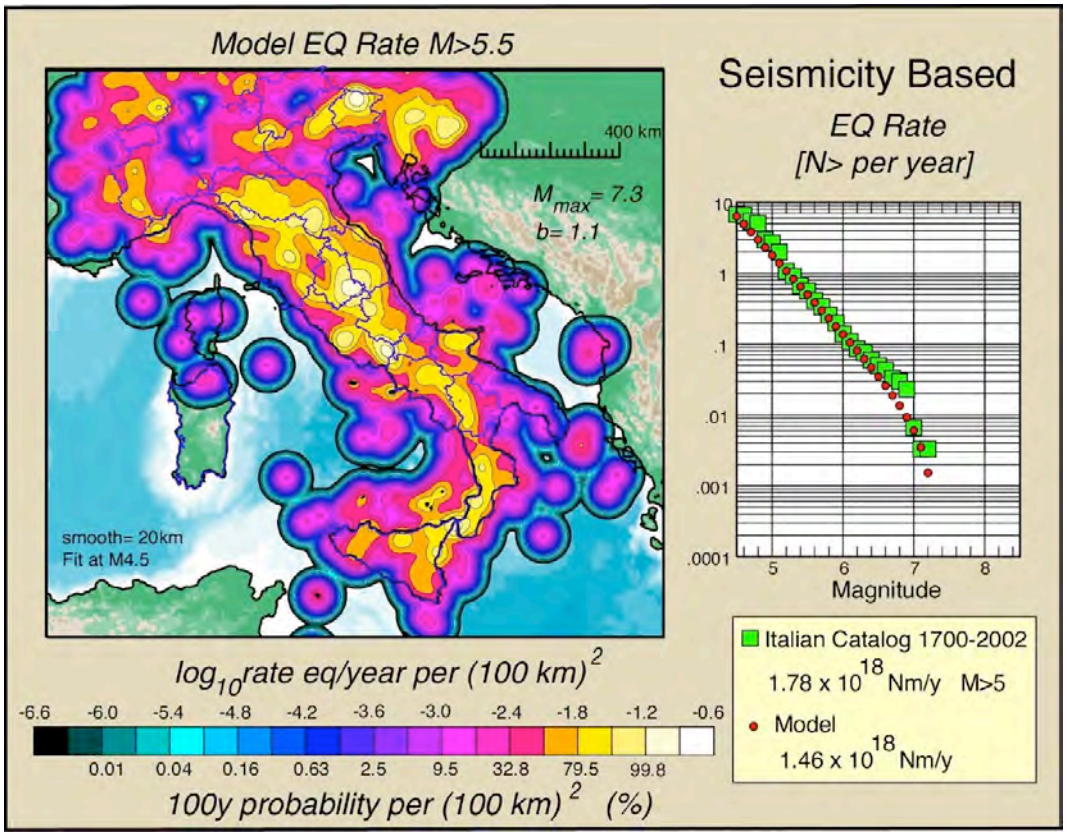

Fig. A4 –Model obtained from historical seismicity only ("Seismological"). See also D 4.3.6.

The "Seismological" model (Figure A4) used all earthquakes of M>4.5 from 1700 onward taken from the reference catalogue CPTI04 [*CPTI Working Group*, 2004]. Because earthquake magnitude was only used for a "in (M>4.5) or out (M<4.5)" selection, bias in the maps due to magnitude estimation should be limited. Still, I understand that macroseismic derived magnitudes for older events in the catalogue are widely thought to be overestimated. If this is so, efforts should be made to quantify and correct the situation.

Finally, the "Geodetic" model (Fig. A5) used velocity vectors from all permanent GPS sites plus a few "selected" campaign stations to compute strain rate. The selected stations filled gaps in coverage and were picked largely on my perception of the agreement of the local site motion with regional trends. Truth to say, there is quite a bit of noise in the Italian GPS data, however after several years, I believe that geodetic Italian deformation models are beginning to show similarities with geological and seismological ones. Seeing that geodesy offers a third, completely independent means to estimate seismic hazard, heavy effort should be made in the next few years toward expanding, integrating and improving the Italian GPS network. Likewise, because the geodetic approach to hazard requires a reliable "seismogenic thickness", continued efforts ought to be made to map this out as well as possible.

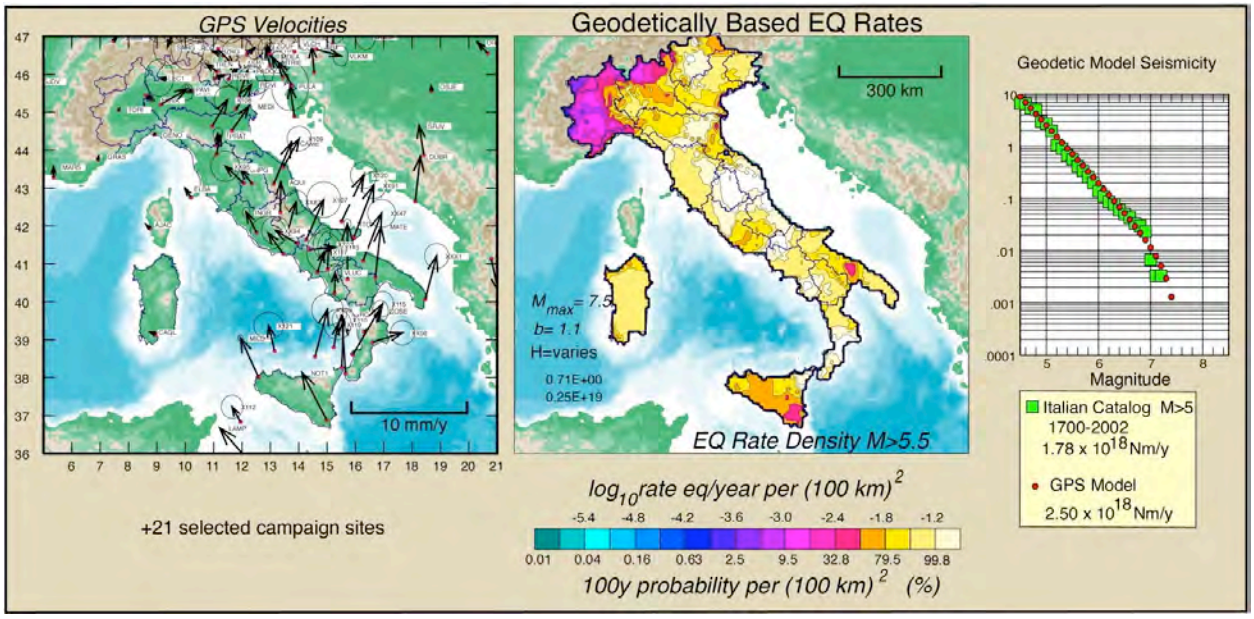

Fig. A5 –Model obtained from 241 GPS velocities from permanent and non-permanent stations ("Geodetic"). Calculations assume variable thickness of the seismogenic layer based on a preliminary model supplied by RU 3.1. See also D 4.3.9.

In the future, I visualize augmenting the hazard maps mentioned above with ones derived from a physical earthquake simulator. Earthquake simulators employ physical laws of stress accumulation and release to generate long catalogues of synthetic earthquakes. Earthquake simulators have found success in California (see http://es.ucsc.edu/~ward/ALLCAL-1100.mov/) and I see no reason why modest inroads might not be started toward the construction of an earthquake simulator for the fault system of Italy.

Main difficulties and countermeasures

In consideration of the innovative nature of the project, it was quite difficult to define from the very beginning all the branches in which the project was to be organized. While the general frame as well as the details of the majority of tasks were rather well delineated from the beginning of the work, important details were missing for some crucial activities. For example, different subjects had been proposed for Task 4, but in the first few months of activity the project coordination failed to devise a detailed plot merging all activities into a common framework.

For this reason a complete restyling of Task 4 was operated soon after the beginning of the project. In its original formulation, Task 4 was subdivided into 3 sub-tasks: 1) occurrence probability supported by physical models; 2) seismicity characteristics of the tectonic structures; 3) probabilities of main events on identified tectonic structures. After the initial meetings and comprehensive discussions with the concerned RUs on their expectations from the project, the project coordinators and the task leaders proposed a new structure that was discussed and agreed upon with the panel of international reviewers.

The restyling led to the following 3 sub-task, that are similar to the original ones but more tightly focused: 1) probability of an imminent earthquake using instrumental data-sets; 2) occurrence probabilities supported by physical model; 3) probabilities of main events supported by statistical models. The modified structure of Task 4 turned out to be fully satisfactory and all expected results have been achieved.

It is worth noting that time dependent analyses request a complete (non-declustered) catalogue, that is not currently available for Italy. Some of the estimates suffered from this circumstance but no viable solution could be found within the framework of S2.

A further limitation concerned GPS analyses. The Italian GPS record is still rather patchy and its accuracy is highly variable for different parts of the country. For this reason it was used essentially as a constraint for the Finite Elements Model developed in Task 3 and only secondarily as a source of primary information to evaluate earthquake probabilities.

A very general and recurrent issue concerns the timing of the different activities. The structure of S2 required that all of its components work sequentially rather than in parallel; the project implied a transfer of data from Task 2 (and secondarily Task 3) to Task 1, and then from Task 1 and Task 3 to Task 4. This implied that all scientists contributing to Task 2 and 3 should have worked principally in Year 1, those working on Task 1 at the end of Year 1, and those working on Task 4 Year 2 (Task 4). Although things can be somehow optimized (during Year 1 Task 4 scientists worked on testing procedures), such a forced schedule is clearly not acceptable in a two-year project. The problem was at least partially solved thanks to the circumstance that only a few weeks after beginning of the project scientists from Task 1 were able to supply a version of the DISS database that already had the final structure. A further version, that was released at the beginning of Year 2, is the one on which most of the calculations were based. Clearly, DISS' last version will be useful only for future work.

List of deliverables

The project generated a large number of deliverables that can all be accessed from a dedicated web-page (www.ingv.it/progettiSV/Progetti/Sismologici/sismologici.htm/). Following is a summary of the deliverables, organized by Task. Further information on the characteristics of the deliverable and on their input data are given in the same web-page. All deliverables have been hotlinked to their name and can hence be accessed from this page. Some of the deliverables (D 1.1., D 1.2., D 1.4., D 3.8.) are hosted on the server installed, set up, and maintained with resources coming from this project.

Notice that all results of Task 2 are presented as research accomplishments rather than as Deliverables. The main accomplishments are delivered to the final user in the form of updates of the DISS database.

Finally, notice that the Deliverables of Task 1 and 3 can be accessed freely, while access to those of Task 4 requires a password.

Task 1

Task 1 generated a large amount of significant deliverables that served as a basis for other activities of the project and for the other projects launched within the INGV-Department of Civil Defence agreement 2004-2006. The deliverables include also the results of the elaborations conducted jointly by **RU 1.1** and **RU 2.19b** on tsunami scenarios. The reader is ecouraged to refer to individual RU reports for further details.

D 1.1.: the DISS database is fully available on the Internet and can be accessed using two independent interfaces. From the DISS web portal (http://www.ingv.it/DISS/) users can start two cartographic interfaces (web browser oriented and Google Earth), seamlessly download data tables in several (most common) GIS formats, and gain insights about the scientific and technical background of the database itself.

D 1.2.: thematic maps obtained either by splicing multiple relational DISS layers or by cross examining DISS layers with external databases.

D 1.3.: the EMMA database on the internet. From the database main page users can download the EMMA main files and then install it on their own computers.

D 1.4.: tsunami scenarios of the maximum water elevation on Southern Italy coastlines obtained by a joint effort of RU 1.1 and RU 2.19b.

From Project S3: In-depth analyses on a number of seismogenic sources that have been used as input data for shaking scenarios (URL on S3 Project web site).

Deliverables 1.1, 1.2, 1.4 are hosted on the server installed, set up, and maintained with resources coming from this project.

Task 3

The deliverables of Task 3 report on the construction of the reference velocity and strain model derived by **RU 3.1**, **RU 3.2a**, **RU 3.2b**, **RU 3.3** and **RU 3.4**, on the Finite Element Modelling developed by **RU 3.1** and on the calculation of slip rates to be used for probability calculations in Task 4. The reader may refer to individual RU reports for further details.

D 3.1.: GPS-derived velocity map elaborated by the RU 3.2a, RU 3.2b and RU 3.1 using a large set of GPS velocities from permanent Italian and non-Italian stations.

D 3.2.: GPS-derived strain map obtained by RU 3.2a for northern Italy using all data presented in D 3.1.

D 3.3.: GPS-derived strain map obtained by RU 3.2a for central Italy using all data presented in D 3.1.

D 3.4.: GPS-derived strain map obtained by RU 3.2a for central Italy using all data presented in D 3.1.

D 3.5.: Velocity map derived by RU 3.1 from averaging results of the best 50 among 33,000 forward finite-element anelastic models. The data are also supplied in tabular form .
D 3.6.: Strain map derived by RU 3.1 from finite-element anelastic models (see D 3.5.).
D 3.7.: Slip-rate map derived finite-element anelastic models (see D 3.5.) and spatial averaging over DISS seismogenic areas. The data are also supplied in tabular form.
D 3.8.: Strain rates and slip rates for DISS v3.0.2 Seismogenic Areas derived finite-element anelastic models (see D 3.5.), in map and tabular form. The data are also supplied in tabular form.

Task 4

The deliverables of Task 4 comprise a set of elaborations aimed at parameterizing the behavior of a given set of seismogenic sources taken from the DISS database and to assign each source a probability of giving a large earthquake. The reader is encouraged to refer to individual RU reports for further details.

Following the structure of the task, also the deliverables refer to three distinct themes:

Theme 1 - Occurrence of an impending earthquake based on instrumental data

D 4.1.1.: Backward probability of an impending earthquake (24 hours) based on Epidemic Type Aftershock Sequence (ETAS) method for all M>5.0 eqs (1987-2005), by RU 4.7.
D 4.1.2.: Application of the Accelerating Moment Release method (AMR) to selected Italian earthquakes, by RU 4.2.
D 4.1.3.: Probability of an earthquake of magnitude 3 (above) and 4 (below) in 30 years after the occurrence of the last event in the catalogue (based on CSI catalogue 1981-2002), by RU 4.5.

Theme 2 - Occurrence of a significant earthquake based on physical models

D 4.2.1.: Synthetic catalogues and analysis of Inter-Event Times (IET) for individual earthquake sources from fault interaction, modeled by co-seismic Coulomb Failure Function and empirical post-seismic relaxation, by RU 4.3.
D 4.2.2.: Numerical simulation of transient strain perturbations due to post-seismic relaxation effects, by RU 4.6.
D 4.2.3.: Perturbation on time-dependent renewal probability of activation of individual geologic sources, resulting from static Coulomb stress changes (permanent and transient effects), by RU 4.7.

Theme 3 - Occurrence of a significant earthquake based on statistical analysis of earthquake and fault data

D 4.3.1.: Time-dependent probability of occurrence of main earthquake in the next 30 years, based on combined exponential-Weibull distributions of empirical interevent times in Seismogenic Areas or macroregions, by RU 4.4.
D 4.3.2.: Time-dependent probability of occurrence of main earthquake in the next 5 and 30 years, based on nonparametric analysis (Polya trees) of empirical interevent times in Seismogenic Areas or macroregions, by RU 4.9.
D 4.3.3.: Time-dependent probability of occurrence of main characteristic earthquake in the next 30 years for the central Apennines and Calabria, obtained using BPT distribution on DISS v3.0.2 Individual Seismogenic Sources, by RU 4.1.
D 4.3.4.: Time-dependent probability of occurrence of main characteristic earthquake in the next 30 years for Italy, obtained using BPT distribution on on DISS v3.0.2 Individual Seismogenic Sources, by RU 4.8.
D 4.3.5.: Time-independent (Poissonian) probability of occurrence of target earthquake in 30

years with geodetic and regional seismicity constraints on DISS v3.0.2 Seismogenic Areas, by RU 4.8.

D 4.3.6.: Time-independent (Poissonian) probability of occurrence of a significant earthquake, based on a smoothed seismicity approach. The data are also supplied in tabular form. Elaboration by Steven Ward.

D 4.3.7.: Time-independent (Poissonian) probability of occurrence of significant earthquake, based on based on DISS v3.0.2 Seismogenic Areas and associated slip rates. The data are also supplied in tabular form. Elaboration by Steven Ward.

D 4.3.8.: Time-independent (Poissonian) probabilty of occurrence of significant earthquake, based on DISS v3.0.2 Seismogenic Areas and on Finite Elements Model by RU 3.1. The data are also supplied in tabular form. Elaboration by Steven Ward.

D 4.3.9.: Time-independent (Poissonian) probabilty of occurrence of significant earthquake, based on GPS velocities. Elaboration by Steven Ward.

Referenced papers

Bird P. (1999). Thin-plate and thin-shell finite-element programs for forward dynamic modeling of plate deformation and faulting. *Computers & Geosciences*, 25, 383-394.

Bird, P. (2003). An updated digital model of plate boundaries, Geochem. Geophys. Geosyst., 4(3), 1027, doi:10.1029/2001GC000252.

CPTI Working Group (2004). Catalogo Parametrico dei Terremoti Italiani, version 2004 (CPTI04). INGV, Milan, available from http://emidius.mi.ingv.it/CPTI/.

Di Stefano, R., F. Aldersons, E. Kissling, P. Baccheschi, C. Chiarabba, D. Giardini (2006). Automatic seismic phase picking and consistent observation error assessment: application to the Italian seismicity. *Geophys. J. Int.*, 165, p. 121-134.

Hardebeck, J.L., K.R. Felzer, A.J. Michael (2007). Rigorous Observational Tests Contradicts the Accelerating Moment Releas Hypothesis. submitted. Manuscript circulated at STATSeis Workshop, Erice 2007.

Garavaglia, E., et al. (2007). La predicibilità di un terremoto caratteristico nell'ipotesi dei processi di rinnovo del tipo mistura, in Quaderni del Dipartimento di Matematica. Politecnico di Milano: Milano. p. http://www.mate.polimi.it/biblioteca/qddview.php?id=1329&L=i.

Gasperini, P., G. Vannucci (2003). FPSPACK: a package of FORTRAN subroutines to manage earthquake focal mechanism data. *Computers & Geosciences*, 29, 893–901.

Grant, D.N., et al. (2006). Defining Priorities and Timescales for Seismic Intervention in School Buildings in Italy, in ROSE Report, I. Press, Editor. ROSE: Pavia. p. 2006/03.

Gruppo di Lavoro, Redazione della mappa di pericolosità sismica prevista dall'Ordinanza PCM 3274 del 30 marzo 2003 (2004). Rapporto conclusivo per il Dipartimento di Protezione Civile, INGV, Milano-Roma, 65 pp., http://zonesismiche.mi.ingv.it/.

Montone, P., M.T. Mariucci, S. Pondrelli, A. Amato (2004). An improved stress map for Italy and surrounding regions (Central Mediterranean). *J. Geophys. Res.*, 109, B10410, doi:10.1029/2003JB002703.

Okal, E.A. and Synolakis C.E (2004). Source discriminants for near-field tsunamis. *Geophys. J. Int.*, 158, 899-912.

Pace, B., et al. (2006). Layered Seismogenic Source Model and Probabilistic Seismic-Hazard Analyses in Central Italy. *Bull. Seismi. Soc. Am.*, 96(1), 107-132.

Rotondi, R. (2007). Time-dependent hazard through nonparametric Bayesian estimation of the interevent time probability density. in Statistical Seismology: Physical and Stochastic Modelling of Earthquake Occurrence and Forecasting. 2007. Erice, 31 May-6 June 2007: 5th International Workshop.

Serpelloni, E., M. Anzidei, P. Baldi, G. Casula, A. Galvani (2005). Crustal velocity and strain-rate fields in Italy and surrounding regions: new results from the analysis of permanent and non-permanent GPS networks. *Geophys. J. Int.*, 161, 861-880.

Serpelloni E., Vannucci G., Pondrelli S., Argnani A., Casula G., Anzidei M., Baldi P. and Gasperini P. (2007). Kinematics of theWestern Africa-Eurasia plate boundary from focal mechanisms and GPS data. Geophys. J. Int., 169/3, 1180-1200, doi: 10.1111/j.1365-246X.2007.03367.x.

Vannucci, G., P. Gasperini (2003). A database of revised fault plane solutions for Italy and surrounding regions. *Computers & Geosciences*, 29, 903–909.

Various Authors, Earthquake and shaking probabilities: helping society to make the right choice, in 26th Workshop of Geophysics. 2006, EMCSC: Erice, Sicily.

Ward, S. N. (2007). Methods for evaluating earthquake potential and likelihood in and around California. Seism. Res. Letters, 78, 121-133.

Papers published or submitted during the project

This section contains papers that were written based on results and activities of the project, or that were partially funded by the project. Given its two-year length, many of the papers are still at the stage of first or second submission. All papers are rated according to the following scheme:

CP - Conference Proceedings
JP - JCR paper, Published or in press
JU – JCR paper, Unpublished (submitted)
NJ – Non-JCR paper, published or unpublished

Task 1

1) Basili, R., G. Valensise, P. Vannoli, P. Burrato, U. Fracassi, S. Mariano, M.M. Tiberti, E. Boschi (2007). The Database of Individual Seismogenic Sources (DISS), version 3: summarizing 20 years of research on Italy's earthquake geology. *Tectonophysics*, in press. **JP**

Task 2

1) Argnani, A., G. Brancolini, M. Rovere, F. Accaino, F. Zgur, M. Grossi, F. Fanzutti, P. Visnovic, D. Sorgo, E. Lodolo, C. Bonazzi and N. Mitchell (2006). Indizi di tettonica attiva nello Stretto di Messina e nelle aree adiacenti: risultati preliminari della campagna geofisica TAORMINA-2006. *Rend. Soc. Geol. It.*, 4, 138-139. **JP**
2) Argnani, A., G. Brancolini, M. Rovere, F. Accaino, F. Zgur, M. Grossi, F. Fanzutti, P. Visnovic, D. Sorgo, E. Lodolo, C. Bonazzi, and N. Mitchell (2006). Hints on active tectonics in the Messina Straits and surroundings: preliminary results from the TAORMINA-2006 seismic cruise. XXV Convegno del Gruppo Nazionale di Geofisica della Terra Solida. Roma, 28-30 Novembre 2006. **CP**
3) Argnani, A., Brancolini G., Rovere M., Accaino F., Zgur F., Grossi M., Fanzutti F., Visnovic P., Sorgo D., Lodolo E., Bonazzi C., and Mitchell N. (2007). Hints on active tectonics in the Messina Straits and surroundings: preliminary results from the TAORMINA-2006 seismic cruise. *Boll. Geof. Teorica Appl.*, submitted. **NJ**
4) Barberi, G., L. Beranzoli, P. Favali, G. Neri and T. Sgroi (2006). Seismic location improvements from an OBS/H temporary network in southern Tyrrhenian Sea. *Ann. Geophys.*, 49, 739-749. **JP**
5) Burrato, P., e G. Valensise (2007). Rise and fall of an hypothesized seismic gap: source complexity in the 1857, southern Italy earthquake (Mw 7.0). *Bull. Seism. Soc. Am.*, submitted. **JU**
6) Burrato, P., M.E. Poli, P. Vannoli, A. Zanferrari, R. Basili, F. Galadini (2007). Sources of Mw 5+ earthquakes in northeastern Italy and western Slovenia: an updated view based on geological and seismological evidence. *Tectonophysics*, in press. **JP**
7) Billi, A., Barberi, G. , Faccenna, C., Neri, G., Pepe, F., Sulli, A. (2006). Tectonics and seismicity of the Tindari Fault System, southern Italy: crustal deformations at the transition between ongoing contractional and extensional domains located above the edge of a subducting slab. *Tectonics*, 25, TC2006, doi:10.129/2004TC001763. **JP**
8) Billi, A., Presti, D., Faccenna, C., Neri, G., and Orecchio, B. (2007). Seismotectonics of the Nubia plate compressive margin in the south-Tyrrhenian region, Italy: clues for subduction inception. *J. Geophys. Res.*, 112, B08302, doi:10.1029/2006JB004837. **JP**
9) Catalano, S., G. De Guidi, C. Monaco, G. Romagnoli, S. Torrisi, G. Tortorici, L. Tortorici (2006). Evidence of a Late Quaternary tectonic inversion in the Hyblean Plateau. XXV Convegno del Gruppo Nazionale di Geofisica della Terra Solida. Roma, 28-30 Novembre 2006. **CP**
10) Catalano, S., G. De Guidi, G. Lanzafame, C. Monaco, S. Torrisi, G. Tortorici and L. Tortorici (2006). Inversione tettonica positiva tardo-quaternaria nel Plateau Ibleo (Sicilia SE). *Rend. Soc. Geol. It.*, n. 2, Nuova serie, 118-120. **JP**
11) Catalano, S., G. De Guidi, G. Romagnoli, S. Torrisi, G. Tortorici and L. Tortorici (2006). Evidence of a Late Quaternary tectonic inversion along the Scicli line: implications for the sismotectonics of SE Sicily. GNGTS 25° Convegno Nazionale Roma 28-30 Novembre 2006 Consiglio Nazionale delle Ricerche. **CP**

12) Catalano, S., G. Romagnoli, G. De Guidi, S. Torrisi, G. Tortorici and L. Tortorici (2007). Evoluzione neogenico-quaternaria della Linea del Tellaro: relazioni con la dinamica del Plateau Ibleo (Sicilia SE). *Rend. Soc. Geol. It.*, 4 , NS, 177-180. **JP**
13) Catalano, S., S. Torrisi, G. De Guidi, G. Grasso, G. Lanzafame, G. Romagnoli, G. Tortorici and L. Tortorici (2007). Sistema a pieghe tardo-quaternarie nell'area di Catania: un esempio di fronte orogenico attivo. *Rend. Soc. Geol. It.*, 4, NS, 181-183. **JP**
14) Catalano, S., G. De Guidi, G. Romagnoli, S. Torrisi, G. Tortorici and L. Tortorici (2007). The role of the Scicli Line in the seismotectonic picture of the Hyblean Plateau (SE Sicily). *Tectonophysics*, submitted. **JU**
15) Cucci L. e A. Tertulliani (2006). I terrazzi marini nell'area di Capo Vaticano (Arco Calabro): solo un record di sollevamento regionale o anche di deformazione cosismica? *Il Quaternario*, 19(1), 89-101. **NJ**
16) Di Bucci D., S. Coccia, U. Fracassi, V. Iurilli, G. Mastronuzzi, G. Palmentola, P. Sansò, G. Selleri e G. Valensise (2007). Late Quaternary deformation of the southern Adriatic foreland: new mesostructural data from southern Apulia (Italy). *Tectonophysics*, submitted. **JU**
17) Di Bucci,, D., Massa, B., Tornaghi, M., Zuppetta, A. (2006). Structural setting of the Southern Apennine fold-and-thrust belt (Italy) at hypocentral depth: the Calore Valley case history. *Journal of Geodynamics*, 175-193. doi:10.1016/j.jog.2006.07.001. **JP**
18) Di Bucci, D., B. Massa, A. Zuppetta (2006). Relay ramps in active normal fault zones: a clue to the location of seismogenic sources (1688 Sannio earthquake, Italy). *Geological Society of America Bulletin*, 118, 430–448. **JP**
19) Ditta, M., P. Bonfanti, A. Caracausi, F. Italiano, G. Martinelli, R. Maugeri, R. Petrini, S. Pizzullo, A. Riggio, M. Santulin, F. Slejko. (2006). I fluidi come strumento per individuare e valutare l'attività di strutture tettoniche: risultati nell'area Friuli-Slovenia. XXV Convegno del Gruppo Nazionale di Geofisica della Terra Solida. Roma, 28-30 Novembre 2006, 312-313. **CP**
20) Favali, P., A. De Santis, B. Di Sabatino, M. Sedita e E. Rubino (2006). An active volcano in the Tyrrhenian Sea? *Ann. Geophys.*, 49, 793-800. **JP**
21) Fracassi, U., G. Valensise (2007). Unveiling the sources of the catastrophic 1456 multiple earthquake: hints to an unexplored tectonic mechanism in southern Italy. *Bull. Seism. Soc. Am.*, **97(3)**, 725-748. **JP**
22) Galadini, F. and M. Stucchi (2007). La sismicità del settore atesino delle Alpi centrali (Italia settentrionale): alcuni problemi aperti, limiti ed implicazioni dell'approccio multidisciplinare (geologico, storico-sismologico, archeosismologico e archeologico-architettonico). *Geographica Historica*, 24, 82-98. **NJ**
23) Gerardi, F., De Martini P.M., Barbano M.S., Pantosti D. (2006). Nature of tsunami sources (earthquake or landslide) in eastern Sicily and southern Calabria as inferred from historical data. XXV Convegno del Gruppo Nazionale di Geofisica della Terra Solida. Roma, 28-30 Novembre 2006, 63-66. **CP**
24) Gerardi, F., Barbano M.S., De Martini P.M., Pantosti D. (2007). Discrimination of the nature of tsunami sources (earthquake vs. landslide) in eastern Sicily and southern Calabria as inferred from historical data. *Marine Geology*, submitted. **JU**
25) Giocoli, A., C. Macrì, P. Vannoli, S. Piscitelli, E. Rizzo, A. Siniscalchi, P. Burrato, C. Basso, S. Di Nocera (2007). Electrical resistivity tomography investigations in the Ufita Valley (Southern Italy). *Annals of Geophysics*, submitted. **JU**
26) Gori, S., F. Dramis, F. Galadini, P. Messina (2007). The use of geomorphological markers in the footwall of active faults for kinematic evaluation: examples from the central Apennines. *Boll. Soc. Geol. It.*, 126, in press. **NJ**
27) Guarnieri, P. (2006). Plio-Quaternary segmentation of the south Tyrrhenian forearc basin. *Int. J. Earth Sci.*, 95, 107-118, doi: 10.1007/s00531-005-0005-2. **JP**
28) Guarnieri, P. and Pirrotta C. (2007). The response of drainage basins to the development of the modern Messina Strait (NE-Sicily). *Geomorphology*, in press. **JP**
29) Guarnieri, P., Pirrotta C., Barbano M.S., De Martini P.M., Gerardi F., Pantosti D. and Smedile A. (2007). Geological evidence of seismically-induced liquefaction in eastern Sicily. *Engineering Geology*, submitted. **JU**
30) Guerra, I., C. De Rose, A. Gervasi, G. Neri, B. Orecchio, D. Presti (2006). Attività sismica recente in Calabria Centro-Meridionale. In: Guerra I. e Savaglio A. (a cura di): 8 settembre 1905 Terremoto in Calabria, Univ. della Calabria. **CP**
31) Italiano, F., P. Bonfanti, A. Caracausi, M. Ditta, G. Martinelli, R. Maugeri, R. Petrini, S. Pizzullo, A. Riggio, and F. Slejko. (2006). I fluidi come strumento per individuare e valutare l'attività di strutture tettoniche: risultati nell'area Friuli-Slovenia. XXV Convegno del Gruppo Nazionale di Geofisica della Terra Solida. Roma, 28-30 Novembre 2006, 305-307. **CP**
32) Italiano, F., P. Bonfanti, A. Caracausi, M. Ditta, R. Favara, E. Gagliano Candela, R. Maugeri, F. Nigro, P. Renda, and C. Scaletta. (2006). Attività di emissione di fluidi lungo strutture tettoniche: risultati nell'area della Sicilia Nord-Orientale. XXV Convegno del Gruppo Nazionale di Geofisica della Terra

Solida. Roma, 28-30 Novembre 2006, 302-305. **CP**
33) Italiano, F., D'Alessandro W., Martelli M. (2007). Gas geochemistry as a tool to investigate the Earth degassing through volcanic and seismic areas: the soul of the 8th International Conference on Gas Geochemistry. *J. Volc. Geoch. Res.* , in press. **JP**
34) Lorito, S., M.M. Tiberti, R. Basili, A. Piatanesi, G. Valensise (2007). Earthquake-generated tsunamis in the Mediterranean Sea: scenarios of potential threats to Southern Italy. *J. Geophys. Res.*, suitable for publication after minor revision (as of July 2007). **JU**
35) Maschio, L., L. Ferranti (2006). Tettonica medio pleistocenico-olocenica al confine tra i Monti del Matese e del Sannio: implicazioni sulla geometria della fagliazione attiva. *Rend. Soc. Geol. It.*, 2, N. S., 150-151. **JP**
36) Massa, B., and Zupetta A. (2006). Indagini geologiche nell'area di massimo danneggiamento del Terremoto del Sannio del 1688 (Appennino meridionale) nell'ambito del Progetto DPC-INGV S2.20. XXV Convegno GNGTS. Riassunti estesi delle comunicazioni. Roma, 28-30 Novembre 2006. **CP**
37) Meletti, C., F. Galadini, G. Valensise, M. Stucchi, R. Basili, S. Barba, G. Vannucci, E. Boschi (2007). The ZS9 seismic source model for the seismic hazard assessment of the Italian territory. Submitted to *Tectonophysics*. **JU**
38) Montuori, C., G.B. Cimini, P. Favali (2007). Teleseismic tomography of the southern Tyrrhenian subduction zone: New results from seafloor and land recordings. *J. Geophys. Res.*, 112, B03311, doi:10.1029/2005JB004114. **JP**
39) Nappi, R., G. Alessio, G. Bronzino, C. Terranova, G. Vilardo (2007). Contribution of the SISCam Web-based GIS to the seismotectonic study of Campania (Southern Apennines): an example of application to the Sannio-area. *Natural Hazards*, submitted. **JU**
40) Nappi, R., G. Alessio, G. Vilardo, E. Bellucci Sessa, G. Ventura (2007). Analisi morfometrica integrata in ambiente GIS applicata ad aree tettonicamente attive come contributo alla valutazione dei rischi ambientali. *Geografia Fisica e Dinamica del Quaternario*, submitted. **NJ**
41) Neri, G., Oliva, G., Orecchio, B., and Presti, D. (2006). A possible seismic gap within a highly seismogenic belt crossing Calabria and Eastern Sicily, Italy. *Bull. Seism. Soc. Am.*, 96, 4, 1321–1331, doi: 10.1785/0120050170. **JP**
42) Petrini, R., F. Slejko, G.B. Carulli, F. Italiano, M. Ditta, P. Bonfanti, R. Maugeri, and A. Caracausi (2006). Caratteristiche chimiche ed isotopiche di acquiferi in zone di faglia nel settore orientale delle Alpi Meridionali: implicazioni sui modelli di flusso in aree sismogeniche. XXV Convegno GNGTS. Riassunti estesi delle comunicazioni. Roma, 28-30 Novembre 2006, 355-356. **CP**
43) Petrini, R., Slejko F., Italiano F., Carulli, G.B. and Ditta M. (2007). Geochemical evidence of a tectonically active regime in the Fella-Sava fault zone (NE Italy): possible implications for long-term fault strength. *Tectonophysics*, submitted. **JU**
44) Pettenati, F., L. Sirovich (2007). Validation of the Intensity-Based Source Inversions of Three Destructive California Earthquakes. *Bull. Seism. Soc. Am.*, in press. **JP**
45) Pino, N.A., Palombo B., Ventura G., Perniola B., Ferrari G. (2007). Waveform modeling of historical seismograms of the 1930 Irpinia earthquake provides insight on 'blind' faulting in Southern Apennines (Italy). *J. Geophys. Res.*, submitted. **JU**
46) Pirrotta, C., Barbano M.S., Guarnieri P., De Martini P.M. and Gerardi F. (2007). New empirical relationships between magnitude and distance for liquefaction in eastern Sicily. *Annals of Geophysics*, submitted. **JU**
47) Pirrotta, C., Guarnieri P., Barbano M.S., De Martini P.M., Gerardi F., Pantosti D., Smedile A.)2006). Geological evidence of seismically-induced liquefaction features in eastern Sicily. XXV Convegno GNGTS. Riassunti estesi delle comunicazioni. Roma, 28-30 Novembre 2006, 307-309. **CP**
48) Poli, M.E., Burrato, P., Galadini, F., A. Zanferrari (2007). Seismogenic sources responsible for destructive earthquakes in NE Italy. *Boll. Geof. Teor. Appl.*, in press. **NJ**
49) Riggio, A., F. Italiano, H. Friedmann, M. Santulin, J. Vaupotic (2007). Geochemical monitoring and seismological parameters in the border zone between Italy, Slovenia and Austria. *J. of Seismology*, submitted. **JU**
50) Riggio, A., P. Bonfanti, M. Ditta, H. Friedmann, F. Italiano, R. Maugeri, M. Santulin, J.Vaupotic. (2006). Continuous and discrete geochemical measurements and seismicity in the border zone between Italy, Slovenia and Austria. XXV Convegno GNGTS. Riassunti estesi delle comunicazioni. Roma, 28-30 Novembre 2006, 296-297. **CP**
51) Scarfì, L., E. Giampiccolo, C. Musumeci, D. Patanè, H. Zhang (2007). New insights on 3D crustal structure in Southeastern Sicily (Italy) and tectonic implications from an adaptive mesh seismic tomography. *Phys. Earth Planet. Inter.*, 161, 74-85, doi:10.1016/j.pepi.2007.01.007. **JP**
52) Sgroi, T., T. Braun, T. Dahm, F. Frugoni (2006). An improved seismicity picture of the Southern Tyrrhenian Area by the use of OBS and land-based networks: the TYDE experiment. *Ann. Geophys.*, 49, 801-817. **JP**

53) Sgroi T., L. Beranzoli, G. Di Grazia, A. Ursino, P. Favali (2007). New observation of local seismicity by the SN-1 seafloor observatory in the Ionian Sea, off-shore Eastern Sicily (Italy). *Geophys. J. Int.*, 169, 490-501. **JP**
54) Smedile, A., Barbano M.S., De Martini P.M., Gerardi F., Pantosti D., Pirrotta C., Azzaro R., Cosentino M., D'Addezio G., Del Carlo P., Guarnieri P. (2006). Multidisciplinary study to identify tsunami deposits in eastern Sicily. XXV Convegno GNGTS. Riassunti estesi delle comunicazioni. Roma, 28-30 Novembre 2006, 325-328. **CP**
55) Tortorici, G., G. De Guidi, G. Sturiale (2006). Evoluzione tettonica quaternaria del margine settentrionale del Plateau Ibleo (Sicilia sud-orientale). *Boll. Soc. Geol. It.*, 125, 21-37. **NJ**
56) Turino C., Scafidi D., Eva E. and Solarino S. (2006). Estensione e caratteristiche di una faglia non cartografata rivelate da studi sismotettonici. 25° Convegno Nazionale GNGTS, 60-62. **CP**

Task 3

1) Braitenberg, C., B. Grillo, I. Nagy, S. Zidarich, A. Piccin (2007). La stazione geodetico-geofisica ipogea del Bus de la Genziana (1000VTV) - Pian Cansiglio. *Atti e Memorie della Commissione Grotte "E. Boegan"*, Società Alpina della Giulie CAI, 41, 105-120. **NJ**
2) Caporali, A. (2006). Adding geodetic strain rate data to a seismogenic context. *Boll. Geofis. Teor. Appl.*, 47, 455-479. **NJ**
3) Cenni, N., M. Viti, P. Baldi, E. Mantovani , M. Ferrini, V. D'Intinosante, D. Babbucci, D. Albarello (2007). Short-term (geodetic) and long-term (geological) velocity fields in the Northern Apennines. *Boll. Soc. Geol. It.*, submitted. **NJ**
4) Del Gaudio, C., V. Sepe, I. Aquino, S. Borgstrom, G. Brandi, G. Cecere, A. D'Alessandro, P. De Martino, V. D'Errico, M. Dolce, G. Milano, F. Obrizzo, G.P. Ricciardi, C. Ricco, V. Siniscalchi, U. Tammaro (2007). La rete GPS dell'area Sannio – Matese - Open File Report N. 4 2007 OV-INGV http://www.ov.ingv.it/italiano/pubblicazioni/openfile/04_07.htm. **NJ**
5) Mantovani, E., M. Viti, D. Babbucci, C. Tamburelli, D. Albarello (2006). Geodynamic correlation between the indentation of Arabia and the Neogene tectonics of the central-eastern Mediterranean region, Post-collisional tectonics and magmatism in the eastern Mediterranean region. In: Dilek Y., Pavlides S. (eds), *Geol. Soc. of Am. Special Paper*, 409, 15-41. **JP**
6) Milano, G., R. Di Giovambattista, G. Ventura (2006). Seismicity and stress field in the Sannio-Matese area. *Annals of Geophysics*, 48, 881-890. **JP**
7) Pinato Gabrieli, C., C. Braitenberg, I. Nagy, D. Zuliani (2006). Tilting and horizontal movement at and across the northern border of the Adria plate. In: Gil A.J. and Sansò F. (eds), Geodetic Deformation Monitoring: From Geophysical to Engineering Roles, Springer Verlag, 129-137. **NJ**
8) Viti, M., E. Mantovani, D. Babbucci, C. Tamburelli (2006). Quaternary geodynamics and deformation pattern in the Southern Apennines: implications for seismic activity. *Boll. Soc. Geol. It.*, 125, 273-291. **NJ**

Task 4

1) Console, R., M. Murru, F. Catalli (2006). Physical and stochastic models of earthquake clustering. *Tectonophysics*, 417, 141-153. **JP**
2) Console, R., M. Murru, F. Catalli, G. Falcone (2007). Real time forecasts through an earthquake clustering model constrained by the rate-and-state constitutive law: comparison with a purely stochastic ETAS model. *Seismological Research Letters*, 78, 49-56. **JP**
3) Garavaglia, E., R. Pavani (2007). About earthquake forecasting by Semi – Markov renewal processes. *Jour. Methodology and Computing in Applied Probability*, submitted. **JU**
4) Guagenti Grandori, E., L. Petrini, E. Garavaglia (2007). Ipotesi e modello di terremoto caratteristico perturbato In: F. Braga e W. Salvatore (eds), Atti di ANIDIS07, XII Conv. Naz. "L'Ingegneria sismica in Italia", Pisa, 10 – 14 Giugno 2007, Edizioni PLUS, Pisa, CD-ROM, paper n. 5, ISBN 978-88-8492-458-2. **CP**
5) Garavaglia, E., E. Guagenti, R. Pavani, L. Petrini (2007). La predicibilità di un terremoto caratteristico nell'ipotesi dei processi di rinnovo del tipo mistura. Quaderni del Dipartimento di Matematica, QDD 20, Politecnico di Milano. Also in: http://www.mate.polimi.it/biblioteca/qddview.php?id=1329&L=i. **NJ**
6) Garavaglia, E., E. Guagenti, L. Petrini (2007). The earthquake predictability in mixture renewal models.

In: Proc. of Società Italiana di Statistica, SIS Intermediate Conference 2007 Risk and Prediction, Venezia, June 6 – 8 2007, Invited Section, Editor Società Italiana di Statistica, Ed. CLEUP, Venezia, Vol. I, pp 361-372, ISBN 978-88-6129-093-8. **CP**

7) Lippiello, E., C. Godano, L. de Arcangelis (2007). Dynamical scaling in branching models for seismicity. *Phys. Rev. Lett.*, 98, (9):098501 17359207. **JP**

8) Rotondi, R., E. Varini (2007). Bayesian inference of stress release models applied to some Italian seismogenic zones. *Geophys. J. Int.*, 169, 301-314. **JP**

9) Stirling, M., L. Peruzza, D. Slejko, B. Pace (2007). Seismotectonic modelling in northeastern Italy. GNS Science Consultancy Report 2007/84, GNS, Wellington, 22 pp. **NJ**